

DTIC FILE COPY

2

SC5485.FR

AD-A202 248

SC5485.FR

AFOSR-TR- 88 - 1249 Copy No. 2

**OHMIC CONTACTS TO  
GALLIUM ALUMINUM ARSENIDE  
FOR HIGH TEMPERATURE APPLICATIONS**

**FINAL TECHNICAL REPORT FOR THE PERIOD  
July 1, 1985 through February 29, 1988**

Approved for public release;  
distribution unlimited.

CONTRACT NO. F49620-85-C-0120

Prepared for

**Air Force Office of Scientific Research  
Directorate of Electronic and Material Sciences  
Building 410  
Bolling AFB, Washington, DC 20332-6448**

**R.W. Grant and J.R. Waldrop  
Principal Investigators**

NOVEMBER 1988

Approved for public release; distribution unlimited

"The views and conclusions contained in this document are those of the authors and should not be interpreted as necessarily representing the official policies, either expressed or implied, of the Air Force Office of Scientific Research or the U.S. Government."

AIR FORCE OFFICE OF SCIENTIFIC RESEARCH (AFOSR)  
NOTICE OF TRANSMITTAL OF DTIC  
This technical report has been reviewed and is  
approved for public release (AV) AFR 190-12.  
Distribution is unlimited.  
MATTHEW J. KERPER  
Chief, Technical Information Division



**Rockwell International  
Science Center**

**DTIC  
ELECTE**

DEC 09 1988

S  
H

88 12 9 007

UNCLASSIFIED

SECURITY CLASSIFICATION OF THIS PAGE

REPORT DOCUMENTATION PAGE				FORM APPROVED OMB No. 0704-0188	
1a. REPORT SECURITY CLASSIFICATION <b>UNCLASSIFIED</b>		1b. RESTRICTIVE MARKINGS			
2a. SECURITY CLASSIFICATION AUTHORITY		3. DISTRIBUTION/AVAILABILITY OF REPORT <b>Approved for public release; distribution unlimited</b>			
2b. CLASSIFICATION/DOWNGRADING SCHEDULE					
4. PERFORMING ORGANIZATION REPORT NUMBER(S) <b>SC5485.FR</b>		5. MONITORING ORGANIZATION REPORT NUMBER(S) <b>AFOSR-TR-88-1249</b>			
6a. NAME OF PERFORMING ORGANIZATION <b>ROCKWELL INTERNATIONAL Science Center</b>		6b. OFFICE SYMBOL <i>(If Applicable)</i>	7a. NAME OF MONITORING ORGANIZATION <b>Same as 8a</b>		
6c. ADDRESS (City, State, and ZIP Code) <b>1049 Camino Dos Rios Thousand Oaks, CA 91360</b>		6b. OFFICE SYMBOL <i>(If Applicable)</i> <b>NE</b>	7b. ADDRESS (City, State and ZIP Code) <b>Same as 8b</b>		
8a. NAME OF FUNDING/SPONSORING ORGANIZATION <b>Air Force Office of Scientific Research</b>		8b. OFFICE SYMBOL <i>(If Applicable)</i> <b>NE</b>	9. PROCUREMENT INSTRUMENT IDENTIFICATION NUMBER <b>CONTRACT NO. F49620-85-C-0120</b>		
8c. ADDRESS (City, State and ZIP Code) <b>Bldg. 410, Bolling Air Force Base Washington, DC 20332-6448</b>		10. SOURCE OF FUNDING NOS.	PROGRAM ELEMENT NO. <b>61102F</b>	PROJECT NO. <b>2306</b>	TASK NO. <b>B1</b>
			WORK UNIT ACCESSION NO.		
11. TITLE (Include Security Classification) <b>OHMIC CONTACTS TO GALLIUM ALUMINUM ARSENIDE FOR HIGH TEMPERATURE APPLICATIONS</b>					
12. PERSONAL AUTHOR(S) <b>Grant, R.W. and Waldrop, J.R.</b>					
13a. TYPE OF REPORT <b>Final Technical Report</b>		13b. TIME COVERED <b>FROM 07/01/85 TO 02/29/88</b>		14. DATE OF REPORT (Year, Month, Day) <b>1988, NOVEMBER</b>	15. PAGE COUNT
16. SUPPLEMENTARY NOTATION "The views and conclusions contained in this document are those of the authors and should not be interpreted as necessarily representing the official policies, either expressed or implied, of the Air Force Office of Scientific Research or the U.S. Government."					
17. COSATI CODES			18. SUBJECT TERMS (Continue on reverse if necessary and identify by block number)		
FIELD	GROUP	SUB-GROUP			
		<b>PHI B</b>	<b>GaAs, Nonalloyed Ohmic Contacts, Schottky Barrier Modification</b>		
			<b>Germanium Silicon Field Effect Transistor</b>		
19. ABSTRACT (Continue on reverse if necessary and identify by block number)			<b>Gallium Arsenide PHI B</b>		
<p>A new approach for fabricating nonalloyed ohmic contacts to GaAs was developed. The approach uses ultrathin (15-30 Å) layers of heavily doped Ge or Si in contact with GaAs to alter the Schottky barrier height (<math>\phi_B</math>) at the GaAs interface. For n-type GaAs <math>\phi_B</math> could be varied from about 0.3 to 1.0 eV. The low barriers are useful for tunneling ohmic contacts to n-GaAs while the high barriers should be useful for p-GaAs ohmic contacts and for FET gate applications. In some instances it was necessary to interpose a thin nonmetallic electrically conducting barrier between the contact metal and the thin Ge or Si layer to preserve optimum contact properties. Specific contact resistivity measurements indicated that <math>\rho_c &lt; 10^{-6} \Omega\text{-cm}^2</math> should be obtainable in practical contacts to heavily doped material. It is generally observed that <math>\phi_B</math> at most GaAs interfaces is confined to a relatively narrow range presumably <math>\rho_c &lt; 10^{-6} \Omega\text{-cm}^2</math> at <math>\phi_B = 0.6</math> ohms/cm<sup>2</sup>.</p>					
20. DISTRIBUTION/AVAILABILITY OF ABSTRACT UNCLASSIFIED/UNLIMITED <input type="checkbox"/> SAME AS RPT. <input type="checkbox"/> DTIC USERS <input type="checkbox"/>			21. ABSTRACT SECURITY CLASSIFICATION <b>UNCLASSIFIED</b>		
22a. NAME OF RESPONSIBLE INDIVIDUAL <b>Dr. Kevin Malloy</b>		22b. TELEPHONE NUMBER <i>(Include Area Code)</i> <b>202/767-4931</b>		22c. OFFICE SYMBOL <b>NE</b>	

DD FORM 1473, JUN 86

Previous editions are obsolete.

UNCLASSIFIED

SECURITY CLASSIFICATION OF THIS PAGE

19. ABSTRACT (Cont'd)

due to a large concentration of acceptor and donor states closely spaced in energy near midgap. The new approach for normalized ohmic contact fabrication suggests that these states can be saturated with carriers from the heavily doped Ge or Si so as to substantially modify  $\phi_B$ . The resulting contact  $\phi_B$  is virtually independent of contact metallization; the heterojunction band alignment characteristics at the Ge or Si interface with GaAs determine the  $\phi_B$  of the contact. (FLW)



TABLE OF CONTENTS

	<u>Page</u>
1.0 INTRODUCTION .....	1
2.0 EXPERIMENTAL APPROACH .....	5
2.1 XPS .....	5
2.2 I-V and C-V Measurements .....	9
2.3 TLM .....	10
3.0 MATERIALS .....	12
4.0 RESULTS .....	13
4.1 Ge Overlayers .....	13
4.1.1 $E_F^1$ Measurements .....	13
4.1.2 Model AuGeNi Contacts .....	18
4.1.3 TLM Measurements .....	23
4.2 Si Overlayers .....	25
4.2.1 $E_F^1$ Measurements .....	26
4.2.2 Electrical Characterization of Contacts .....	32
5.0 SUMMARY .....	37
6.0 REFERENCES .....	39
7.0 APPENDIX .....	41



Accession For	
NTIS GRA&I	<input checked="" type="checkbox"/>
DTIC TAB	<input type="checkbox"/>
Unannounced	<input type="checkbox"/>
Justification	
By _____	
Distribution/ _____	
Availability Codes	
Avail and/or	
Dist	Special
A-1	



LIST OF FIGURES

<u>Figure</u>		<u>Page</u>
1	Photograph of XPS apparatus.....	6
2	Schematic band diagram that illustrates the use of XPS to determine $E_F^{\uparrow}$ . . . . .	7
3	Analysis method of Ga3d peak used to determine $E_F^{\uparrow}$ from XPS data. . . . .	8
4	TLM measurement test pattern.. . . . .	11
5	XPS Ga3d core-level spectra for several GaAs(100) samples with thin overlayers.. . . . .	14
6	Summary of several $E_F^{\uparrow}$ measurements. . . . .	16
7	XPS Ga3d core level spectra for various thin overlayer structures on initially clean GaAs(100) surfaces. . . . .	19
8	Representative I-V data for a selection of contacts to GaAs that have a variety of structures . . . . .	22
9	TLM measurements for a $10^3\text{\AA}$ Au- $500\text{\AA}$ NiAs <sub>x</sub> - $10\text{\AA}$ Ge(As) ohmic contact to n-GaAs.....	24
10	XPS As3d core level spectra for thin p-type and thin n-type Si layers deposited on clean n-type GaAs(100) surfaces. . . . .	27
11	Summary of several $E_F^{\uparrow}$ measurements with Si overlayers.....	30
12	XPS As3d core level spectra for various thin overlayers on clean n-type GaAs(100) surfaces. . . . .	31
13	Representative I-V data for Cr-Si(Ga) and Ti-Si(Ga) contacts compared to corresponding ideal contacts. . . . .	33
14	Representative I-V data for Au-Si(Ga), Cr-Si(B), and Au-Si(P) contacts compared to Au-ideal and Cr-ideal contacts. . . . .	35
15	Representative C-V data for Au-Si(Ga), Au-Si(P), and Au-ideal contacts.....	36



LIST OF TABLES

<u>Table</u>		<u>Page</u>
1	Values of $E_{\text{Ga3d}}^{\text{GaAs}}$ and $E_F^i$ for Several n-GaAs (100) Interfaces .....	15
2	Correlation of Interface Composition and Barrier Height for Model Nonalloyed AuGeNi Contacts to GaAs .....	21
3	TLM Results for $10^3 \text{ \AA}$ Au - $\sim 500 \text{ \AA}$ NiAs <sub>x</sub> - $10 \text{ \AA}$ Ge(As) Ohmic Contact to n-GaAs (100) .....	25
4	Interface Fermi Energy $E_F^i$ After Deposition of Various Thin Si Layers Which Contain n-Type or p-Type Impurities onto Clean n-Type GaAs(100) Surfaces .....	28
5	XPS Measured $E_F^i$ After Deposition of Thin Si Overlayers and After Subsequent Deposition of Thin Metal Overlayers .....	31
6	Schottky Barrier Height $\phi_B$ of Metal Contacts to GaAs that Include a Thin Si Interface Layer .....	34



## 1.0 INTRODUCTION

This is the final report for Contract No. F49620-85-C-0120 entitled, "Ohmic Contacts to Gallium Aluminum Arsenide for High Temperature Applications," for the period 07/01/85 through 02/29/88. The material properties of GaAs (e.g., high electron mobility, radiation hardness and ease of heterojunction fabrication) make it an attractive semiconductor for use in advanced DoD systems applications that require high frequency operation and high data processing rates. New types of heterostructure devices are being developed in the rapidly progressing area of GaAs IC technology. These heterostructure devices include the GaAs heterojunction bipolar transistor (HBT) for which remarkable current gain cutoff frequencies above 120 GHz have been reported.<sup>1</sup> Increased circuit complexity and high-frequency operation require decreased device dimensions. This size reduction puts greater importance on ohmic contact quality, especially with regard to spatial uniformity of electrical properties and surface morphology. Nonideal ohmic contacts can limit frequency response and nonuniform contacts can affect the yield of ICs.

Although GaAs IC technology has developed rapidly, the rather empirical nature of ohmic contact metallurgy indicates that the basic contact formation mechanism is not well understood.<sup>2</sup> Improved ohmic contacts to both n- and p-type  $\text{Ga}_{1-x}\text{Al}_x\text{As}$  material are needed. The most widely used ohmic contact to n- GaAs is the alloyed AuGeNi metallization.<sup>3</sup> Several studies have shown that these alloyed contacts have multiphase structures with the phase size and composition being dependent on alloying conditions.<sup>4-7</sup> The alloying process involves melting and resolidification of material on a  $10^3\text{\AA}$  scale. Consequently, alloying requires careful control to achieve reproducibility. It appears that alloyed ohmic contacts are not fully adaptable for small dimension device applications and that to obtain contacts with better uniformity, reproducibility, and reliability nonalloyed contacts need to be developed.

The development of stable nonalloyed ohmic contacts to  $\text{Ga}_{1-x}\text{Al}_x\text{As}$  is of considerable technological importance and could benefit several GaAs device structures. As an example, the Rockwell HBT development effort uses a material structure that consists of several thin layers of  $\text{Ga}_{1-x}\text{Al}_x\text{As}$  or related materials to



achieve high speed response.<sup>1</sup> To optimize HBT performance, parasitic resistances and capacitances must be minimized. The emitter contact resistance is a key parameter; typically, an emitter specific contact resistance of  $\leq 5 \times 10^{-7} \Omega\text{-cm}^2$  is required for high performance HBT operation. The base contact is also critical to HBT performance. Heavily doped p-layers are necessary to minimize base resistance and very thin layers are used to optimize current gain. It is important not to alloy the p-type ohmic contact through the base layer during processing. As GaAs device dimensions decrease to improve performance, self-aligned processing techniques based on ion implantation become increasingly important. A self-aligned structure places severe constraints on contact properties if the contact metallurgy is required to withstand the annealing conditions necessary to activate the ion-implanted dopants used in self-aligned processing. The above considerations emphasize the need to develop nonalloyed ohmic contacts to  $\text{Ga}_{1-x}\text{Al}_x\text{As}$  that have good thermal stability.

Tunneling across a thin barrier region is the most common method of forming an ohmic contact. For n-type GaAs, it is generally observed that metal contacts exhibit Schottky barrier heights ( $\phi_B$ ) in the fairly narrow range of 0.7-0.9 eV. By maximizing the dopant concentration at the semiconductor interface, the barrier width is reduced and the contact resistance is minimized. For the commonly used AuGeNi ohmic contact metallization, it is usually assumed that a sizeable Schottky barrier exists at the n-type GaAs interface and that tunneling occurs because of heavy Ge doping of the GaAs near-interface region.<sup>2,8</sup> The tunneling contact model<sup>9</sup> has  $\rho_C \sim \exp(C\phi_B N_D^{-1/2})$ , where  $\rho_C$  is the specific contact resistance,  $N_D$  is the net donor concentration, and C is a constant. For n-GaAs, a maximum  $N_D$  limit of  $\sim 5 \times 10^{19} \text{ cm}^{-3}$  (Sn) has been reported.<sup>10</sup> For this  $N_D$  and a  $\phi_B = 0.7$  eV, one can estimate a lower limit of  $\sim 1.5 \times 10^{-6} \Omega\text{-cm}^2$  for  $\rho_C$ .<sup>11</sup> Consistent with this limit are specific contact resistances of  $\sim 1 \times 10^{-6} \Omega\text{-cm}^2$  for the AuGeNi metallization<sup>4</sup> and of low  $10^{-6} \Omega\text{-cm}^2$  for Ge/Mo sintered contacts<sup>12</sup> (i.e., contacts in which a thin layer of dopant at the GaAs interface is capped with a high melting point metal). As mentioned above, this lower limit is not acceptable for some GaAs heterostructure device applications.

If the barrier height at a tunneling contact could be reduced, a substantial reduction in  $\rho_C$  could be achieved because  $\rho_C$  depends exponentially on  $\phi_B$ . Although the



barrier height of most n-type GaAs interfaces is confined to the fairly narrow limits indicated above, there is growing evidence that at some n-GaAs interfaces, much smaller barriers can be obtained.<sup>12-17</sup> Some of these small barrier interfaces are unstable and would not be suitable for contact applications. A major objective of the present program was to develop methods of producing low barrier tunneling contacts to GaAs. The very stable oxides and hydroxides of Al can complicate attainment of good ohmic contacts to  $\text{Ga}_{1-x}\text{Al}_x\text{As}$ . This difficulty is often circumvented by making contact to  $n^+$  or  $p^+$  GaAs layers grown on  $\text{Ga}_{1-x}\text{Al}_x\text{As}$  and thus, this program focused on making low barrier contacts to the end member GaAs.

A promising new approach for nonalloyed ohmic contact development was discovered in this program based on the use of ultrathin heterojunction layers (UTHL). Low barrier height contacts to n-GaAs were achieved by using thin (15-30Å) layers of heavily n-type doped Ge and Si. With appropriate diffusion barriers, these low barrier contacts could be preserved in practical contacts. The low barrier nature of the contact was determined by both x-ray photoemission (XPS) and electrical (I-V and C-V) measurements and a model based on the heterojunction characteristics of the contact is proposed to explain the results. The UTHL contact has a barrier height that is virtually independent of the contact metallization. Specific contact resistivity was determined by transmission line measurements (TLM) for a model contact with  $N_D = 2 \times 10^{18} \text{ cm}^{-3}$ . Extrapolation of this result to a contact with  $N_D = 5 \times 10^{19} \text{ cm}^{-3}$  indicated that  $\rho_c \sim 2 \times 10^{-7} \Omega\text{-cm}^2$  should be obtained. The UTHL approach to ohmic formation should be applicable for p-type ohmic contact formation. A low barrier p-type contact should correspond to a high barrier n-type contact. By using thin (15-30Å) layers of heavily p-type doped Si on n-type GaAs, Schottky barriers of 1 eV were observed which demonstrate the generality of the UTHL method for modifying contact barriers and is consistent with the proposed heterojunction model of contact formation.

The UTHL method for GaAs barrier modification was demonstrated for both Ge and Si interface layers with both n-type (As and P) and p-type (Ga and B) dopants. The associated model offers a means to design a stable high temperature low barrier tunneling ohmic contact by using materials expected to be thermodynamically stable under the annealing conditions used in self-aligned processing.



This report is organized into seven sections. Section 2 discusses the experimental approach used to characterize the GaAs contacts. The materials used in the program are documented in Section 3. In Section 4, the results of XPS interface potential measurements for the Ge and Si overlayers are discussed and related to the heterojunction characteristics of the samples; electrical measurements of corresponding thick contacts obtained by I-V, C-V and TLM are also given. The program is summarized in Section 5 and references are provided in Section 6. The Appendix (Section 7) reproduces four journal publications, three conference talk abstracts and two patent disclosures based on work supported by this program.



## 2.0 EXPERIMENTAL APPROACH

The XPS system in which the GaAs contacts were prepared and analyzed is discussed in this section. In addition, the current-voltage (I-V), capacitance-voltage (C-V) and transmission line measurement (TLM) apparatus used for electrical characterization of GaAs contacts is described.

### 2.1 XPS

A Hewlett-Packard 5950 electron spectrometer was used for the XPS investigations of interface chemistry and potential in this program. A photograph of the instrument is shown in Fig. 1. The spectrometer utilizes a monochromatic AlK $\alpha$  ( $h\nu = 1486.6$  eV) x-ray source to excite photoelectrons. A custom sample preparation chamber is attached to the spectrometer to provide various in-situ specimen treatments. These treatments include sample heating, material deposition and low energy electron diffraction (LEED) analysis. Both the XPS spectrometer and sample preparation chamber operate at UHV with a base pressure of  $\sim 10^{-10}$  Torr.

The deposition sources for Ge and most metals were resistively heated W wire baskets. A W wire basket was also used for initial Si depositions although an enclosed Ta wire basket was subsequently found to improve source stability. The As $_4$  and Te sources were small quartz ovens, the P $_2$  source was an InP crystal heated by a W wire while avoiding direct line of sight between source and sample and elemental B was included in the Si source to deposit boron-doped silicon, Si(B).

The ability of XPS to determine interface chemistry by analyzing chemical shifts is well known.<sup>18</sup> The technique also provides a method to determine the interface Fermi level ( $E_F^i$ ) of a sample.<sup>19</sup> The determination of  $E_F^i$  is illustrated in Fig. 2, which shows a schematic GaAs band diagram. In this figure, all binding energies ( $E_B$ ) are referred to the Fermi level ( $E_F$ ). The conduction band minimum is  $E_C^{GaAs}$ , the valence band maximum is  $E_V^{GaAs}$ , the Ga3d and As3d core level binding energies are  $E_{Ga3d}^{GaAs}$  and  $E_{As3d}^{GaAs}$ , respectively.  $E_F^i$  is measured relative to  $E_V^{GaAs}$  at the interface and  $W$  is the depletion width. The typical electron escape depth ( $\approx 25\text{\AA}$ )<sup>20</sup> is much shorter than  $W$  for moderately doped GaAs. For our experimental geometry, the effective photoelectron



Rockwell International  
Science Center

13855

SC5485.FR



Fig. 1 Photograph of XPS apparatus.

6  
C9553D/bje

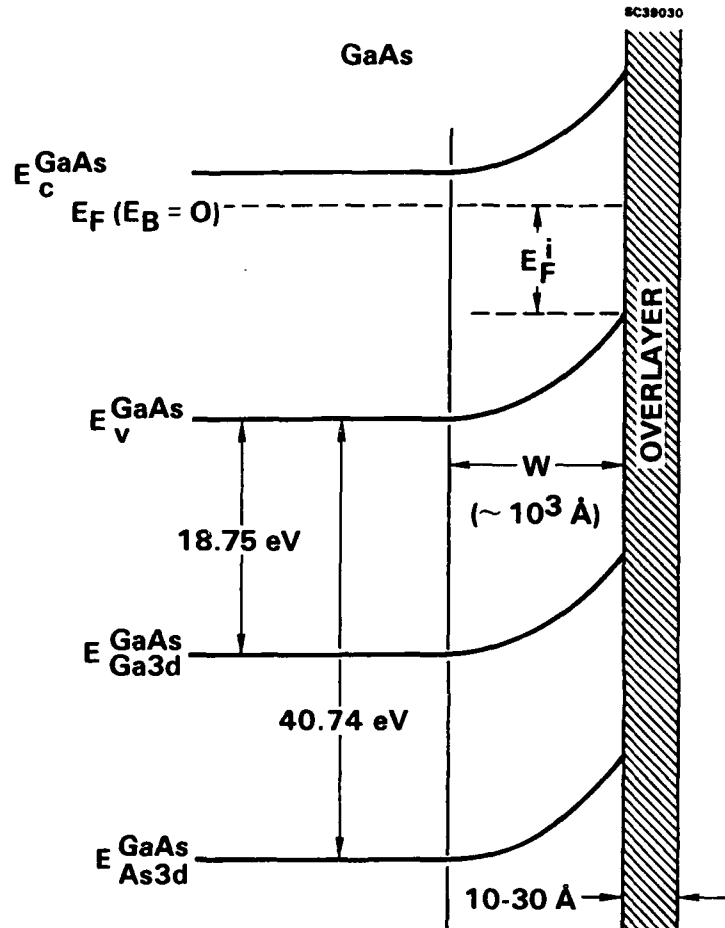


Fig. 2 Schematic band diagram that illustrates the use of XPS to determine  $E_F^1$ .

escape depth was always  $\sim 16 \text{ \AA}$ . Thus, an XPS measurement of a clean GaAs surface or a surface with a very thin overlayer ( $\leq 25 \text{ \AA}$ ) will determine  $E_{Ga3d}^{GaAs}$  and/or  $E_{As3d}^{GaAs}$  at the interface, as shown in Fig. 2. For GaAs, the binding energy differences  $E_{Ga3d}^{GaAs} - E_V^{GaAs} = 18.75 \pm 0.03 \text{ eV}$  and  $E_{As3d}^{GaAs} - E_V^{GaAs} = 40.74 \pm 0.03 \text{ eV}$  have been determined previously.<sup>21</sup> As can be seen in Fig. 2, the interface potential is determined as  $E_F^1 = E_{Ga3d}^{GaAs} - 18.75 \text{ eV} = E_{As3d}^{GaAs} - 40.74 \text{ eV}$  and  $\phi_B = 1.43 \text{ eV} - E_F^1$ .



To determine the absolute  $E_B$  of either the Ga3d or As3d core levels, a background function proportional to the integrated photoelectron intensity was first subtracted from the XPS spectrum in the vicinity of the core level peak. The resulting peak was least-squares fit to a third order polynomial near the peak maximum and near the half height on both sides of the peak to determine the peak center (position of the half width point at half height) and the peak width,  $r$  (the full width at half height). A representative example of this analysis for a Ga3d peak is shown in Fig. 3. At the conclusion of most experiments, a thick ( $> 10^3 \text{ \AA}$ ) Au metal layer was evaporated onto the sample surface and an absolute  $E_F^1$  value was obtained by indexing the Au4f<sub>7/2</sub> XPS peak position to 84.00 eV.<sup>22</sup>

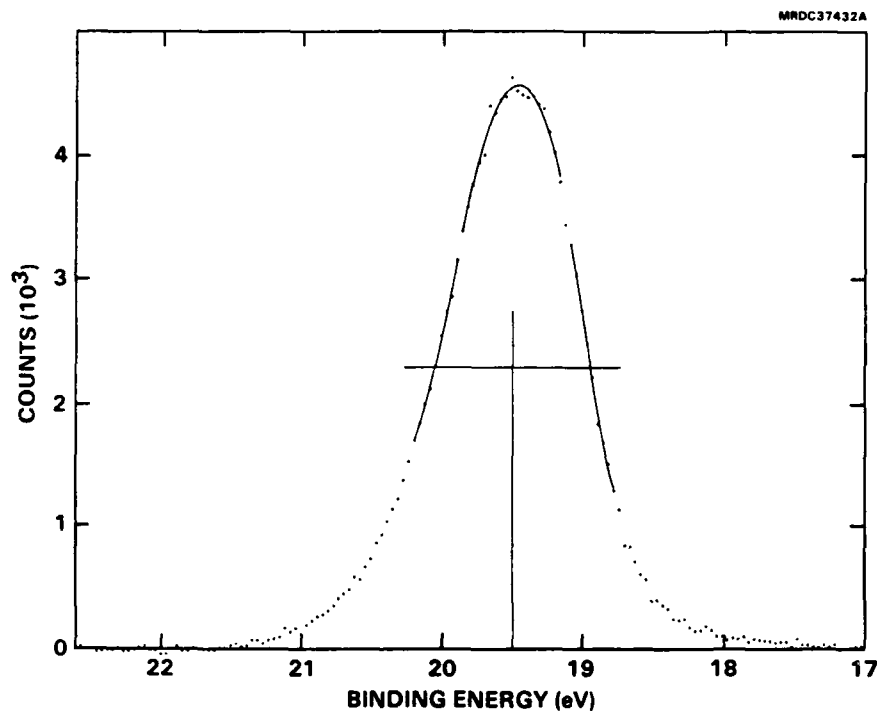


Fig. 3 Analysis method of Ga3d peak used to determine  $E_F^1$  from XPS data. Curves are least-square fits to third order polynomials; the peak center and full width at half maximum are indicated.



## 2.2 I-V and C-V Measurements

The electrical properties of GaAs contacts were characterized by I-V and C-V measurements. I-V data are obtained in 0.01 V forward bias increments by using a computerized system that includes a HP4140B pA meter/voltage source. Both room temperature and low temperature measurements were performed. The low temperature cold stage uses a nitrogen gas Joule-Thomson expansion system. Low temperature measurements were necessary to analyze the low  $\phi_B$  samples. The I-V data were analyzed by use of the Schottky barrier thermionic emission model with

$$I = I_s \exp(qV/nkT) [1 - \exp(-qV/kT)]A$$

where both the ideality factor  $n$  (at  $T = 295K$ ,  $n = 1.02$  is ideal; however there is often an increase in  $n$  at low  $T$ ) and  $I_s$  (the saturation current) were determined by a least-squares fit. The  $\phi_B$  was extracted from  $I_s$  by

$$I_s = SA^* T^2 \exp[-q(\phi_B - \Delta\phi)/kT]A$$

where  $S$  is the contact area,  $A^* = 8.16$  is the effective Richardson constant, and  $\Delta\phi$  is the calculated image force correction ( $\Delta\phi \pm 0.04$  eV for  $\phi_B \geq 0.7$  eV and  $+0.03$  eV for  $\phi_B < 0.7$  eV). Good reproducibility of results between contacts on a given sample was observed and thus average values (approximately seven contacts per sample) of  $\phi_B$  and  $n$  were determined; the measurement uncertainty for  $\phi_B$  was  $< \pm 0.01$  eV.

The C-V measurements employed a HP 4275A LCR meter operating at 1 MHz. The C-V data were analyzed according to the conventional model<sup>23</sup> that gives  $\phi_B^{CV}$  in terms of the intercept  $V_i$  (found by a least-squares fit) on the voltage axis of a  $C^{-2}$  vs  $V$  plot.

The interface potential determined by XPS could be compared with corresponding barrier heights determined by I-V or C-V by making measurements on the same sample. First,  $E_F^1$  was determined for a thin ( $\sim 25\text{\AA}$ ) overlayer; following this determination, a thicker ( $\geq 10^3\text{\AA}$ ) metallization was deposited in situ. After removal from the ultrahigh vacuum (UHV) system, circular dots were fabricated by chemically



etching a photoresist pattern. In this way, both electrical measurements and XPS measurements could be obtained on the same interface.

### 2.3 TLM

The specific contact resistance ( $\rho_c$ ) was measured by the transmission line method (TLM).<sup>24</sup> The contacts were formed on an MBE-grown GaAs layer on a semi-insulating GaAs substrate. A schematic of the test structure is shown in Fig. 4. Two contact masks were fabricated, one to provide test patterns, as shown in Fig. 4(a), and one to facilitate a mesa etch for isolating each test pattern, Fig. 4(b). The rectangular mesa etch mask had dimensions  $+1 \mu\text{m}$  larger than the test pattern. A constant current was passed between the large rectangular end contact pads of the test pattern and the subsequent voltage drop between neighboring contact pads was measured. The transmission line model gives the measured resistance as

$$R = R_s \frac{L}{w} + \frac{2L_T}{w} R_s \coth \frac{z}{L_T}$$

where  $R_s$  is the sheet resistance,  $L$  is the separation between contact pads,  $w$  is the contact pad width,  $L_T$  is the transfer length, and  $z$  is the contact length. When  $z \gg L_T$ , that is, if the portion of the contact length from which current is flowing is small compared to the total contact length (which is the condition in our measurements), the TLM model reduces to:

$$R = \frac{R_s}{w} L + 2L_T \frac{R_s}{w} .$$

In practice, a plot of  $R$  vs  $L$  is made from which the slope of a linear least square fit yields  $\frac{R_s}{w}$  and the intercept on the  $L$  axis for  $R = 0$  yields  $2L_T$ . The transfer length is related to the contact resistance  $\rho_c$  by:

$$\rho_c = R_s L_T^2 .$$



SC47284

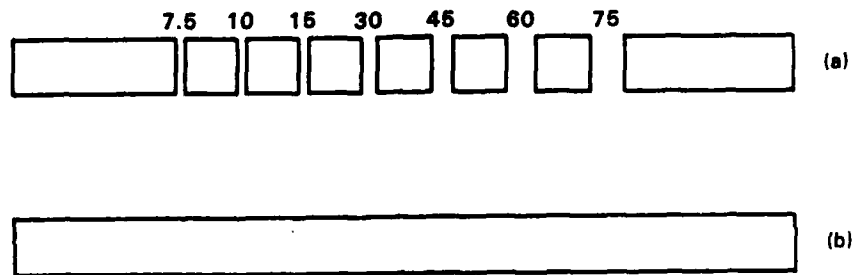


Fig. 4 TLM measurement test pattern. (a) Spacings between squares (in  $\mu\text{m}$ ) are indicated; square dimensions were  $125 \times 125 \mu\text{m}$ , rectangle dimensions were  $375 \times 125 \mu\text{m}$ . (b) Rectangular mesa isolation pattern—dimensions  $1743.5 \times 126 \mu\text{m}$ .



### 3.0 MATERIALS

Most of the GaAs material used in this program was bulk grown, (100) oriented, and doped in the  $3\text{-}5 \times 10^{16} \text{ cm}^{-3}$  range with either Se or Si. This moderately doped material was utilized so that barrier heights determined by I-V could be analyzed by the thermionic emission model and XPS measurements were not complicated by excessive band bending in the interface region. The material was either grown by the liquid encapsulated Czochralski or horizontal Bridgman techniques. The wafers were obtained in cut and polished form with a 20 mil thickness.

A few GaAs samples were prepared by molecular beam epitaxy at Rockwell for use in TLM measurements. These samples consisted of a 5000Å semi-insulating buffer layer and a 1500Å n-type GaAs layer grown on a semi-insulating GaAs substrate. Net donor densities ranged from  $3 \times 10^{17}$  to  $2.3 \times 10^{18} \text{ cm}^{-3}$ , as determined by Hall effect measurements.

To prepare a bulk sample for XPS analysis, the GaAs wafer was cut into an approximate  $8 \times 8$  mm square, etched in fresh 4:1:1  $\text{H}_2\text{SO}_4:\text{H}_2\text{O}_2:\text{H}_2\text{O}$  solution for ~ 30 s to remove polishing damage, mounted with indium on a Mo plate and immediately placed into the UHV environment of the XPS system. The In mounting involved heating in air to ~ 160°C for a few seconds. The ~ 10Å native oxide layer was removed by momentary heating, either in vacuum or in an  $\text{As}_4$  overpressure, to the minimum necessary temperature (~ 550°C); this heating also forms an ohmic contact between the bulk GaAs and the Mo plate. The thermally cleaned surface is ordered (displays a characteristic LEED pattern) and is shown by XPS to be free of oxygen, carbon, or other contaminants. Following XPS analysis and deposition of thick ( $> 10^3 \text{Å}$ ) overlayers, circular  $2.54 \times 10^{-2}$  cm diameter dots (for contact electrical characterization) were defined by using photolithography and chemical etching.

The MBE samples used for TLM measurements were prepared in a similar manner except the initial surface was only degreased and not chemically etched. Following contact metallization deposition, the TLM test patterns and isolating mesas were defined by ion milling.



## 4.0 RESULTS

A new approach for fabricating nonalloyed ohmic contacts is described in this section. The approach uses heavily doped UTHL to alter  $E_F^{\uparrow}$  in GaAs. The results for UTHL ohmic contacts formed with either Ge or Si interlayers are presented.

### 4.1 Ge Overlayers

As noted in Section 1.0, there is growing evidence that at some GaAs interfaces,  $E_F^{\uparrow}$  values outside the commonly observed narrow pinning range can be obtained. Specifically relevant to this section is the wide range of  $E_F^{\uparrow}$  values reported for the Ge/GaAs interface.<sup>14,15,24-27</sup> If either large  $E_F^{\uparrow}$  values could be obtained for n-type contacts or small  $E_F^{\uparrow}$  values for p-type contacts, substantial lowering of  $\rho_C$  for tunneling contacts could be expected. In Section 4.1.1, we present XPS measurements which show the wide range of  $E_F^{\uparrow}$  values obtainable with thin Ge overlayers. The most commonly used ohmic contact to n-type GaAs is the AuGeNi metallization. In Section 4.1.2, we discuss investigations of nonalloyed layer structures of Au, Ge, and Ni which establish a correlation of interface composition and  $E_F^{\uparrow}$ . Section 4.1.3 describes TLM measurements of a model UTHL contact which are used to predict expected  $\rho_C$  for various  $N_D$ .

#### 4.1.1 $E_F^{\uparrow}$ Measurements

The variation in  $E_F^{\uparrow}$  for thin overlayers of Ge on n-GaAs can be easily detected by XPS. Representative XPS Ga3d core-level spectra for several samples are compared in Fig. 5. A spectrum from a thermally cleaned surface is shown for reference in Fig. 5(a) (the vertical line shown in the figure marks the center of this Ga3d line). The two spectra shown in Figs. 5(b) and 5(c) are for GaAs samples on which thin layers of Ge were deposited in vacuum at 325 and 250°C, respectively. A LEED pattern was observed for the Ge layers deposited (either in vacuum or in the presence of an  $As_4$  background pressure) in the 200-325°C temperature range, although the pattern had a high background at 200°C. The Ga3d binding energy decrease noted in Figs. 5(b) and 5(c) spectra relative to the thermally clean surface represents a decrease in  $E_F^{\uparrow}$ , and thus a corresponding increased band bending. The spectrum shown in Fig. 5(d) is for the same

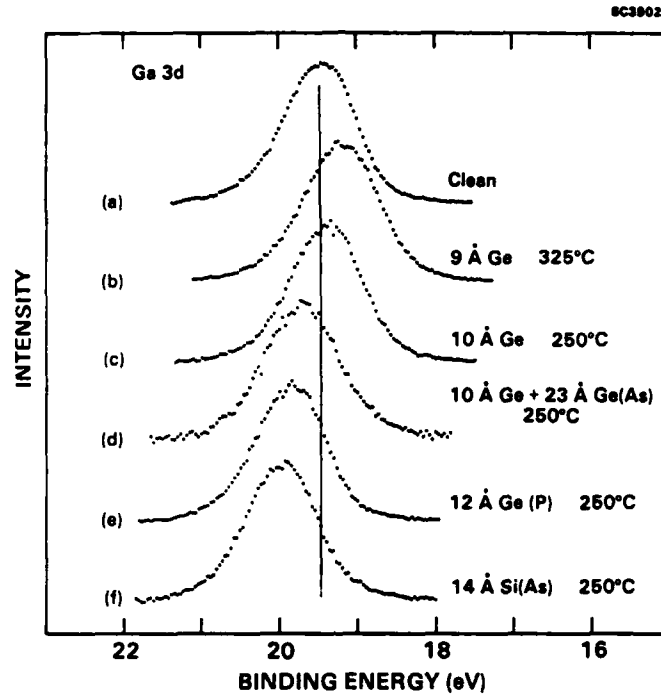


Fig. 5 XPS Ga3d core-level spectra for several GaAs(100) samples with thin overlayers. The overlayer composition and deposition temperatures are noted in the figure. The spectra shown as (c) and (d) are for the same sample, except for the additional Ge(As) layer.

sample that was studied in Fig. 5(c), but with the addition of a 23Å-thick layer of Ge deposited at 250°C under conditions ( $1 \times 10^{-7}$  Torr  $As_4$  background pressure) where As incorporation occurs [this layer is designated Ge(As)]. A marked shift to higher  $E_B$  (lower band bending) occurs.

Two additional spectra are shown in Figs. 5(e) and 5(f). The first is from a sample on which a 12Å Ge layer was deposited at 250°C in the presence of a  $10^{-6}$  Torr  $P_2$  background. This sample has a substantially lower band-bending than the thermally cleaned surface. Figure 5(f) is a spectrum from a sample on which a 14Å layer of Si was deposited at 250°C; these data will be discussed in Section 4.2.1. Values of  $E_{GaAs}^{Ga3d}$  and of



the corresponding  $E_F^1$  are given in Table I for the representative samples shown in Figs. 5(a-e) and for several other samples.

Table I  
Values of  $E_{GaAs}^{GaAs}$  and  $E_F^1$  for Several n-GaAs (100) Interfaces

Sample No.	Overlayer	Deposition Temp. (°C)	Overlayer Thickness (Å)	Background Pressure during Deposition (Torr)	$E_{GaAs}^{GaAs}$ (eV)	$E_F^1$ (eV)
1	Thermally clean (ave. of 16 samples)	---	---	---	19.46	0.71
2	Ge	200	9	Vacuum	19.45	0.70
3	Ge <sup>a</sup>	200	10	Vacuum	19.87	1.12
4	Ge	250	10	Vacuum	19.40	0.65
5	Sample No. 4 + Ge(As)	250	23	10 <sup>-7</sup> As <sub>4</sub>	19.73	0.98
6	Ge	250	6	Vacuum	19.47	0.72
7	Sample No. 6 + Ge(As)	250	6	10 <sup>-7</sup> As <sub>4</sub>	19.88	1.13
8	Ge	325	9	Vacuum	19.20	0.45
9	Sample No. 8 + Exposure to 30 L As <sub>4</sub> at 325°C	---	---	---	19.26	0.51
10	Ge(As)	RT	26	10 <sup>-7</sup> As <sub>4</sub>	19.49	0.74
11	Ge(As)	200	10	10 <sup>-7</sup> As <sub>4</sub>	19.82	1.07
12	Ge(As)	200	7	10 <sup>-7</sup> As <sub>4</sub>	19.79	1.04
13	Ge(As) <sup>b</sup>	200	9	10 <sup>-7</sup> As <sub>4</sub>	19.78	1.03
14	Ge(As)	200	11	10 <sup>-7</sup> As <sub>4</sub>	19.78	1.03
15	Ge(As) <sup>a</sup>	200	4	10 <sup>-7</sup> As <sub>4</sub>	19.78	1.03
16	Ge(As)	250	9	10 <sup>-7</sup> As <sub>4</sub>	19.96	1.21
17	Ge(As)	250	9	10 <sup>-7</sup> As <sub>4</sub>	19.90	1.15
18	Ge(As)	250	8	10 <sup>-7</sup> As <sub>4</sub>	19.78	1.03
19	Ge(As)	250	7	10 <sup>-7</sup> As <sub>4</sub>	19.89	1.14
20	Ge(As)	325	11	10 <sup>-7</sup> As <sub>4</sub>	19.85	1.10
21	Ge(As)	325	9	10 <sup>-6</sup> As <sub>4</sub>	19.96	1.21
22	Ge(P)	250	11	10 <sup>-6</sup> P <sub>2</sub>	19.87	1.12

- a Substrate cleaned in 10<sup>-6</sup> Torr As<sub>4</sub>.  
b Substrate cleaned in 10<sup>-7</sup> Torr As<sub>4</sub>.

Several of the results listed in Table I are shown pictorially in Fig. 6. The overlayer characteristics are noted at the bottom of the figure, and the corresponding  $E_F^1$  value is shown on the vertical scale. The positions of  $E_V^{GaAs}$  and  $E_C^{GaAs}$  are listed on the vertical scale ( $E_F^1 = 0$  at  $E_V^{GaAs}$ ). As will be noted below, the interface heterojunction band alignment characteristics appear to play a role in determining the

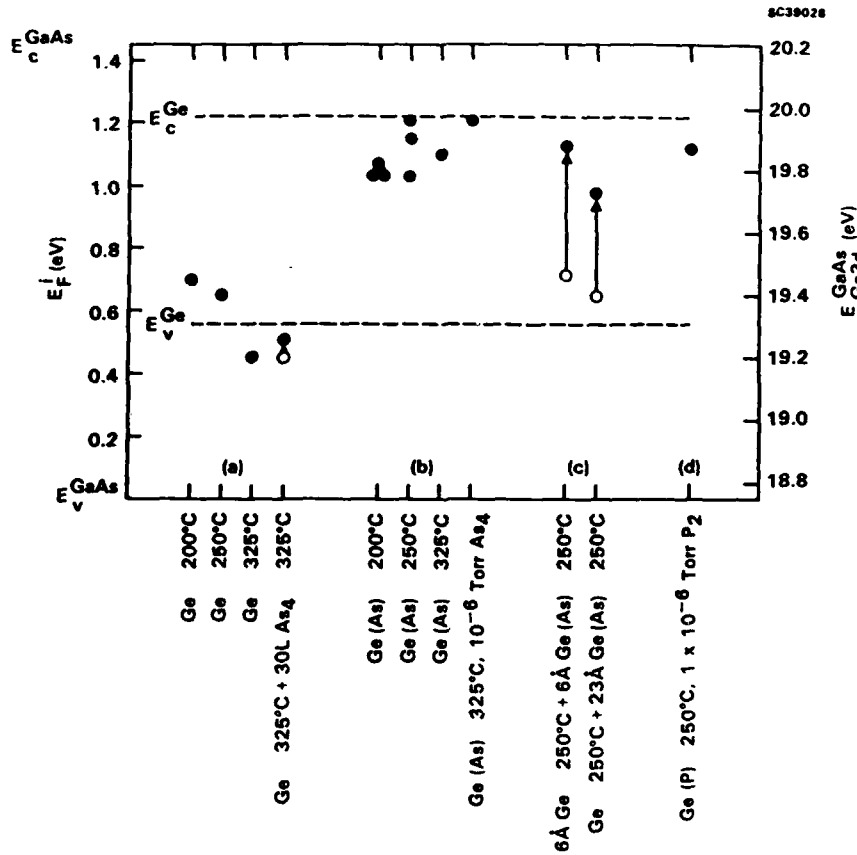


Fig. 6 Summary of several  $E_F^1$  measurements. Germanium overlayer characteristics are given at bottom of figure. Unless noted otherwise, overlayer thicknesses are nominally  $\sim 10\text{\AA}$  and depositions intended to incorporate As or P in the overlayer were carried out in  $10^{-7}$  Torr background pressure of As<sub>4</sub> or P<sub>2</sub>: (a) overlayers deposited in vacuum; (b) overlayers deposited in As<sub>4</sub>; (c) overlayers initially deposited in vacuum, but completed with deposition in As<sub>4</sub>; (d) overlayer deposited in P<sub>2</sub>.

observed  $E_F^1$  positions. Thus, also shown in this figure by dashed lines are the  $E_v$  and  $E_c$  positions for Ge measured at Ge/GaAs<sup>28</sup> heterojunction interfaces.



The data shown in Fig. 6 are grouped into four sets (a)-(d). The first set (a) shows  $E_F^i$  values obtained with Ge overlayers that were deposited in vacuum between 200 and 325°C. The data indicate that band bending in the GaAs increases slightly with increasing Ge deposition temperature. Vacuum-deposited Ge is almost always found to be p-type,<sup>29</sup> independent of the substrate. The results shown in Fig. 6(a) suggest that the acceptor density (associated with either the deposition process and/or Ga incorporation from the substrate) increases with increasing deposition temperature. The Ge is degenerate p-type when vacuum deposited at 325°C on thermally cleaned GaAs substrates, in agreement with previous results.<sup>25</sup> Exposure of the Ge overlayer grown at 325°C to 30 L of  $As_4$  with the sample held at 325°C caused only a small (~ 0.06 eV) decrease in GaAs band bending, as indicated by the arrow in Fig. 6(a).

The  $E_F^i$  values shown in Fig. 6(b) are for Ge(As) overlayers deposited between 200 and 325°C. The net donor density associated with As-doped, molecular beam epitaxy (MBE)-grown Ge films on GaAs (100) has been studied<sup>11,30</sup> as a function of substrate temperature and found to vary relatively slowly in this temperature range. This behavior may be related to the relatively small variation of  $E_F^i$  with substrate temperature observed in Fig. 6(b), where there is a tendency for  $E_F^i$  to increase with increasing substrate temperature and with increasing  $As_4$  background pressure during Ge deposition. The observed  $E_F^i$  values are in the same range as those previously observed for n-Ge layers grown on several GaAs(100) surfaces,<sup>15</sup> and support the conclusion that As doping of Ge is important in determining  $E_F^i$  while deposition-induced defects are not.<sup>26</sup>

To investigate the role of As in determining  $E_F^i$ , two additional experiments were performed in an effort to separate the effect of As at the Ge/GaAs interface from As incorporated in the Ge overlayer. The results of these two experiments are shown in Fig. 6(c). In this case, the sample has two overlayers. The first layer was Ge deposited in vacuum at 250°C; the  $E_F^i$  value associated with this layer is shown by the open circles. The second Ge(As) overlayer was deposited at 250°C in the presence of  $10^{-7}$  Torr  $As_4$  background pressure. The  $E_F^i$  observed after deposition of the Ge(As) layer is shown by closed circles. The large increase in the  $E_F^i$  position (decrease in GaAs band bending) is indicated by arrows in Fig. 6(c). In Fig. 6(a), it was observed that exposure of



a vacuum-deposited Ge layer to  $As_4$  caused only a minor shift of  $E_F^\dagger$ . Taken together with the results shown in Fig. 6(c), it appears that the role of As is to alter the  $E_F$  in the deposited Ge and thus the Ge/GaAs  $E_F^\dagger$  rather than directly affecting the interface properties per se.

If As acting as a donor in Ge is responsible for the large  $E_F^\dagger$  values, other n-type dopants might be expected to produce a similar effect. Thus, a Ge(P) overlayer was prepared by depositing Ge at 250°C in a  $10^{-6}$  Torr  $P_2$  background pressure. The measured  $E_F^\dagger$  value is shown in Fig. 6(d) and is similar to the results obtained with Ge(As) layers.

The above noted range in  $E_F^\dagger$  indicates that interface heterojunction band alignment characteristics may be responsible for the limits to the large range of observed  $E_F^\dagger$  values at the Ge/GaAs interface. This possibility will be further discussed in Section 4.2.1.

#### 4.1.2 Model AuGeNi Contacts

The alloyed AuGeNi metallization<sup>3</sup> is widely used as an ohmic contact to n-GaAs. The complex contact structure consists of several phases whose individual size and composition depend on the alloying time and temperature.<sup>7,31-33</sup> It is usually assumed that  $\phi_B$  is inevitably ~ 0.7-0.9 eV because, as noted previously, the Schottky barrier height for most metal contacts to GaAs is in this range. According to this viewpoint,  $\rho_C$  is reduced by minimizing  $N_D$ . However, as observed in Section 4.1.1, for certain thin Ge overlayers on clean GaAs,  $E_F^\dagger$  can be > 1.0 eV. If such a high  $E_F^\dagger$  state (low  $\phi_B$ ) can be attained in a tunnel AuGeNi ohmic contact,  $\rho_C$  would be substantially reduced for a given  $N_D$ .

An investigation of model AuGeNi contacts to GaAs was carried out that involved layered structures designed to correlate interface composition with  $\phi_B$ . The contacts were not alloyed so as to retain interfaces of controlled composition. The interface chemistry and  $E_F^\dagger$  during initial contact formation were observed by XPS; the corresponding  $\phi_B$  for a thick contact was obtained by I-V measurement.



The contact interfaces were prepared under UHV conditions in the sample preparation chamber of the XPS system. During initial contact formation, XPS spectra of the Ga3d and As3d core level peaks in GaAs and of other core level peak spectra appropriate for a given interface were obtained. The NiAs<sub>x</sub> layers were formed by depositing Ni onto a room temperature substrate in a 10<sup>-7</sup>-10<sup>-6</sup> Torr As<sub>4</sub> overpressure (XPS analysis indicated that the NiAs<sub>x</sub> layers were As rich).

The representative Ga3d core level peak data plotted in Fig. 7 show how XPS was used to measure E<sub>F</sub><sup>↑</sup> and to monitor composition during interface formation. The upper three spectra are after sequential treatments to the same sample; the lower three are for three other samples with the indicated overlayer structure (peak heights are normalized). The vertical line in Fig. 7 that marks the center of the clean surface Ga3d peak at 19.47 eV is for E<sub>F</sub><sup>↑</sup> (clean) = 0.67 eV.

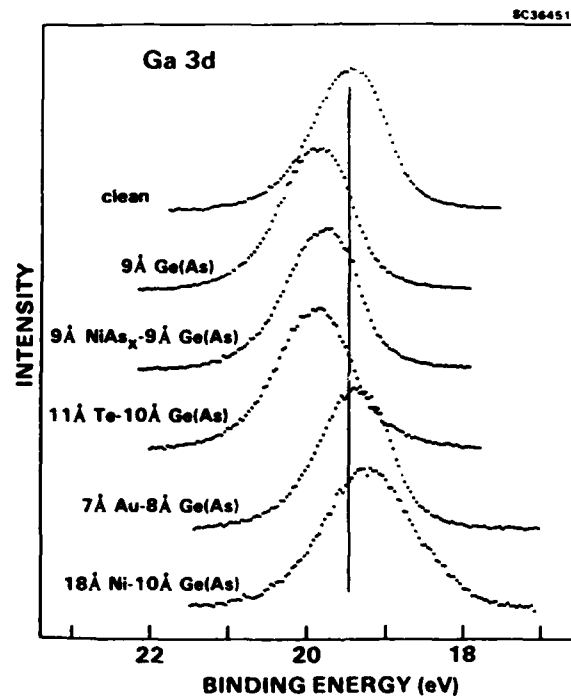


Fig. 7 XPS Ga3d core level spectra for various thin overlayer structures on initially clean GaAs(100) surfaces. Upper three spectra are for successive depositions on the same sample.



After deposition of 9Å of Ge onto the clean GaAs surface at 250°C and in  $1 \times 10^7$  Torr  $As_4$  overpressure, the Ga3d peak shifts 0.43 eV to higher binding energy (compare upper two peaks). This shift represents an increase in  $E_F^\dagger$  to 1.10 eV. The  $E_F^\dagger$  for a thin Ge overlayer on clean GaAs will be defined as  $E_F^\dagger(\text{Ge})$  and the  $E_F^\dagger(\text{Ge})$  data are tabulated in Table 2. An  $E_F^\dagger$  of 1.10 eV corresponds to  $\phi_B = 0.33$  eV which would be attractive for tunneling ohmic contact applications if it can be preserved upon deposition of additional contact material. The third and fourth spectra (from the top) in Fig. 7 demonstrate that the low band bending can still be preserved in certain cases. The third spectrum is for 9Å of  $NiAs_x$  deposited onto the 9Å Ge(As) overlayer where  $E_F^\dagger(\text{Ge}) = 1.1$  eV. Essentially no change in the Ga3d energy, and hence no change in  $E_F^\dagger$ , occurs. To test the generality of this result, another conductive nonmetal, Te, was used. When 11Å of Te is deposited onto a Ge(As) overlayer with high associated  $E_F^\dagger(\text{Ge})$  (fourth spectrum), there is also no change in  $E_F^\dagger$ . The situation is dramatically different when either Au or Ni is deposited directly onto a high  $E_F^\dagger(\text{Ge})$  overlayer of Ge(As) (lower two spectra in Fig. 7). In each case,  $E_F^\dagger$  shifted from  $E_F^\dagger(\text{Ge}) = \sim 1.1$  eV to  $E_F^\dagger = \sim 0.7$  eV after the metal deposition; thus, the lower barrier condition was removed (the low binding energy shoulder in the last peak is due to a Ni-GaAs chemical reaction).

To investigate the correlation of XPS measured  $E_F^\dagger$  values with I-V measured  $\phi_B$ , several kinds of model thick contact structures were formed. The types that include Ge are shown on the right side of Fig. 8; in each case, an initial Ge overlayer is followed (at room temperature) by the indicated depositions. Not shown are structures without the Ge layer (designated ideal), where Au, Ni, or  $NiAs_x$  is deposited directly onto clean GaAs.

Figure 8 also shows representative I-V data ( $T = 295$  or  $150\text{K}$ , the lower measurement temperature was necessary for low  $\phi_B$ ) that demonstrate the wide range in  $\phi_B$  which is associated with the different contact structures. The data were analyzed by the thermionic emission model (Section 2.2.1) and Table 2 lists the average  $\phi_B$  and  $n$  values for the various interface structures ( $\sim$  seven contacts per sample,  $< \pm 0.01$  eV measurement uncertainty).



**Table 2**  
**Correlation of Interface Composition and Barrier Height for**  
**Model Nonalloyed AuGeNi Contacts to GaAs**

Interface Structure	Ge Depos. Temp. (°C)	$E_F^{\uparrow}(\text{Ge})^a$ (eV)	$\phi_B^{b,c}$ (eV)	n
Au-NiAs <sub>x</sub> -9Å Ge(As)	200	0.98	0.31 <sup>d</sup>	1.27
Au-NiAs <sub>x</sub> -11Å Ge(As)	200	0.98	0.35 <sup>d</sup>	1.23
Au-NiAs <sub>x</sub> -9Å Ge(As)	250	1.10	0.39 <sup>d</sup>	1.11
Au-100Å Te-10Å Ge(As)	200	1.07	0.23 <sup>e</sup>	1.33
Au-100Å Te-9Å Ge(As)	250	1.16	0.39 <sup>d</sup>	1.08
Au-100Å Te-7Å Ge(As)	325	1.05	0.36 <sup>d</sup>	1.10
Au-10Å Ge(As)	200	1.02	0.76	1.05
Au-8Å Ge(As)	250	0.98	0.61	1.05
Au-9Å Ge(As)	325	1.16	0.64	1.05
Ni-10Å Ge(As)	200	0.99	0.81	1.11
Au-100Å Te-9Å Ge	200	0.65	0.65	1.06
Au-9Å Ge	325	0.40	0.71	1.12
Au-100Å Te <sup>f</sup>	---	--	0.79	1.02
NiAs <sub>x</sub> -ideal	---	--	0.80	1.04
Ni-ideal	---	--	0.84	1.05
Au-ideal	---	--	0.89	1.05

- a Ge overlayer only
- b Includes image force correction, see Section 2.2.1
- c Measured at T = 295K unless noted
- d T = 150K
- e T = 100K
- f Reference 16

The Au-NiAs<sub>x</sub>-Ge(As) and Au-Te-Ge(As) contacts that have a high  $E_F^{\uparrow}(\text{Ge})$  (~ 1.0-1.2 eV) also have a low  $\phi_B$  (~ 0.25-0.4 eV). In contrast, the Au-Ge(As) and Ni-Ge(As) contacts that have a similarly high  $E_F^{\uparrow}(\text{Ge})$  value have, without an intervening NiAs<sub>x</sub> or Te layer, a high  $\phi_B$  (~ 0.6-0.8 eV). These values for  $\phi_B$  can be compared to those for the Au and Ni ideal contacts,  $\phi_B(\text{Au}) = 0.89$  eV and  $\phi_B(\text{Ni}) = 0.84$  eV. Thus, a high  $E_F^{\uparrow}$  state induced by a Ge(As) layer can be preserved by a NiAs<sub>x</sub> or Te layer that prevents Au or Ni from reaching the Ge-GaAs interface.



8C36463

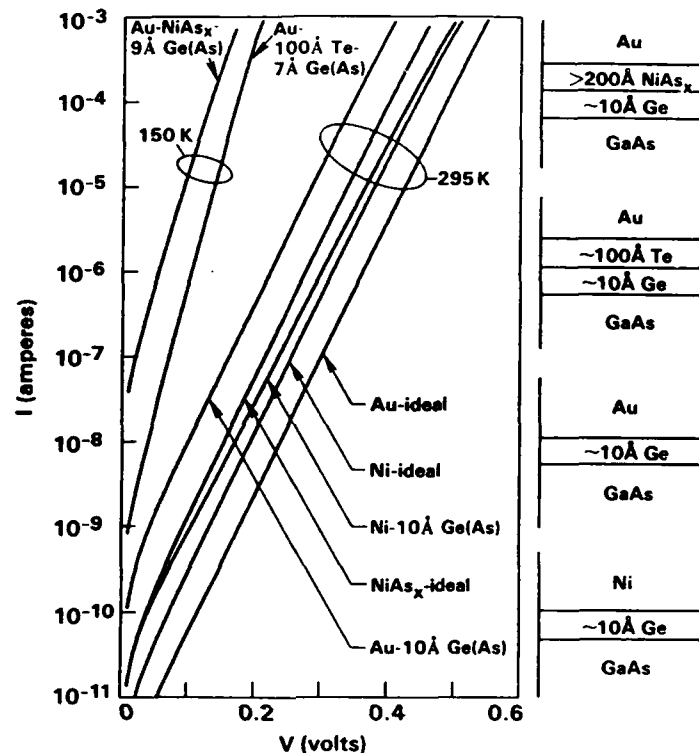


Fig. 8 Representative I-V data for a selection of contacts to GaAs that have a variety of structures (contact area =  $5.07 \times 10^{-4} \text{ cm}^2$ ). Multilayered contact structures are shown schematically on right.

The  $\text{NiAs}_x$ -ideal and the Au-100 Å Te contacts have  $\phi_B = 0.79\text{-}0.80 \text{ eV}$ , which corresponds to  $E_F^{\dagger} = 0.63\text{-}0.64 \text{ eV}$ ; this value of  $E_F^{\dagger}$  is essentially that of the clean GaAs surface. Thus,  $\text{NiAs}_x$  and Te have no effect on the Ge-GaAs interface electronic structure while also providing a conducting electrical contact (other nonmetal conductors with this property are likely).

In a careful electron microscopy investigation<sup>33</sup> of alloyed AuGeNi contacts,  $\rho_C$  was found to depend on the relative contact areas of several  $\text{Ni}_2\text{GeAs}$ ,  $\text{NiAs}$ , and  $\text{Au}(\text{Ga,As})$  phases. It was concluded that a low  $\rho_C$  is achieved when the  $\text{Ni}_2\text{GeAs}$  phase dominates because of heightened Ge indiffusion while a higher  $\rho_C$  occurs when Au areas



predominate. The present results suggest an alternate explanation: the Ni<sub>2</sub>GeAs and NiAs phases may actually be separated from the GaAs by a very thin layer (not yet observed) of interface Ge and are thus associated with a low  $\phi_B$  (~ 0.25-0.4 eV); the Au phase is associated with a high  $\phi_B$  (~ 0.7-0.9 eV). Consequently, with this model, the minimum  $\rho_C$  for an alloyed AuGeNi ohmic contact is obtained when the interface area of phases associated with a low  $\phi_B$  is greatest.

The large variation in  $\phi_B$ , from ~ 0.25 to 0.9 eV, for the different model interface structures suggests that low  $\rho_C$  nonalloyed ohmic contacts that use Au, Ge, and Ni can be made to n<sup>+</sup>-GaAs ( $N_D > 5 \times 10^{18} \text{ cm}^{-3}$ ) if interface composition is controlled to minimize  $\phi_B$ . For example, a properly fabricated Au-NiAs<sub>x</sub>-Ge(As) contact should have a low  $\phi_B$  over the entire contact area. The ~ 0.65 eV range in  $\phi_B$  also has implications for GaAs Schottky barrier models in that  $\phi_B$  at GaAs interfaces cannot be assumed a priori to be restricted to values of ~ 0.7-0.9 eV.

#### 4.1.3 TLM Measurements

As noted in Section 4.1.2, a properly fabricated Au-NiAs<sub>x</sub>-Ge(As) contact to n-GaAs should have a low  $\phi_B$  over the entire contact area and would be expected to exhibit a low  $\rho_C$ . A contact that consisted of 10<sup>3</sup>Å Au - ~ 500Å NiAs<sub>x</sub> - 10Å Ge(As) was fabricated on an MBE sample with a 1500Å n-type GaAs layer ( $N_D = 2.3 \times 10^{18} \text{ cm}^{-3}$ ). The Ge(As) was deposited at 250°C. XPS measurements obtained following the 10Å Ge(As) deposition indicated that  $E_F^i$  was 1.0 eV which gives  $\phi_B = 0.43 \text{ eV}$ .

An array of TLM test patterns was defined as described in Section 2.2.2. The data plotted in Fig. 9 are the average of data obtained from five patterns (there was only a very minor variation in the sample-to-sample data). R was measured at a current of 1 mA (sample ohmic behavior was confirmed by repeating a measurement at 0.1 mA with no change in measured R observed). The R vs L data have been least squares fit to a straight line to determine  $R_S$  and  $L_T$ . As discussed previously,  $\rho_C = R_S L_T^2$ . The uppermost plot in Fig. 9 is for the as-formed contacts. The three subsequent data sets are after 5 min rapid thermal anneals (in argon) at 300, 400 and 500°C, respectively. The values of  $\rho_C$  derived from these data are listed in Table 3. The sharp decrease in  $\rho_C$  after



SC5485.FR

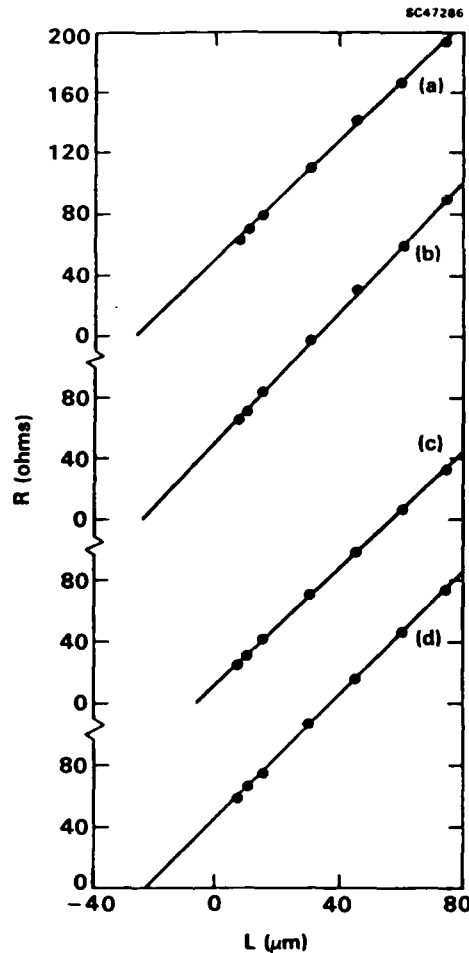


Fig. 9 TLM measurements for a  $10^3 \text{ \AA}$  Au- $500 \text{ \AA}$  NiAs<sub>x</sub>- $10 \text{ \AA}$  Ge(As) ohmic contact to n-GaAs ( $2.3 \times 10^{18} \text{ cm}^{-3}$ ). Test pattern is shown schematically in Fig. 4. (a) Initially fabricated sample, (b) annealed  $300^\circ\text{C}$ , 5 min, (c) annealed  $400^\circ\text{C}$ , 5 min, and (d) annealed  $500^\circ\text{C}$ , 5 min.

the  $400^\circ\text{C}$  anneal may be attributed to Ge indiffusion causing an increase in n-type doping near the contact interface. The increase in  $\rho_c$  after the  $500^\circ\text{C}$  anneal may be due to Au indiffusion through the NiAs<sub>x</sub> that causes an increase in  $\phi_B$  at the Ge-GaAs interface, which would act to cancel the lowering of  $\rho_c$  by any Ge indiffusion; discoloration of the Au metallization was noted after this anneal. A full understanding of this variation in  $\rho_c$  with annealing, however, requires further study.



Table 3  
TLM Results for  $10^3 \text{ \AA}$  Au - -  $500 \text{ \AA}$  NiAs<sub>x</sub> -  $10 \text{ \AA}$  Ge(As)  
Ohmic Contact to n-GaAs (100)

Anneal Temperature (°C)	$R_s$ ( $\Omega \square^{-1}$ )	$L_T$ ( $\mu\text{m}$ )	$\rho_c^b$ ( $\Omega\text{-cm}^2$ )	Extrapolated <sup>c</sup>	Extrapolated <sup>c</sup>
				$N_D = 1 \times 10^{19} \text{ cm}^{-3}$ ( $\Omega\text{-cm}^2$ )	$N_D = 5 \times 10^{19} \text{ cm}^{-3}$ ( $\Omega\text{-cm}^2$ )
Initial	240	13.3	$4.3 \times 10^{-4}$	$3 \times 10^{-6}$	$2 \times 10^{-7}$
300 <sup>a</sup>	265	12.1	$3.9 \times 10^{-4}$	---	---
400 <sup>a</sup>	237	3.11	$2.3 \times 10^{-5}$	---	---
500 <sup>a</sup>	249	11.5	$3.3 \times 10^{-4}$	---	---

a - annealed 5 min in argon

b - measured experimentally on  $N_D = 2.3 \times 10^{18} \text{ cm}^{-3}$  sample

c - extrapolation based on model of Ref. 34

Because practical nonalloyed ohmic contacts should be formed on heavier doped material than was used in the present case, extrapolated values of  $\rho_c$  at higher values of  $N_D$  are also given in Table 3. We obtained these predicted values by assuming a simplified model in which  $\rho_c$  is approximated in the form  $\rho_c - \exp(C\phi_B N_D^{-1/2})$ . A value for the constant C of  $3.4 \times 10^{-10}$  was derived from a curve ( $\phi_B = 0.6 \text{ eV}$ ) calculated in the tunneling model given in Ref. 34. This value of C and  $\phi_B = 0.43 \text{ eV}$  were used to extrapolate the measured value of  $\rho_c = 4.3 \times 10^{-4} \Omega\text{-cm}^2$  at  $N_D = 2.3 \times 10^{18} \text{ cm}^{-3}$ .

#### 4.2 Si Overlayers

As indicated in Section 4.1.1, the interface heterojunction band alignment characteristics appear to be responsible for the limits to the range of  $E_F^{\uparrow}$  values observed at the Ge/GaAs contacts. Because Si has a larger band gap than Ge, a wider range of  $E_F^{\uparrow}$  values might be obtained for UTHL contacts utilizing Si. Improved thermal stability might also be expected for Si contacts. Section 4.2.1 describes  $E_F^{\uparrow}$  measurements for Si UTHL contacts to n-GaAs and Section 4.2.2 reports I-V and C-V characterization of these contacts.



#### 4.2.1 $E_F^{\uparrow}$ Measurements

The range over which  $E_F^{\uparrow}$  in n-GaAs could be varied by using heavily doped n- or p-type Si overlayers was investigated. The Si overlayer thickness was in the 10-30Å range. Large  $E_F^{\uparrow}$  values were obtained by using heavily n-type doped Si layers (P or As dopants) while small  $E_F^{\uparrow}$  values were observed by using p-type doped Si layers (Ga or B dopants).

Si layers of ~ 10-30Å thickness were deposited at ~ 0.1Å/s onto clean GaAs surfaces held between 200 and 350°C (measurement of layer thickness was by noting the attenuation of the As3d peak from the underlying GaAs). For the B-doped Si layers, designated Si(B), material from the Si source was evaporated in vacuum. The procedure for the Ga-doped layers, Si(Ga), was somewhat more complex. The same Si source as for the Si(B) layers was used. Gallium was introduced into the Si by depositing a monolayer of Ga during the first few seconds of Si growth. This amount of Ga is more than can be incorporated into the Si in the thickness range used, which ensures that sufficient Ga is available to produce degeneracy. The most consistent low  $E_F^{\uparrow}$  Si(Ga)-GaAs interfaces were obtained when the chamber was back-filled with ~  $2 \times 10^{-6}$  Torr  $H_2$  during the Si deposition. Evidently, the hydrogen assists in the p-type doping process by minimizing the number of electrically active deep levels in the Si, but the precise mechanism(s) involved is not obvious. Silicon layers with incorporated P or As, Si(P) and Si(As), were obtained by evaporation of lightly n-type (P) Si in an ~  $2 \times 10^{-6}$  Torr  $P_2$  or  $10^{-7}$  Torr  $As_4$  background pressure.

Figure 10 shows representative As3d core level spectra to demonstrate the range in  $E_F^{\uparrow}$  that results from Si(P), Si(B), and Si(Ga) overlayers deposited onto clean GaAs (100) surfaces (peak heights are normalized). The upper two peaks are for the same sample. Thus, the vertical line that indicates the center (midpoint of the width at half-maximum) of the clean surface As3d peak at  $E_{As3d} = 41.52$  eV corresponds to  $E_F^{\uparrow}(\text{clean}) = 0.78$  eV. Deposition of a 14Å Si(P) overlayer onto this clean surface results in a 0.30 eV increase in binding energy to  $E_{As3d} = 41.82$  eV, which is a  $E_F^{\uparrow}$  increase to  $E_F^{\uparrow} = 1.08$  eV. In contrast, overlayers of Si(B) (third peak,  $E_{As3d} = 41.24$  eV) and Si(Ga) (bottom peak,  $E_{As3d} = 41.07$  eV) have a decrease in  $E_B$  relative to the clean surface, which is thus a  $E_F^{\uparrow}$  decrease to 0.50 and 0.33 eV, respectively.

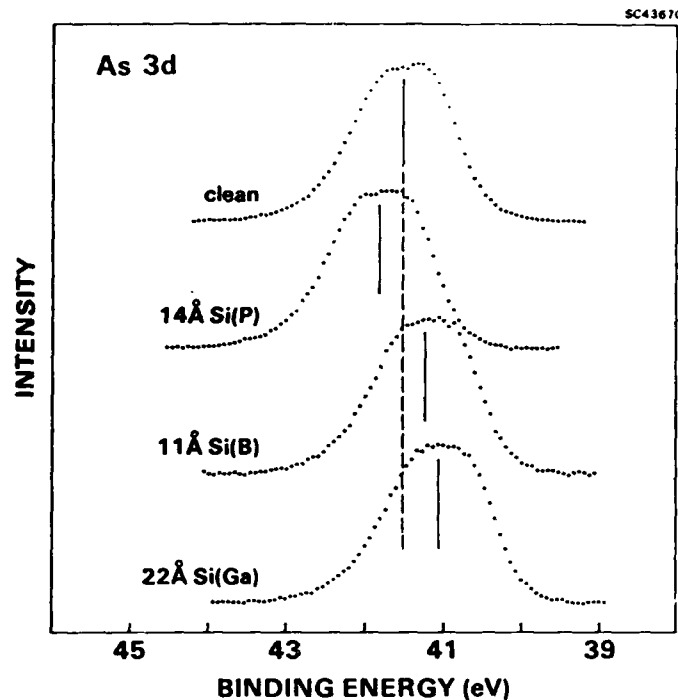


Fig. 10 XPS As3d core level spectra for thin p-type and thin n-type Si layers deposited on clean n-type GaAs(100) surfaces.

The Ga3d core level peak was used to characterize the Si(As) overlayer on n-GaAs to avoid possible overlap of As3d lines from the GaAs substrate and the overlayer. These data are shown in Fig. 5(f) for a 14 Å layer of Si deposited at 250°C.

Table 4 lists  $E_F^{\dagger}$  data for a number of samples in which Si(Ga), Si(B), Si(P), and Si(As) overlayers were deposited onto clean GaAs surfaces. The maximum range in  $E_F^{\dagger}$  for the Si-GaAs interfaces in Table 4 is 0.90 eV.

Low  $E_F^{\dagger}$  (high  $\phi_B$ ) values have been obtained both with Ga and B heavily doped Si layers and high  $E_F^{\dagger}$  (low  $\phi_B$ ) values both with P and with As heavily doped layers (in principle, the Si layer should be degenerate and undepleted). Deposition temperatures between 200 and 350°C were used. A LEED pattern was observed for the 350°C growth which indicated epitaxy, but the lower temperature growths were either amorphous or polycrystalline. (LEED studies of Si growth on Si (100) have demonstrated epitaxy as low



Table 4  
Interface Fermi Energy  $E_F^{\uparrow}$  After Deposition of Various  
Thin Si Layers Which Contain n-Type or p-Type Impurities  
onto Clean n-Type GaAs(100) Surfaces

Impurity	Si Thickness <sup>a</sup> (Å)	$E_{As3d}^b$ (eV)	$E_{Ga3d}^c$ (eV)	$E_F^{\uparrow}$ (eV)
Ga	17	41.13	---	0.39
Ga	22	41.07	---	0.33
Ga	26	41.21	---	0.47
Ga	28	41.15	---	0.41
B	11 <sup>d</sup>	41.24	---	0.50
B	24 <sup>d</sup>	41.28	---	0.54
B	25 <sup>e</sup>	41.23	---	0.49
P	14	41.82	---	1.08
P	25	41.84	---	1.10
As	14	---	19.98	1.23

- a Except as noted, Si deposited at 250°C.
- b As3d binding energy in GaAs with Si overlayer.
- c Ga3d binding energy in GaAs with Si overlayer.
- d 200°C.
- e 350°C.

as 300°C<sup>35</sup>). Thus, neither a precise Si growth temperature (although the lower and upper limits have not been determined) nor a particular Si impurity are crucial. The large lattice mismatch of Si and GaAs and the generally nonepitaxial nature of the Si layers also show that the degree of Si-GaAs interface perfection is unimportant. The essential condition influencing  $E_F^{\uparrow}$  at the Si-GaAs interface is that the Si be heavily either n-type or p-type.

Some difficulty was encountered in growing sufficiently heavily p-type Si films. The results with the B dopant were erratic with the method employed and there were some samples where the Si-GaAs  $E_F^{\uparrow}$  was not low because the Si apparently failed to be heavily p-type. Although lower  $E_F^{\uparrow}$  values were obtained with Ga, this should not be considered an inherent limitation of using B as a dopant but rather a requirement for good control over the Si dopant incorporation process. In this respect, the procedure for the Ga-doped films yielded better consistency in producing low  $E_F^{\uparrow}$  interfaces, although



the importance of the hydrogen background needs to be clarified. On the other hand, heavily n-type Si by P or As incorporation was readily obtained. Under the conditions used, the Si(P) layer had a large P excess detected by XPS; the amount of P can probably be controlled by changing the level of P overpressure or the substrate temperature.

The  $E_F^{\uparrow}$  data from Table 4 are plotted in Fig. 11. Also shown in this figure by dashed lines are the  $E_V$  and  $E_C$  positions of Si measured at Si/GaAs<sup>36</sup> heterojunction interfaces. Similar to the Ge overlayer results discussed in Section 4.1.1, the range in  $E_F^{\uparrow}$  values observed for Si overlayers seems to be bounded by the Si band gap. A range of 0.76 eV in  $E_F^{\uparrow}$  was observed for n- or p-type Ge layers on n-GaAs in Table 1. This range is similar to the 0.66 eV band gap of Ge and consistent with the Ge-GaAs heterojunction band lineup. A range of 0.9 eV in  $E_F^{\uparrow}$  was observed for n- or p-type Si layers on n-GaAs in Table 4. This range is somewhat less than would be predicted by the 1.12 eV crystalline Si band gap. Thus, an additional increase in  $E_F^{\uparrow}$  range at Si/GaAs interfaces of ~ 0.2 eV is probable by refinement of the Si deposition process.

It is usually assumed that the fairly narrow range of pinning positions observed at most GaAs interfaces is associated with acceptor and donor interface states closely spaced in energy.<sup>12,37</sup> The results of this work suggest that these states can be saturated with carriers from a heavily doped semiconductor overlayer so as to move  $E_F^{\uparrow}$  from the GaAs pinning level to near the dopant level in the overlayer (i.e., near the overlayer band edges). Thus, the band alignment characteristics of the Ge/GaAs and Si/GaAs heterojunction interfaces are what determines  $E_F^{\uparrow}$  at a UTHL contact.

In Section 4.1.2, metal deposition on UTHL contacts that involved Ge was shown to affect  $E_F^{\uparrow}$ . Experiments were carried out to determine variations in  $E_F^{\uparrow}$  after thin (~ 10-20Å) metal depositions on Si overlayers. The results of XPS measurements on As3d core levels are shown in Fig. 12 for Au and Ti depositions on Si(Ga) overlayers. The top three spectra are for sequential treatments to the same sample; the bottom peak is for the indicated two overlayers (the peak heights are normalized). The vertical line indicates the center (half width at half maximum) of the As3d peak. Deposition of 22Å of Si(Ga) onto the clean n-GaAs surface caused an 0.51 eV decrease of the As3d binding energy to 41.07 eV which corresponds to  $E_F^{\uparrow} = 0.33$  eV (compare the upper two peaks in Fig. 12). Similar  $E_F^{\uparrow}$  data for other Si(Ga) and Si(P) overlayer samples are given in

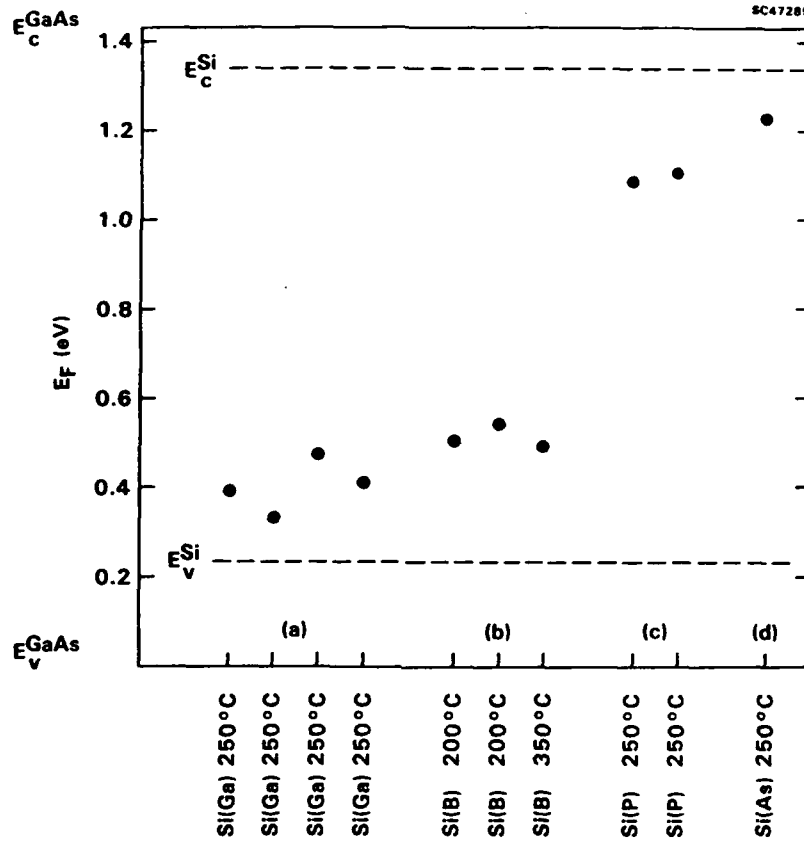


Fig. 11 Summary of several  $E_F^1$  measurements with Si overlayers. Overlayer thicknesses ranged from 11 to 28Å and are given in Table 4. Conditions used to incorporate dopants are specified in text. Silicon deposition temperatures are noted in figure. Dopants used were (a) Ga, (b) B, (c) P and (d) As.

Table 5. As shown in the third spectrum of Fig. 12, deposition of an ~ 9Å thick Au overlayer essentially did not change  $E_F^1$  for the 22Å Si(Ga) sample;  $E_F^1$  in this case was 0.32 eV (see Table 5). Similarly, the bottom As3d peak at 41.12 eV ( $E_F^1 = 0.38$  eV) is for a 15Å Ti overlayer on the 17Å Si(Ga)-GaAs interface. Thus, deposition of Au or Ti does not increase the low  $E_F^1$  value established by the Si(Ga) layer. Deposition of Au onto Si(P) overlayer samples, however, caused an ~ 0.1 eV decrease in  $E_F^1$ . A large, ~ 1 eV, barrier





( $\phi_B = 1.43 \text{ eV} - E_F^1$ ) is therefore predicted for thick contacts to Si(Ga)-GaAs and a small  $\sim 0.4 \text{ eV}$  barrier for contacts to Si(P)-GaAs.

The  $\sim 0.1 \text{ eV}$  decrease in  $E_F^1$  observed for Au deposited on Si(P)-GaAs samples may occur for other metals. For ohmic contact applications to n-GaAs, it may be desirable to avoid this decrease. It is likely that the highest  $E_F^1$  at Si(n-type)-GaAs interfaces can be retained by interposition of a thin nonmetal electrical conductor between the contact metal and the Si (n-type)-GaAs interface. This was the approach used to maintain high  $E_F^1$  values at Ge(As)-GaAs UTHL contacts for example by using a  $\text{NiAs}_x$  conducting diffusion barrier layer (see Section 4.1.2).

#### 4.2.2 Electrical Characterization of Contacts

Thick ( $\sim 10^3 \text{ \AA}$ ) metal layer contacts were also formed on  $\sim 20 \text{ \AA}$  Si-GaAs samples to allow I-V and C-V measurements. Representative I-V data for thick metal Cr-28 $\text{ \AA}$  Si(Ga) and Ti-17 $\text{ \AA}$  Si(Ga) contacts are plotted in Fig. 13. Data for Au-22 $\text{ \AA}$  Si(Ga) contacts were also obtained but are not shown because of overlap with the Cr-Si(Ga) data. For comparison, I-V data for ideal contacts of these metals (metal deposited onto a clean n-GaAs surface) are also shown. These data were analyzed by using the thermionic emission model and results are given in Table 6. In several cases, XPS was used to measure the barrier height ( $\phi_B^{\text{XPS}}$ ) on thin metal-Si-GaAs samples prior to deposition (in situ) of the thick metal ( $\sim 10^3 \text{ \AA}$ ) overlayers. The  $\phi_B^{\text{XPS}}$  values are also given in Table 6. The significant increase in  $\phi_B$  for the metal-Si(Ga) contacts compared to the respective ideal contacts is obvious from Fig. 13 and Table 1. In addition, the metal-Si(Ga)  $\phi_B$  is independent of the contact metal, which is in contrast with the ideal contacts.

The variation in I-V characteristics that can be achieved by changing the doping characteristics of the thin Si layer is demonstrated in Fig. 14. Representative I-V data for thick metal Au-22 $\text{ \AA}$  Si(Ga), Cr-24 $\text{ \AA}$  Si(B), and Au-25 $\text{ \AA}$  Si(P) contacts are shown. Again for comparison, data for ideal contacts are also presented. A significant increase in  $\phi_B$  is apparent for Si(Ga) and Si(B) UTHL contacts as is a significant decrease for the Si(P) contact. Table 6 gives the average  $n$  and  $\phi_B^{\text{IV}}$  measured for these contacts.

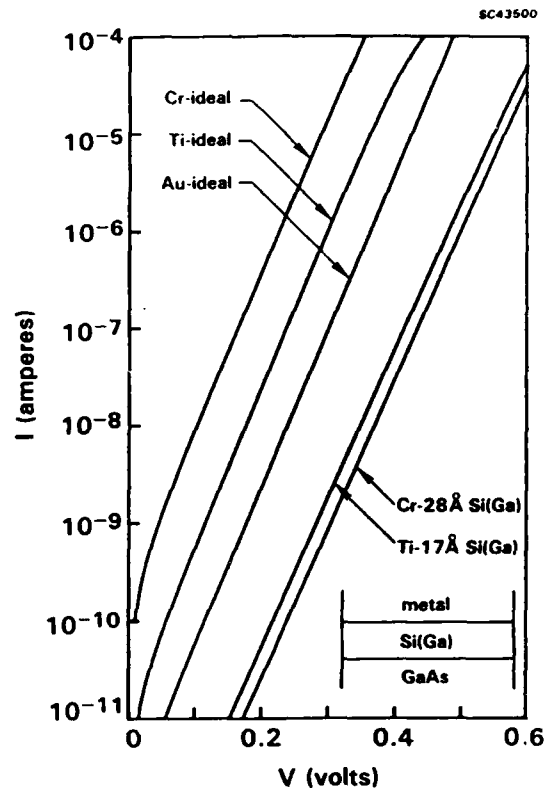


Fig. 13 Representative I-V data for Cr-Si(Ga) and Ti-Si(Ga) contacts compared to corresponding ideal contacts (Au-Si(Ga) data not shown because of overlap with Cr-Si(Ga) data). Contact area =  $5.07 \times 10^{-4}$  cm<sup>2</sup>.

Representative C-V data for the Au-Si(Ga), Au-Si(P), and Au-ideal contacts are shown in the  $1/C^2$  vs V plots of Fig. 15. The C-V data for the other contact samples were similar in form. The average  $\phi_B^{CV}$  measured for each sample is listed in Table 6.

The I-V and C-V electrical measurements of  $\phi_B$  on thick contacts are consistent with the  $E_F^1(\phi_B)$  values measured by XPS with thin overlayers. Why  $\phi_B^{CV}$  is  $\sim 0.1$  eV  $> \phi_B^{IV}$  for the Cr and Ti contacts with Si(Ga) and Si(B) interlayers and an opposite sign difference of 0.07 eV is measured for the Au-Si(P) contact is not clear. The agreement between I-V and C-V values for the Au-Si(Ga) contact, however, indicates that such disparities are not an intrinsic characteristic of all metal-Si-GaAs contacts. Since the



Table 6  
Schottky Barrier Height  $\phi_B$  of Metal Contacts to GaAs  
that Include a Thin Si Interface Layer

Contact	XPS $\phi_B$ (eV)	n	IV <sup>a</sup> $\phi_B$ (eV)	CV $\phi_B$ (eV)
Au-22Å Si(Ga)	1.11	1.08	1.01	1.01
Cr-28Å Si(Ga)	----	1.11	0.99	1.10
Ti-17Å Si(Ga)	1.05	1.11	0.98	1.14
Ti-26Å Si(Ga)	1.01	1.10	0.97	1.06
Cr-24Å Si(B)	----	1.09	0.92	0.97
Au-14Å Si(P)	0.43	1.05	0.53	0.46
Au-25Å Si(P)	0.42	1.06	0.49	0.42
Au-ideal		1.05	0.89	
Cr-ideal		1.05	0.76	
Ti-ideal		1.04	0.83	

a Includes image force correction.

discrepancies are comparatively minor and may be an artifact of the C-V model, for discussion purposes, the I-V values will be used: for the thick Si(Ga) contacts  $\phi_B = 1.0$  eV; for the Cr-Si(B) contact  $\phi_B = 0.92$  eV; and for the Au-Si(P) contact  $\phi_B = 0.5$  eV. The I-V ideality factors are acceptably small. Compared to the respective ideal contacts, the  $\phi_B$  increase ranges from 0.1 eV (Au) to 0.23 eV (Cr) while the  $\phi_B$  decrease for Au is 0.4 eV. By use of the metal-Si(p-type)-GaAs structure,  $\phi_B$  can be made essentially independent of the contact metal.

The XPS measurements show that the wide range in  $\phi_B$  for these metal-Si contacts is a direct consequence of the wide range in  $E_F^{\uparrow}$  that can be induced at the Si-GaAs interface. This mechanism for achieving a wide range in  $\phi_B$  is thus quite unlike methods<sup>38</sup> in which a variable effective barrier height is created by tailoring the impurity profile, and therefore the potential, in the GaAs depletion region adjacent to the metal-GaAs interface where  $\phi_B$  itself remains constant.

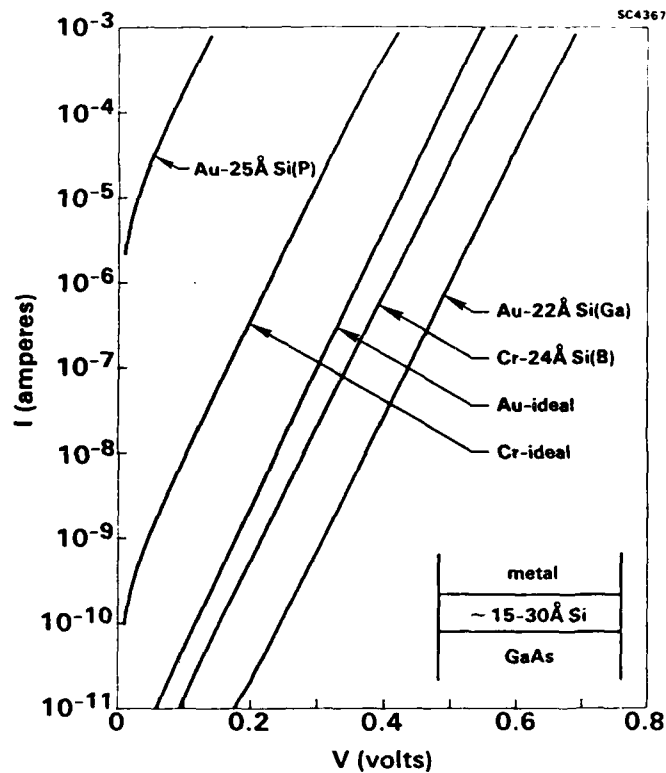


Fig. 14 Representative I-V data for Au-Si(Ga), Cr-Si(B), and Au-Si(P) contacts compared to Au-ideal and Cr-ideal contacts (contact area =  $5.07 \times 10^{-4}$  cm<sup>2</sup>).

Our results offer a possible basis for understanding the high barrier measured for thick amorphous Si-Ge-B contacts<sup>39</sup> to GaAs. If heavily p-type material in intimate contact with the GaAs was produced by the chemical vapor deposition process that was used, then  $E_F^1$  may have been unpinned in the same way as at the Si(Ga)-GaAs interfaces described here.

The low barrier contacts obtained by using Si(n-type) interfaces should be useful in the design of ohmic contacts to n-GaAs. Because a high  $\phi_B$  contact to n-GaAs should correspond to a low  $\phi_B$  contact to p-GaAs, the high barrier contacts obtained by using Si(p-type) interlayers should be of use in the design of nonalloyed ohmic contacts to p-GaAs.

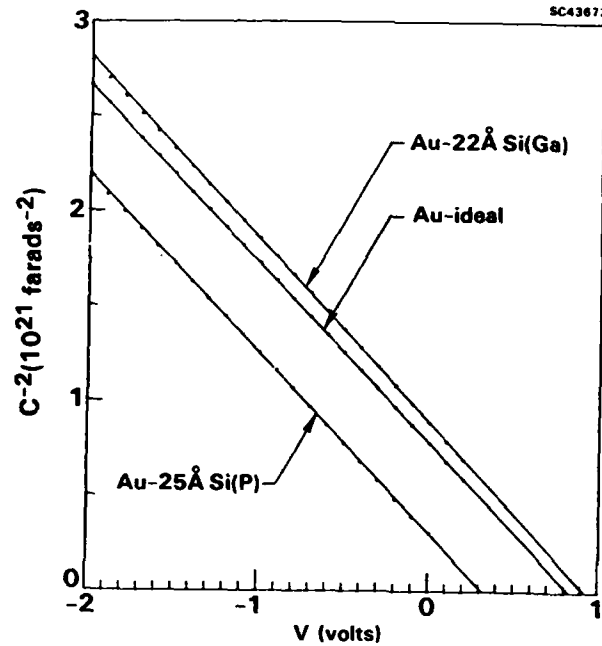


Fig. 15 Representative C-V data for Au-Si(Ga), Au-Si(P), and Au-ideal contacts. Line is least squares fit extrapolation to  $V_i$ .

Like GaAs, other III-V compound semiconductors (InP, for example) tend to have a limited range of  $\phi_B$  for metal contacts. If the mechanism that restricts  $\phi_B$  in other III-V semiconductors is analogous to that for GaAs, the present results suggest that appropriately doped Si or Ge interlayers will also increase the  $\phi_B$  range for metal contacts to such semiconductors.



## 5.0 SUMMARY

A new approach for fabricating nonalloyed ohmic contacts to GaAs has been developed. The approach uses heavily doped ultrathin heterojunction layers (UTHL) of Ge or Si in contact with GaAs to alter the GaAs interface Fermi level position ( $E_F^i$ ); typical Ge or Si layer thicknesses are 15-30Å.

The most common method of forming an ohmic contact to GaAs involves tunneling across a thin barrier region. For a tunneling ohmic contact, the specific contact resistance ( $\rho_c$ ) depends exponentially on Schottky barrier height ( $\phi_B$ ). Thus, if the barrier height is reduced, a substantial reduction in  $\rho_c$  can be achieved. Most metal contacts to n-GaAs exhibit  $\phi_B$  in the 0.7-0.9 eV range which corresponds to a 0.7-0.5 eV range in  $E_F^i$ . By using thin Ge or Si layers heavily doped n-type with As or P,  $E_F^i$  values between 1.0 and 1.2 could be obtained. For thin Si layers heavily doped p-type with Ga or B, or for vacuum-deposited Ge layers (normally heavily p-type),  $E_F^i$  values in GaAs ranged from 0.3 to 0.5 eV. Thus, it is possible to substantially extend the range of  $\phi_B$  that can be obtained at a n-GaAs interface.

If the high  $E_F^i$  (low  $\phi_B$ ) n-GaAs interfaces can be retained in thick metallizations, they should be useful for ohmic contacts. Low barrier UTHL contacts to n-GaAs were demonstrated by both I-V and C-V measurements. To retain the high  $E_F^i$  values at Ge(Ga) - GaAs interfaces, it was necessary to interpose a thin nonmetal electrically conducting barrier (e.g., NiAs<sub>x</sub>) between the contact metal and the Ge(As) layer to prevent the metal from reaching the GaAs interface. Although metallization of Si(P)-GaAs interfaces did not drastically reduce  $E_F^i$ , it is likely that the highest  $E_F^i$  at Si(n-type)-GaAs interfaces can also best be retained by using a nonmetallic electrically conducting barrier layer. With a nonalloyed Au-NiAs<sub>x</sub>-GaAs UTHL contact structure, a  $\rho_c = 4 \times 10^{-4} \Omega\text{-cm}^2$  was measured for a GaAs sample with donor concentration ( $N_D$ ) =  $2 \times 10^{18} \text{ cm}^{-3}$ ; extrapolating this result to  $N_D = 5 \times 10^{19} \text{ cm}^{-3}$ , which is more typical of a practical n-GaAs ohmic contact, suggests that  $\rho_c = 2 \times 10^{-7} \Omega\text{-cm}^2$  would be obtained for the UTHL contact. At 400°C and above, the Au-NiAs<sub>x</sub>-GaAs UTHL contact was not stable which indicates the need to use thermodynamically stable components in future UTHL contact designs for high temperature applications.



High barrier UTHL contacts to n-GaAs were demonstrated by I-V and C-V measurements. For metallizations to Si(Ga)-GaAs UTHL contacts, an unusually large  $\phi_B$  of  $\sim 1.0$  eV was observed. Because a large  $\phi_B$  to n-GaAs should correspond to a low  $\phi_B$  to p-GaAs, the UTHL method of  $E_F^\dagger$  modification should be applicable for p-GaAs ohmic contact design.

It is usually assumed that the fairly narrow range of pinning positions observed at most GaAs interfaces is associated with a large concentration of acceptor and donor states closely spaced in energy near midgap. The variation in GaAs  $E_F^\dagger$  obtained by using heavily doped Ge or Si layers suggests that these states can be saturated with carriers from a heavily doped semiconductor overlayer so as to move  $E_F^\dagger$  from the usual mid gap GaAs pinning level to near the dopant level in the overlayer (i.e., near the overlayer band edges). Thus, the band alignment characteristics of the Ge/GaAs and Si/GaAs heterojunction interfaces determine  $E_F^\dagger$  at a UTHL contact.

The generality of the UTHL method for modifying  $E_F^\dagger$  was demonstrated by forming both low and high  $\phi_B$  contacts to n-GaAs. While low  $\phi_B$  interfaces have ohmic contact applications, high  $\phi_B$  interfaces have FET gate applications. The UTHL contact has a  $\phi_B$  that is virtually independent of contact metallization. The proposed heterojunction model for UTHL contact formation offers a means to design stable high temperature contacts by using materials expected to be thermodynamically stable at elevated temperatures. Like GaAs, other III-V semiconductors (e.g., InP) tend to have a limited range of  $\phi_B$  for metal contacts. If the mechanism that limits this range is analogous to GaAs, the UTHL contact method may have more general applicability.



## 6.0 REFERENCES

1. P.M. Asbeck, M.F. Chang, K.-C. Wang, D.L. Miller, G.J. Sullivan, N.H. Sheng, E. Sovero and J.A. Higgins, *IEEE Trans. on Microwave Theory and Tech.* MTT-35, 1462 (1987).
2. N. Braslau, *J. Vac. Sci. Technol.* A4, 3085 (1986).
3. N. Braslau, J.B. Gunn and J.L. Staples, *Solid State Electron.* 10, 381 (1967).
4. T.S. Kuan, P.E. Batson, T.N. Jackson, H. Rupprecht and E.L. Wilkie, *J. Appl. Phys.* 54, 6952 (1983).
5. T.K. Higman, M.A. Emanuel, J.J. Coleman, S.J. Jeng and C.M. Wayman, *J. Appl. Phys.* 60, 677 (1986).
6. M. Murakami, K.D. Childs, J.M. Baker and A. Callegari, *J. Vac. Sci. Technol.* B4, 903 (1986).
7. C.J. Palmstrom and D.V. Morgan, *Gallium Arsenide*, M.J. Howes and D.V. Morgan, eds., Wiley, Chichester, Chapt. 6 (1985), and references therein.
8. N. Braslau, *J. Vac. Sci. Technol.* 19, 803 (1981).
9. C.Y. Chang, Y.K. Fang and S.M. Sze, *Solid State Electron.* 14, 541 (1971).
10. J.V. Dilozenzo, W.C. Niehaus and A.Y. Cho, *J. Appl. Phys.* 50, 951 (1979).
11. See, e.g., C.E.C. Wood, *J. Vac. Sci. Technol.* 18, 772 (1981).
12. R.W. Grant, J.R. Waldrop, S.P. Kowalczyk and E.A. Kraut, *J. Vac. Sci. Technol.* 19, 477 (1981).
13. J. Massies, J. Chaplart, M. Laviron and N.T. Linh, *Appl. Phys. Lett.* 38, 693 (1981).
14. H. Brugger, F. Schäffler and G. Abstreiter, *Phys. Rev. Lett.* 52, 141 (1984).
15. P. Chiaradia, A.D. Katnani, H.W. Sang, Jr., and R.S. Bauer, *Phys. Rev. Lett.* 52, 1246 (1984).
16. J.R. Waldrop, *Appl. Phys. Lett.* 47, 1301 (1985).
17. S.D. Offsey, J.M. Woodall, A.C. Warren, P.D. Kirchner, T.I. Chappel and G.D. Pettit, *Appl. Phys. Lett.* 48, 475 (1986).
18. K. Siegbahn et al, *ESCA: Atomic, Molecular and Solid-State Structure Studied by Means of Electron Spectroscopy*, Almquist and Wiksells, Uppsala, 1967.
19. R.W. Grant, E.A. Kraut, S.P. Kowalczyk and J.R. Waldrop, *J. Vac. Sci. Technol.* B1, 320 (1983).
20. M.P. Seah and W.A. Dench, *Surf. Interface Anal.* 1, 2 (1979).



21. J.R. Waldrop, R.W. Grant and E.A. Kraut, J. Vac. Sci. Technol. B5, 1209 (1987).
22. F.R. McFeely, S.P. Kowalczyk, L. Ley, R.A. Pollak and D.A. Shirley, Phys. Rev. B7, 5228 (1973).
23. A.M. Goodman, J. Appl. Phys. 34, 329 (1963).
24. Reviewed in: B.L. Sharma, Semiconducting and Semimetals 15, 1 (1981).
25. S.P. Kowalczyk, R.W. Grant, J.R. Waldrop and E.A. Kraut, J. Vac. Sci. Technol. B1, 684 (1983).
26. A.D. Katnani, P. Chiaradia, H.W. Sang, Jr., and R.S. Bauer, J. Electron. Mater. 14, 25 (1985).
27. P. Chen, D. Bolmont and C.A. Sebenne, J. Phys. C 15, 6101 (1982).
28. J.R. Waldrop, E.A. Kraut, S.P. Kowalczyk and R.W. Grant, Surf. Sci. 132, 513 (1983).
29. J.E. Davey, Appl. Phys. Lett. 8, 164 (1966).
30. R.A. Stall, C.E.C. Wood, K. Board, N. Dandekar, L.F. Eastman and J. Devlin, J. Appl. Phys. 52, 4062 (1981).
31. G.Y. Robinson, Solid State Electron. 18, 331 (1975).
32. M. Ogawa, J. Appl. Phys. 51, 406 (1980).
33. T.S. Kuan, P.E. Batson, T.N. Jackson, H. Rupprecht and E.L. Wilkie, J. Appl. Phys. 54, 6952 (1983).
34. W.J. Boudville and T.C. McGill, J. Vac. Sci. Technol. B3, 1192 (1985).
35. R.N. Thomas and M.H. Francombe, Appl. Phys. Lett. 11, 108 (1967).
36. R.S. List, J. Woicik, P.H. Mahowald, I. Lindau, and W.E. Spicer, J. Vac. Sci. Technol. A5, 1459 (1987).
37. W.E. Spicer, I. Lindau, P. Skeath and C.Y. Su, J. Vac. Sci. Technol. 17, 1019 (1980).
38. See, e.g., J.M. Shannon, Solid State Electron. 19, 537 (1976).
39. M. Suzuki, K. Murase, K. Asai and K. Kurumada, Jpn. J. Appl. Phys. 22, L709 (1983).



## 7.0 APPENDIX

This appendix contains four publications, three conference abstracts and two patent disclosures that were based on work supported by this contract.

### Publications

1. "Correlation of Interface Composition and Barrier Height for Model AuGeNi Contacts to GaAs," J.R. Waldrop and R.W. Grant, Appl. Phys. Lett. 50, 250 (1987).
2. "Variation of n-GaAs(100) Interface Fermi Level by Ge and Si Overlayers," R.W. Grant and J.R. Waldrop, J. Vac. Sci. Technol. B5, 1015 (1987).
3. "Metal Contacts to GaAs with 1 eV Schottky Barrier Height," J.R. Waldrop and R.W. Grant, Appl. Phys. Lett. 52, 1794 (1988).
4. "Wide Range of Schottky Barrier Height for Metal Contacts to GaAs Controlled by Si Interface Layers," J.R. Waldrop and R.W. Grant, J. Vac. Sci. Technol. B6, 1432 (1988).

### Conference Abstracts

1. "Variations of GaAs(100) Interface Fermi Level for Model AuGeNi Ohmic Contacts," R.W. Grant and J.R. Waldrop, Physics and Chemistry of Semiconductor Interfaces Conference, Salt Lake City, UT, Jan 27-29, 1987.
2. "Large Range of Interface Fermi Energy in n-GaAs(100) Induced by Thin Si Layers," J.R. Waldrop and R.W. Grant, Physics and Chemistry of Semiconductor Interfaces Conference, Asilomar, CA, Feb 1-4, 1988.
3. "Effect of Si and Ge Interface Layers on the Schottky Barrier Height of Metal Contacts to GaAs," J.R. Waldrop and R.W. Grant, Materials Research Society Conference, San Diego, CA, April 24-29, 1989.



Patent Disclosures

1. "Design of Nonalloyed Ohmic Contacts with Low Barrier Heights," J.R. Waldrop and R.W. Grant.
2. "Method for Obtaining Metal Contacts with Large Schottky Barrier," J.R. Waldrop and R.W. Grant.

# Correlation of interface composition and barrier height for model AuGeNi contacts to GaAs

J. R. Waldrop and R. W. Grant

Rockwell International Corporation, Thousand Oaks, California 91360

(Received 23 July 1986; accepted for publication 2 December 1986)

Model contacts to GaAs that include nonalloyed layered structures of Au, Ge, and Ni in various combinations are used to establish a correlation between interface composition and large changes in barrier height  $\phi_B$ . The interface Fermi level  $E_F^i$  and chemistry during initial contact formation were investigated by x-ray photoemission spectroscopy; the corresponding  $\phi_B$  for the thick contact was obtained by current-voltage ( $I$ - $V$ ) measurement. The circumstances under which a thin ( $\sim 10$  Å) Ge layer at the GaAs interface can produce  $\phi_B = \sim 0.25$ – $0.4$  eV (as measured by  $I$ - $V$ ) are described. For all model contacts examined a  $\phi_B$  range from  $\sim 0.25$  to  $0.9$  eV is observed. This result questions the usual assumption of a relatively fixed  $\phi_B$  of  $\sim 0.8$  eV for the alloyed AuGeNi contact and offers an alternative explanation for the mechanism of ohmic contact formation. The conditions that define the exceptionally low  $\phi_B$  contacts provide a guide for the design of nonalloyed tunnel ohmic contacts.

The alloyed AuGeNi metallization<sup>1</sup> is widely used as an ohmic contact to  $n$ -type GaAs. The complex contact structure consists of several phases whose individual size and composition depend on the alloying time and temperature.<sup>2-5</sup> The familiar ohmic contact tunneling<sup>6</sup> model that gives<sup>7</sup>  $\rho_c \propto \exp(a\phi_B/N_D^{1/2})$ , where  $\rho_c$  is the specific contact resistance,  $\phi_B$  is the interface barrier height,  $N_D$  is the donor concentration in the GaAs ( $> 5 \times 10^{18}$  cm<sup>-3</sup>), and  $a = 5 \times 10^{10}$  cm<sup>-3/2</sup> eV<sup>-1</sup>, is troublesome to apply quantitatively to the alloyed contact. This difficulty arises from not knowing precisely either  $\phi_B$  or the effect of Ge, Au, or Ni indiffusion on  $N_D$ . It is usually assumed that  $\phi_B$  is inevitably  $\sim 0.7$ – $0.9$  eV because the Schottky barrier height<sup>8,9</sup> for most metal contacts to GaAs is in this range. According to this viewpoint  $\rho_c$  is reduced by maximizing  $N_D$ . However, for certain thin ( $\sim 10$ – $40$  Å) Ge overlayers on clean GaAs surfaces the interface Fermi energy  $E_F^i$  can be  $> 1$  eV.<sup>10,11</sup> Hence, if such a high  $E_F^i$  state (low  $\phi_B$ ) can be attained in a tunnel AuGeNi ohmic contact then  $\rho_c$  would be substantially reduced for a given  $N_D$ .

This letter reports an investigation of model AuGeNi contacts to GaAs that involve layered structures designed to correlate interface composition with  $\phi_B$ . The contacts were not alloyed to retain interfaces of controlled composition. The interface chemistry and  $E_F^i$  during initial contact formation were observed by x-ray photoemission spectroscopy (XPS); the corresponding  $\phi_B$  for a thick contact was obtained by current-voltage ( $I$ - $V$ ) measurement. Since the current transport for a tunnel contact depends on both  $\phi_B$  and  $N_D$ , GaAs with  $N_D$  appropriate for thermionic emission transport ( $< 10^{17}$  cm<sup>-3</sup>) was used to simplify the  $I$ - $V$  analysis.

The contact interfaces were prepared under ultrahigh vacuum conditions ( $10^{-10}$  Torr range base pressure) in an XPS system comprised of a HP5950A electron spectrometer ( $h\nu = 1486.6$  eV monochromatic x-ray source,  $\sim 16$  Å effective photoelectron escape depth) and attached custom sample preparation chamber. During initial contact formation XPS spectra of the Ga 3d and As 3d core level peaks in

the GaAs and of other core level peak spectra appropriate for a given interface composition were obtained.  $I$ - $V$  data were obtained in 0.01 V forward bias increments.

The GaAs (100) material is liquid encapsulated Czochralski grown  $n$  type ( $\sim 5 \times 10^{16}$  cm<sup>-3</sup> Se). To prepare a sample, the GaAs is etched in fresh 4:1:1 H<sub>2</sub>SO<sub>4</sub>:H<sub>2</sub>O<sub>2</sub>:H<sub>2</sub>O solution for  $\sim 30$  s to remove polishing damage, mounted on a Mo plate with In and immediately put into the XPS system. The  $\sim 10$  Å native oxide layer is removed by momentary heating, either in vacuum or in an As overpressure, to the minimum necessary temperature ( $\sim 550$  °C, which also forms an ohmic contact between the GaAs and the Mo plate). This thermally cleaned surface is ordered [displays a characteristic low-energy electron diffraction (LEED) pattern] and is shown by XPS to be free of oxygen, carbon, or other contaminants. The Ge, Au, and Ni were evaporated from W baskets; the As and Te sources were small quartz ovens. The NiAs layers were formed by depositing the Ni onto a room-temperature substrate in a  $10^{-7}$ – $10^{-6}$  Torr As overpressure [although XPS analysis indicates the resulting Ni and As layer is As rich, and thus a compound(s) of the form NiAs<sub>*x*</sub>, for simplicity it will be referred to as NiAs]. After XPS analysis of thin overlayers, a total overlayer thickness of  $> 2000$  Å was deposited. Circular  $2.54 \times 10^{-2}$  cm diameter contacts were defined by using photolithography and chemical etching.

The representative Ga 3d core level peak data plotted in Fig. 1 show how XPS was used to measure  $E_F^i$  and to monitor composition during interface formation. The upper three spectra are after sequential treatments to the same sample; the lower three are for three other samples with the indicated overlayer structure (peak heights are normalized). The upper inset in Fig. 2 shows the relationship between the interface Ga 3d core level binding energy in GaAs and  $E_F^i$ :  $E_F^i = E_{Ga\ 3d} - 18.80$  eV, where  $(E_{Ga\ 3d} - E_c) = 18.80 \pm 0.03$  eV is the energy difference<sup>12</sup> between the Ga 3d core level and the valence-band maximum. Note that the binding energy  $E_B$  scale is referenced to the sample Fermi energy  $E_F$  (other details on the use of XPS to measure  $E_F^i$  can be found

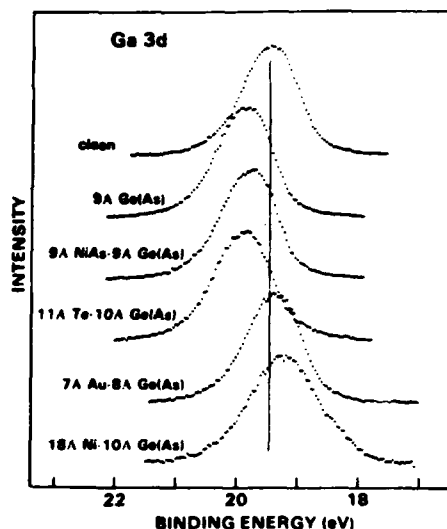


FIG. 1. XPS Ga 3d core level spectra for various thin overlayer structures on initially clean GaAs (100) surfaces. Upper three spectra are for successive depositions on the same sample.

elsewhere).<sup>13</sup> Thus, the vertical line in Fig. 1 that marks the center of the clean surface Ga 3d peak at 19.47 eV is for  $E_F^i(\text{clean}) = 0.67$  eV (the average for 16 samples is 0.66 eV, as indicated in Fig. 2).

After deposition of 9 Å of Ge onto the clean GaAs surface at 250 °C and in  $1 \times 10^{-7}$  Torr As overpressure the Ga 3d peak shifts 0.43 eV to higher binding energy (compare upper two peaks). This shift represents an increase in  $E_F^i$  to 1.10 eV. The  $E_F^i$  for a thin Ge overlayer on clean GaAs will be defined as  $E_F^i(\text{Ge})$ . Figure 2 gives the value of  $E_F^i(\text{Ge})$  for 13 different samples in which  $\sim 10$  Å of Ge was deposited onto clean GaAs (see lower inset) at several different substrate temperatures and As overpressure conditions. These  $E_F^i(\text{Ge})$  data are also tabulated in Table I.

For Ge deposited in a 200–325 °C temperature range under conditions where As incorporation occurs [designat-

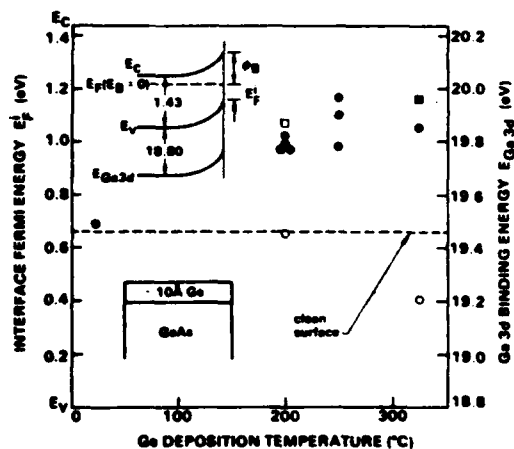


FIG. 2. Interface Fermi energy  $E_F^i(\text{Ge})$  for thin ( $\sim 10$  Å) Ge overlayers deposited on GaAs (100) surfaces at several different temperatures. The closed circles and square are for  $10^{-7}$  and  $10^{-6}$  Torr As overpressure during Ge evaporation, respectively; the open circles are for a GaAs surface cleaned and Ge deposited in vacuum; the open square is for GaAs cleaned in  $10^{-6}$  Torr As and Ge deposited in vacuum.

ed Ge(As)], which presumably makes the Ge  $n$  type,  $E_F^i(\text{Ge}) = 1.0$ – $1.2$  eV. A LEED pattern from the Ge was observed for these layers (with a high background at 200 °C). Room-temperature Ge deposition (no LEED pattern), or 200–325 °C Ge deposition on a vacuum cleaned surface without an As overpressure, yields  $E_F^i(\text{Ge}) = 0.4$ – $0.7$  eV.

The relation  $\phi_B = 1.43$  eV  $- E_F^i$  indicates that barriers in the 0.2–0.4 eV range can be achieved if the low band bending state (high  $E_F^i$ ) can be preserved upon deposition of additional contact material. For example, the third (from top) spectrum in Fig. 1 is for 9 Å of NiAs deposited onto the 9 Å Ge(As) overlayer where  $E_F^i(\text{Ge}) = 1.1$  eV. Essentially no change in the Ga 3d energy, and hence no change in  $E_F^i$ , occurs. To test the generality of this result another conductive nonmetal, Te, was used. When 11 Å of Te is deposited onto a Ge(As) overlayer with high associated  $E_F^i(\text{Ge})$  (fourth spectrum) there is also no change in  $E_F^i$ . The situation is dramatically different when either Au or Ni is deposited directly onto a high  $E_F^i(\text{Ge})$  Ge(As) overlayer (lower two spectra in Fig. 1). In each case  $E_F^i$  shifted from  $E_F^i(\text{Ge}) = \sim 1.1$  eV to  $E_F^i = \sim 0.7$  eV after the metal deposition; thus, the low barrier condition was removed (the low binding energy shoulder in the last peak is due to a Ni-GaAs chemical reaction).

Do the XPS measurements of  $E_F^i$  shifts correlate with the  $I$ - $V$   $\phi_B$  data for the same interfaces? To investigate this question several kinds of model thick contact structures were formed. The types that include Ge are shown on the right side of Fig. 3; in each case an initial Ge overlayer is followed (at room temperature) by the indicated deposi-

TABLE I. Correlation of interface composition and barrier height for model nonalloyed AuGeNi contacts to GaAs.

Interface structure	Ge depos. temp. (°C)	$E_F^i(\text{Ge})^a$ (eV)	$\phi_B^{b,c}$ (eV)	$n$
Au-NiAs-9 Å Ge(As)	200	0.98	0.31 <sup>d</sup>	1.27
Au-NiAs-11 Å Ge(As)	200	0.98	0.35 <sup>d</sup>	1.23
Au-NiAs-9 Å Ge(As)	250	1.10	0.39 <sup>d</sup>	1.11
Au-100 Å Te-10 Å Ge(As)	200	1.07	0.23 <sup>e</sup>	1.33
Au-100 Å Te-9 Å Ge(As)	250	1.16	0.39 <sup>d</sup>	1.08
Au-100 Å Te-7 Å Ge(As)	325	1.05	0.36 <sup>d</sup>	1.10
Au-10 Å Ge(As)	200	1.02	0.76	1.05
Au-8 Å Ge(As)	250	0.98	0.61	1.05
Au-9 Å Ge(As)	325	1.16	0.64	1.05
Ni-10 Å Ge(As)	200	0.99	0.81	1.11
Au-100 Å Te-9 Å Ge	200	0.65	0.65	1.06
Au-9 Å Ge	325	0.40	0.71	1.12
Au-100 Å Te <sup>f</sup>	...	...	0.79	1.02
NiAs-ideal	...	...	0.80	1.04
Ni-ideal	...	...	0.84	1.05
Au-ideal	...	...	0.89	1.05

<sup>a</sup> Ge overlayer only.

<sup>b</sup> Includes image force correction, see text.

<sup>c</sup> Measured at  $T = 295$  K unless noted.

<sup>d</sup>  $T = 150$  K.

<sup>e</sup>  $T = 100$  K.

<sup>f</sup> Reference 17.

tions. Not shown are structures without the Ge layer (designated ideal) where Au, Ni, or NiAs is deposited directly onto clean GaAs.

Figure 3 also shows representative  $I$ - $V$  data ( $T = 295$  or  $150$  K, the lower measurement temperature was necessary for low  $\phi_B$ ) that demonstrate the wide range in  $\phi_B$  which is associated with the different contact structures. The  $I$ - $V$  data were analyzed by use of the thermionic emission model<sup>14</sup> for a Schottky barrier:  $I = I_0 \exp(qV/nkT) [1 - \exp(-qV/kT)] A$ , where both the ideality factor  $n$  ( $n \sim 1.02$  at  $T = 295$  K is ideal; there is often, however, an increase in  $n$  at low  $T$ )<sup>14</sup> and  $I_0$  were determined by a least-squares fit. The barrier height  $\phi_B$  is extracted from  $I_0$  by  $I_0 = SA^* T^2 \times \exp[-q(\phi_B - \Delta\phi)/kT] A$ , where  $S$  is the contact area,  $A^* = 8.16$  is the effective Richardson constant, and  $\Delta\phi$  is the calculated<sup>14</sup> image force correction ( $\Delta\phi = +0.04$  eV for  $\phi_B > 0.7$  eV and  $+0.03$  eV for  $\phi_B < 0.7$  eV). Table I lists the average  $\phi_B$  and  $n$  values for the various interface structures ( $\sim$  seven contacts per sample,  $< \pm 0.01$  eV measurement uncertainty).

The Au-NiAs-Ge(As) and Au-Te-Ge(As) contacts that have a high  $E_g^+$  (Ge) ( $\sim 1.0$ – $1.2$  eV) also have a low  $\phi_B$  ( $\sim 0.25$ – $0.4$  eV). In contrast, the Au-Ge(As) and Ni-Ge(As) contacts that have a similarly high  $E_g^+$  (Ge) value have, without an intervening NiAs or Te layer, a high  $\phi_B$  ( $\sim 0.6$ – $0.8$  eV).<sup>15</sup> These values for  $\phi_B$  can be compared to those for the Au and Ni<sup>16</sup> ideal contacts,  $\phi_B$  (Au) =  $0.89$  eV and  $\phi_B$  (Ni) =  $0.84$  eV, and the two contacts where  $E_g^+$  (Ge) was  $0.4$  and  $0.65$  eV. Thus, a high  $E_g^+$  state induced by a Ge(As) layer can be preserved by a NiAs or Te layer that prevents Au or Ni from reaching the Ge-GaAs interface.

The NiAs-ideal and the Au-100 Å Te<sup>17</sup> contacts have  $\phi_B = 0.79$ – $0.80$  eV, which corresponds to  $E_g^+ = 0.63$ – $0.64$  eV; this value of  $E_g^+$  is essentially that of the clean GaAs surface. Thus, NiAs and Te have no effect on the Ge-GaAs interface electronic structure while also providing a conducting elec-

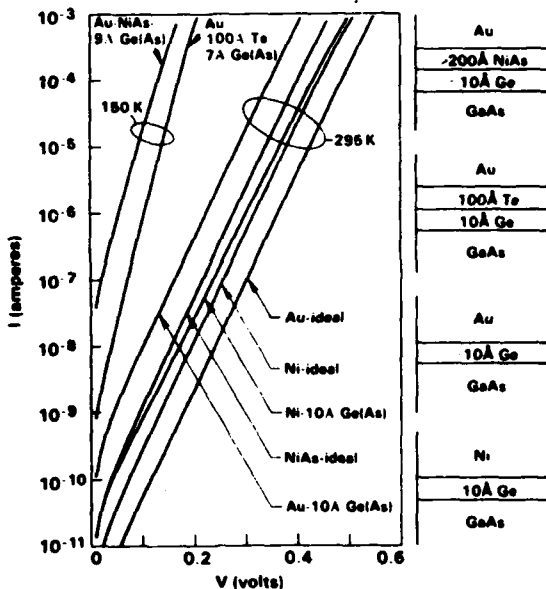


FIG. 3. Representative  $I$ - $V$  data for a selection of contacts to GaAs that have a variety of structures (contact area =  $5.07 \times 10^{-4}$  cm<sup>2</sup>). Multi-layered contact structures are shown schematically on right.

trical contact (other nonmetal conductors with this property are likely).

In a careful electron microscopy investigation<sup>4</sup> of alloyed AuGeNi contacts  $\rho_c$  was found to depend on the relative contact areas of several Ni<sub>2</sub>GeAs, NiAs, and Au(Ga,As) phases. It was concluded that a low  $\rho_c$  is achieved when the Ni<sub>2</sub>GeAs phase dominates because of heightened Ge indiffusion while a higher  $\rho_c$  occurs when Au areas predominate. The present results suggest an alternate explanation: the Ni<sub>2</sub>GeAs and NiAs phases may actually be separated from the GaAs by a very thin layer (not yet observed) of interface Ge and are thus associated with a low  $\phi_B$  ( $\sim 0.25$ – $0.4$  eV); the Au phase is associated with a high  $\phi_B$  ( $\sim 0.7$ – $0.9$  eV). Consequently, with this model the minimum  $\rho_c$  for an alloyed AuGeNi ohmic contact is obtained when the interface area of phases associated with a low  $\phi_B$  is greatest.

The large variation in  $\phi_B$ , from  $\sim 0.25$  to  $0.9$  eV, for the different model interface structures suggests that low  $\rho_c$  nonalloyed ohmic contacts that use Au, Ge, and Ni can be made to  $n^+$ -GaAs ( $N_D > 5 \times 10^{18}$  cm<sup>-3</sup>) if interface composition is controlled to minimize  $\phi_B$ . For example, a properly fabricated Au-NiAs-Ge(As) contact should have a low  $\phi_B$  over the entire contact area.<sup>18</sup> The  $\sim 0.65$  eV range in  $\phi_B$  also has implications for GaAs Schottky barrier models in that  $\phi_B$  at GaAs interfaces cannot be assumed *a priori* to be restricted to values of  $\sim 0.7$ – $0.9$  eV.

This work was supported by Air Force Office of Scientific Research contract No. F49620-85-C-0120.

<sup>1</sup>N. Braslau, J. B. Gunn, and J. L. Staples, *Solid State Electron.* **10**, 381 (1967).

<sup>2</sup>G. Y. Robinson, *Solid State Electron.* **18**, 331 (1975).

<sup>3</sup>M. Ogawa, *J. Appl. Phys.* **51**, 406 (1980).

<sup>4</sup>T. S. Kuan, P. E. Batson, T. N. Jackson, H. Rupprecht, and E. L. Wilkie, *J. Appl. Phys.* **54**, 6952 (1983).

<sup>5</sup>A recent review with an extensive bibliography is C. J. Palmström and D. V. Morgan, in *Gallium Arsenide*, edited by M. J. Howes and D. V. Morgan (Wiley, Chichester, 1985), Chap. 6.

<sup>6</sup>F. A. Kröger, G. Diemer, and H. A. Klasens, *Phys. Rev.* **103**, 279 (1956).

<sup>7</sup>C. Y. Chang, Y. K. Fang, and S. M. Sze, *Solid State Electron.* **14**, 541 (1971).

<sup>8</sup>W. G. Spitzer and C. A. Mead, *J. Appl. Phys.* **34**, 3061 (1963).

<sup>9</sup>J. R. Waldrop, *J. Vac. Sci. Technol. B* **2**, 445 (1984); *Appl. Phys. Lett.* **44**, 1002 (1984).

<sup>10</sup>H. Brugger, F. Schäffler, and G. Abstreiter, *Phys. Rev. Lett.* **52**, 141 (1984).

<sup>11</sup>P. Chiaradia, A. D. Katnani, H. W. Sang, Jr., and R. S. Bauer, *Phys. Rev. Lett.* **52**, 1246 (1984).

<sup>12</sup>E. A. Kraut, R. W. Grant, J. R. Waldrop, and S. P. Kowalczyk, *Phys. Rev. B* **28**, 1965 (1983).

<sup>13</sup>R. W. Grant, J. R. Waldrop, S. P. Kowalczyk, and E. A. Kraut, *J. Vac. Sci. Technol.* **19**, 477 (1981).

<sup>14</sup>E. H. Rhoderick, *Metal-Semiconductor Contacts* (Clarendon, Oxford, 1977).

<sup>15</sup>The large increase in band bending following metal depositions directly on the Ge layers (Fig. 1) in addition to the high and low  $\phi_B$  values measured by  $I$ - $V$  on similarly prepared Ge layers (Table I) rules out tunneling as a dominant conduction mechanism for our samples.

<sup>16</sup>This  $\phi_B$  for Ni-ideal is somewhat higher than the 0.77 eV reported in Ref. 9, which indicates that ideal Ni contacts appear not to have a unique  $\phi_B$ .

<sup>17</sup>J. R. Waldrop, *Appl. Phys. Lett.* **47**, 1301 (1985).

<sup>18</sup>For another nonalloyed GaAs ohmic contact approach, which uses a Au Schottky barrier to a thick Ge-GaAs heterojunction, see R. Stall, C. E. C. Wood, K. Board, and L. F. Eastman, *Electron. Lett.* **15**, 800 (1979). In this case  $\phi_B$  (Au-Ge) =  $\sim 0.5$  eV.

# Variation of *n*-GaAs (100) Interface Fermi level by Ge and Si overlayers

R. W. Grant and J. R. Waldrop

Rockwell International Science Center, Thousand Oaks, California 91360

(Received 29 January 1987; accepted 9 April 1987)

The interface Fermi level ( $E_F^i$ ) for interfaces that were formed by depositing thin ( $\sim 10 \text{ \AA}$ ) layers of Ge and Si onto heated GaAs (100) substrates was studied by x-ray photoelectron spectroscopy. The value of  $E_F^i$  for Ge overlayers (relative to the GaAs valence band maximum) could be varied from  $\sim 0.5 \text{ eV}$  to  $\sim 1.2 \text{ eV}$  by depositing the Ge in vacuum or by depositing it in an  $\text{As}_4$  or  $\text{P}_2$  background pressure ( $\sim 10^{-7}$  Torr). These  $E_F^i$  values roughly correspond to the band edges of Ge at the Ge/GaAs heterojunction interface, which suggests that the dopant type in the Ge overlayer and band alignment play a significant role in determining  $E_F^i$ . A thin Si overlayer with incorporated As also exhibited an  $E_F^i$  of  $\sim 1.2 \text{ eV}$ . The results suggest that heterojunction band alignment characteristics for Ge/GaAs and Si/GaAs based electrical contacts are important in determining the range over which  $E_F^i$  can be varied. The large  $E_F^i$  variation could have an application in the design of nonalloyed GaAs ohmic contacts.

## I. INTRODUCTION

Metal contacts to *n*-GaAs generally have Schottky barrier heights ( $\phi_B$ ) of  $0.7\text{--}0.9 \text{ eV}^{1-3}$ ; the corresponding interface Fermi level position ( $E_F^i$ ) is  $\sim 0.7\text{--}0.5 \text{ eV}$  above the valence band maximum ( $E_v$ ). In addition, oxidized *n*-GaAs surfaces<sup>4</sup> and thin Ge overlayers<sup>5</sup> can exhibit  $E_F^i$  values in this same range. Although most *n*-GaAs  $E_F^i$  positions are confined to the fairly narrow limits indicated above, growing evidence shows that at some *n*-GaAs interfaces much larger  $E_F^i$  values can be obtained.<sup>6-11</sup> An understanding of the factors that influence  $E_F^i$  would clarify the Fermi level ( $E_F$ ) pinning mechanism and be significant for improved GaAs ohmic contact development, where large  $E_F^i$  values are desirable.

The most widely used ohmic contact to *n*-GaAs is the alloyed AuGeNi metallization.<sup>12</sup> Numerous studies have revealed that the heterogeneous contact structure consists of several phases, with phase size and composition dependent on alloying conditions.<sup>13,14</sup> The ohmic contact formation mechanism is not well-known. It is usually assumed that  $E_F^i$  at the GaAs interface is  $\sim 0.6 \text{ eV}$  and that a tunneling contact is formed by heavy Ge donor doping of the GaAs near-interface region.<sup>15</sup> The tunneling contact model<sup>16</sup> has  $\rho_c \sim \exp(C\phi_B N_D^{-1/2})$ , where  $\rho_c$  is the specific contact resistance,  $N_D$  is the net donor concentration, and  $C$  is a constant. Thus, for a fixed  $\phi_B$  (or  $E_F^i$ ),  $\rho_c$  is minimized by maximizing  $N_D$ .

For certain thin ( $\sim 10\text{--}40 \text{ \AA}$ ) Ge overlayers on clean GaAs surfaces,  $E_F^i$  can be  $> 1 \text{ eV}$ .<sup>8,9</sup> It has recently been demonstrated<sup>17</sup> by  $I$ - $V$  measurements that this high  $E_F^i$  value can be retained for thick contacts formed under suitable conditions; a high  $E_F^i$  should make it possible to significantly reduce  $\rho_c$  for a given  $N_D$ . This paper reports further studies of  $E_F^i$  on *n*-GaAs (100), with the goal of investigating factors that can produce large  $E_F^i$  values.

## II. EXPERIMENT

The interfaces studied were prepared in an ultrahigh vacuum (UHV) (base pressure  $10^{-10}$  Torr) custom sample

preparation chamber attached to a Hewlett-Packard (HP) 5950A x-ray photoelectron spectroscopy (XPS) system; a monochromatic  $\text{AlK}\alpha$  ( $h\nu = 1486.6 \text{ eV}$ ) x-ray source was used and the effective photoelectron escape depth was  $\sim 16 \text{ \AA}$ . The bulk GaAs (100) material used was *n*-type ( $\sim 3\text{--}5 \times 10^{16} \text{ cm}^{-3}$ ). To prepare a sample, the GaAs was etched in  $4\text{H}_2\text{SO}_4\text{:H}_2\text{O}_2\text{:H}_2\text{O}$  for  $\sim 30 \text{ s}$  to remove polishing damage, mounted on a Mo plate with In and immediately inserted into the XPS system. The  $\sim 10 \text{ \AA}$  native oxide layer was removed by momentarily heating in vacuum to the minimum necessary temperature ( $\sim 550 \text{ }^\circ\text{C}$ ). This thermally cleaned surface is ordered [displays a characteristic low-energy electron diffraction (LEED) pattern] and shown by XPS to be free of oxygen, carbon, or other contaminants. To prepare an interface, thin layers of Ge or Si were deposited onto the thermally cleaned GaAs (100) substrates. The substrate temperatures were controlled between room temperature and  $325 \text{ }^\circ\text{C}$ , and the depositions were performed in UHV or in background pressures of  $\text{As}_4$  or  $\text{P}_2$ . The Ge and Si were evaporated from W baskets, while the  $\text{As}_4$  source was a small quartz oven and the  $\text{P}_2$  source was an InP crystal heated by a W wire coiled around it. Deposition rates for Ge and Si were  $\sim 0.1 \text{ \AA/s}$ . The deposited overlayer thickness was estimated from the GaAs substrate Ga3d core-level intensity attenuation.

During interface formation, XPS spectra of the Ga3d, As3d, and either the Ge3d or Si2p core-level peaks were obtained. The XPS measurement of  $E_F^i$  for all the interfaces is illustrated schematically in Fig. 1, where  $E_c^{\text{GaAs}}$  and  $E_v^{\text{GaAs}}$  are the GaAs conduction band minimum and valence band maximum, respectively,  $E_{\text{Ga3d}}^{\text{GaAs}}$  is the Ga3d core-level binding energy in GaAs [the binding energy ( $E_B$ ) scale is 0 at  $E_F$ ], and  $W$  is the depletion width. In all cases, the overlayer thicknesses studied were comparable to the Ga3d photoelectron escape depth and  $E_{\text{Ga3d}}^{\text{GaAs}}$  was used to measure  $E_F^i$ . For mid- $10^{16} \text{ cm}^{-3}$  *n*-type GaAs material,  $W$  is  $\sim 1000 \text{ \AA}$ , and thus GaAs band-bending does not complicate the measurement. To determine  $E_F^i$ , the relationship  $E_F^i = E_{\text{Ga3d}}^{\text{GaAs}} - 18.75 \text{ eV}$  was used, where  $18.75 \pm 0.03 \text{ eV}$ <sup>19</sup> is the  $E_B$  difference between  $E_{\text{Ga3d}}^{\text{GaAs}}$  and  $E_c^{\text{GaAs}}$ . At the conclusion of an

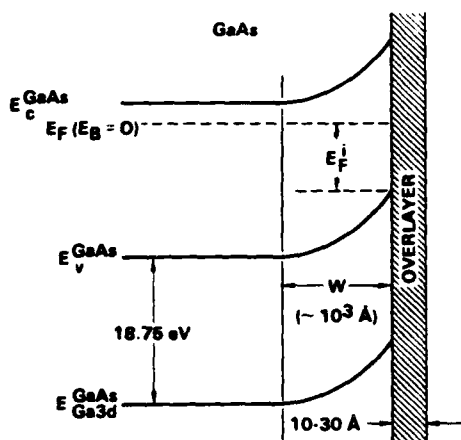


FIG. 1. Schematic energy band diagram that illustrates the XPS measurement of  $E_F^i$  for GaAs.

interface characterization, a thick Au metal layer was evaporated from a W basket onto the sample surface and an absolute  $E_F^i$  value was obtained by indexing the  $Au4f_{7/2}$  XPS peak position to 84.00 eV.<sup>18</sup> Further details on the use of XPS to measure  $E_F^i$  can be found elsewhere.<sup>6</sup>

### III. RESULTS

Representative XPS  $Ga3d$  core-level spectra for several samples are compared in Fig. 2. A spectrum from a thermally cleaned surface is shown for reference in Fig. 2(a) (the vertical line shown in the figure marks the center of this  $Ga3d$  line). The two spectra shown in Figs. 2(b) and 2(c) are for GaAs samples on which thin layers of Ge were deposited in vacuum at 325 and 250 °C, respectively. A low energy electron diffraction (LEED) pattern was observed for the Ge layers deposited (either in vacuum or in the presence of an  $As_4$  background pressure) in the 200–325 °C temperature range, although the pattern had a high background at 200 °C.<sup>17</sup> The  $Ga3d$  binding energy decrease noted in Figs. 2(b) and 2(c) spectra relative to the thermally clean surface represents a decrease in  $E_F^i$ , and thus a corresponding increased band bending. The spectrum shown in Fig. 2(d) is for the same sample that was studied in Fig. 2(c), but with the addition of a 23-Å thick layer of Ge deposited at 250 °C under conditions ( $1 \times 10^{-7}$  Torr  $As_4$  background pressure) where As incorporation occurs [this layer is designated Ge(As)]. A marked shift to higher  $E_B$  (lower band bending) occurs.

Two additional spectra are shown in Figs. 2(e) and 2(f). The first is from a sample on which a 12-Å Ge layer was deposited at 250 °C in the presence of a  $10^{-6}$ -Torr  $P_2$  background. Figure 2(f) spectrum is from a sample on which a 14-Å layer of Si was deposited at 250 °C in the presence of a  $10^{-7}$  Torr  $As_4$  background pressure. Both samples have substantially lower band-bending than the thermally cleaned surface. The Si(As) overlayer did not exhibit a LEED pattern. Subsequent annealing of this sample to 400 °C for 1 min yielded a weak pattern. LEED studies of Si growth on Si (100) have demonstrated epitaxy as low as 300 °C.<sup>20</sup> Pre-

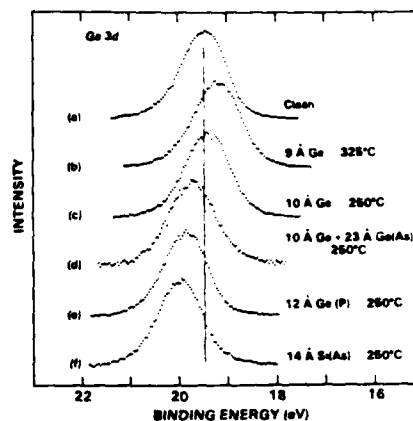


FIG. 2. XPS  $Ga3d$  core-level spectra for several GaAs (100) samples with thin overlayers. The overlayer composition and deposition temperatures are noted in the figure. The spectra shown as (c) and (d) are for the same sample, except for the additional Ge(As) layer.

sumably, 250 °C is slightly too low to achieve epitaxy. Values of  $E_{Ga3d}^{GaAs}$  and of the corresponding  $E_F^i$  are given in Table I for the samples noted in Fig. 2, and for several other samples included in this work (some of these results are from Ref. 17 and are included here for completeness).

### IV. DISCUSSION

Several of the results listed in Table I are shown pictorially in Fig. 3. The overlayer characteristics are noted at the bottom of the figure, and the corresponding  $E_F^i$  value is shown on the vertical scale. The positions of  $E_V^{GaAs}$  and  $E_C^{GaAs}$  are listed on the vertical scale ( $E_F^i = 0$  at  $E_V^{GaAs}$ ). As will be noted below, the interface heterojunction band alignment characteristics appear to play a role in determining the observed  $E_F^i$  positions. Thus, also shown in this figure by dashed lines are the  $E_V$  and  $E_C$  positions for Ge and Si measured at Ge/GaAs<sup>21</sup> and Si/GaAs<sup>22</sup> heterojunction interfaces.

The data shown in Fig. 3 are grouped into five sets (a)–(e). The first set (a) shows  $E_F^i$  values obtained with Ge overlayers that were deposited in vacuum between 200 and 325 °C. The data indicate that band bending in the GaAs increases slightly with increasing Ge deposition temperature. Vacuum-deposited Ge is almost always found to be *p*-type,<sup>23</sup> independent of the substrate. The results shown in Fig. 3(a) suggest that the acceptor density (associated with either the deposition process and/or Ga incorporation from the substrate) increases with increasing deposition temperature. The Ge is degenerate *p*-type when vacuum deposited at 325 °C on thermally cleaned GaAs substrates, in agreement with previous results.<sup>24</sup> Exposure of the Ge overlayer grown at 325 °C to 30 L of  $As_4$  with the sample held at 325 °C caused only a small ( $\sim 0.06$  eV) decrease in GaAs band bending, as indicated by the arrow in Fig. 3(a).

The  $E_F^i$  values shown in Fig. 3(b) are for Ge(As) overlayers deposited between 200 and 325 °C. The net donor den-

TABLE I. Values of  $E_{\text{GaAs}}^{\text{GaAs}}$  and  $E_F^i$  for several *n*-GaAs (100) interfaces.

Sample No.	Overlayer	Deposition Temp. (°C)	Overlayer thickness (Å)	Background pressure during deposition (Torr)	$E_{\text{GaAs}}^{\text{GaAs}}$ (eV)	$E_F^i$ (eV)
1	Thermally clean (ave. of 16 samples)	...	...	...	19.46	0.71
2	Ge	200	9	Vacuum	19.45	0.70
3	Ge*	200	10	Vacuum	19.87	1.12
4	Ge	250	10	Vacuum	19.40	0.65
5	Sample No. 4 + Ge(As)	250	23	$10^{-7}$ As <sub>4</sub>	19.73	0.98
6	Ge	250	6	Vacuum	19.47	0.72
7	Sample No. 6 + Ge(As)	250	6	$10^{-7}$ As <sub>4</sub>	19.88	1.13
8	Ge	325	9	Vacuum	19.20	0.45
9	Sample No. 8 + Exposure to 30 L As <sub>4</sub> at 325 °C	...	...	...	19.26	0.51
10	Ge(As)	RT	26	$10^{-7}$ As <sub>4</sub>	19.49	0.74
11	Ge(As)	200	10	$10^{-7}$ As <sub>4</sub>	19.82	1.07
12	Ge(As)	200	7	$10^{-7}$ As <sub>4</sub>	19.79	1.04
13	Ge(As) <sup>b</sup>	200	9	$10^{-7}$ As <sub>4</sub>	19.78	1.03
14	Ge(As)	200	11	$10^{-7}$ As <sub>4</sub>	19.78	1.03
15	Ge(As)*	200	4	$10^{-7}$ As <sub>4</sub>	19.78	1.03
16	Ge(As)	250	9	$10^{-7}$ As <sub>4</sub>	19.96	1.21
17	Ge(As)	250	9	$10^{-7}$ As <sub>4</sub>	19.90	1.15
18	Ge(As)	250	8	$10^{-7}$ As <sub>4</sub>	19.78	1.03
19	Ge(As)	250	7	$10^{-7}$ As <sub>4</sub>	19.89	1.14
20	Ge(As)	325	11	$10^{-7}$ As <sub>4</sub>	19.85	1.10
21	Ge(As)	325	9	$10^{-6}$ As <sub>4</sub>	19.96	1.21
22	Ge(P)	250	11	$10^{-6}$ P <sub>2</sub>	19.87	1.12
23	Si(As)	250	14	$10^{-7}$ As <sub>4</sub>	19.98	1.23

\*Substrate cleaned in  $10^{-6}$  Torr As<sub>4</sub>.<sup>b</sup>Substrate cleaned in  $10^{-7}$  Torr As<sub>4</sub>.

sity associated with As-doped, molecular-beam epitaxy (MBE)-grown Ge films on GaAs (100) has been studied<sup>25,26</sup> as a function of substrate temperature and found to vary relatively slowly in this temperature range. This behavior may be related to the relatively small variation of  $E_F^i$  with substrate temperature observed in Fig. 3(b), where there is a tendency for  $E_F^i$  to increase with increasing substrate temperature and with increasing As<sub>4</sub> background pressure during Ge deposition. The observed  $E_F^i$  values are in the same range as those previously observed for *n*-Ge layers grown on several GaAs (100) surfaces,<sup>9</sup> and support the conclusion that As doping of Ge is important in determining  $E_F^i$  while deposition-induced defects are not.<sup>27</sup>

To investigate the role of As in determining  $E_F^i$ , two additional experiments were performed in an effort to separate the effect of As at the Ge/GaAs interface from As incorporated in the Ge overlayer. The results of these two experiments are shown in Fig. 3(c). In this case, the sample has two overlayers. The first layer was Ge deposited in vacuum at 250 °C; the  $E_F^i$  value associated with this layer is shown by the open circles. The second Ge(As) overlayer was deposited at 250 °C in the presence of  $10^{-7}$  Torr As<sub>4</sub> background

pressure. The  $E_F^i$  observed after deposition of the Ge(As) layer is shown by closed circles. The large increase in the  $E_F^i$  position (decrease in GaAs band bending) is indicated by arrows in Fig. 3(c). In Fig. 3(a), it was observed that exposure of a vacuum-deposited Ge layer to As<sub>4</sub> caused only a minor shift of  $E_F^i$ . Taken together with the results shown in Fig. 3(c), it appears that the role of As is to alter the  $E_F$  in the deposited Ge and thus the Ge/GaAs  $E_F^i$  rather than directly affecting the interface properties *per se*.

If As acting as a donor in Ge is responsible for the large  $E_F^i$  values, other *n*-type dopants might be expected to produce a similar effect. Thus, a Ge(P) overlayer was prepared by depositing Ge at 250 °C in a  $10^{-6}$  Torr P<sub>2</sub> background pressure. The measured  $E_F^i$  value is shown in Fig. 3(d) and is similar to the results obtained with Ge(As) layers.

The above noted range in  $E_F^i$  indicates that interface heterojunction band alignment characteristics may be responsible for the limits to the large range of observed  $E_F^i$  values at the Ge/GaAs interface. To investigate this possibility, an overlayer of Si(As) was deposited at 250 °C in  $10^{-7}$  Torr As<sub>4</sub> background pressure. The  $E_F^i$  measurement is noted in Fig. 3(e) and indicates very small GaAs band bending.

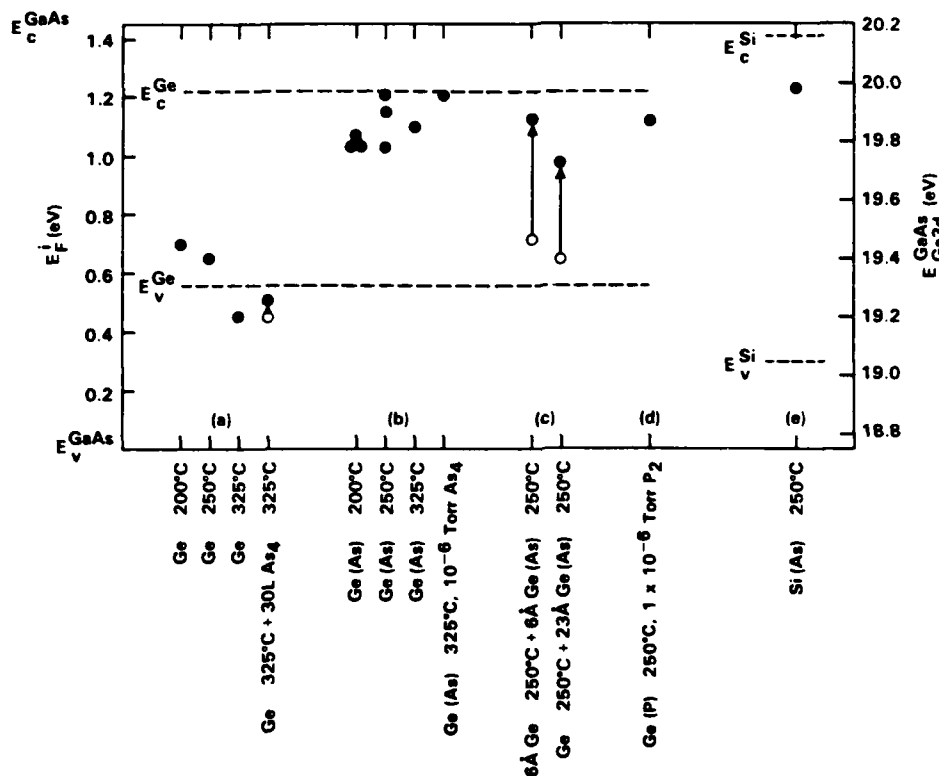


FIG. 3. Summary of several  $E_F^i$  measurements. Overlayer characteristics are given at bottom of figure. Unless noted otherwise, overlayer thicknesses are nominally  $\sim 10$  Å and depositions intended to incorporate As or P in the overlayer were carried out in  $10^{-7}$  Torr background pressure of As<sub>4</sub> or P<sub>2</sub>: (a) Ge overlayers deposited in vacuum; (b) Ge overlayers deposited in As<sub>4</sub>; (c) Ge overlayers initially deposited in vacuum, but completed with deposition in As<sub>4</sub>; (d) Ge overlayer deposited in P<sub>2</sub>; (e) Si overlayer deposited in As<sub>4</sub>.

The above noted range in  $E_F^i$  indicates that interface heterojunction band alignment characteristics may be responsible for the limits to the large range of observed  $E_F^i$  values at the Ge/GaAs interface. To investigate this possibility, an overlayer of Si(As) was deposited at 250 °C in  $10^{-7}$  Torr As<sub>4</sub> background pressure. The  $E_F^i$  measurement is noted in Fig. 3(e) and indicates very small GaAs band bending.

## V. CONCLUSIONS

The widely varying values of  $E_F^i$  that have been observed for the Ge/GaAs interface, both in this work and in many previously published works<sup>5,8,9,17,24,27,28</sup> appear to be approximately confined to within the Ge band gap, as noted in Fig. 3. A very plausible explanation for this limit to the  $E_F^i$  values is that  $E_F^i$  depends on the net donor or acceptor density in the Ge. This model suggests that  $E_F^i$  is not necessarily pinned at the Ge/GaAs interface, but rather is restricted in total movement by the large density of states in the valence and conduction bands of Ge at the heterojunction interface.

The fact that the interface heterojunction characteristics seem important in determining the  $E_F^i$  value is supported by noting that both Ge(As) and Si(As) overlayers can produce very large  $E_F^i$  values. Also, it is well known that two-dimensional electron and hole gases can be observed at the technologically important AlAs/GaAs interface so that in this case

$E_F^i$  in GaAs can be moved across the entire GaAs band gap. It appears therefore that even very thin ( $\sim 10$  Å) semiconductor heterojunction interfaces can overcome or remove the dominant  $E_F$  pinning mechanism observed at most GaAs interfaces. The formation of a heterojunction interface can be expected to remove dangling bond states that may otherwise contribute to pinning at the interface. Alternatively, a heterojunction interface might remove defects associated with pinning or overcome their influence by a charge transfer between carriers in the overlayer and these defects.

It is well-known that  $\rho_c$  for alloyed AuGe based contacts depends sensitively on annealing conditions. In some investigations of alloyed AuGe contacts,<sup>29</sup> epitaxial regions of Ge have been observed in contact with the GaAs. It seems possible that  $E_F^i$  variations associated with the changing size, thickness and doping of thin epitaxial Ge regions could be affecting  $\rho_c$  during alloying. Because  $\rho_c$  for a tunneling contact depends exponentially on  $\phi_B$ , the realization of a stable high  $E_F^i$  GaAs interface could have an important application in nonalloyed ohmic contact design.

## ACKNOWLEDGMENT

This work was supported by the AFOSR under Contract No. F49620-85-C-0120.

- <sup>1</sup>W. G. Spitzer and C. A. Mead, *J. Appl. Phys.* **34**, 3061 (1963).
- <sup>2</sup>J. R. Waldrop, *J. Vac. Sci. Technol. B* **2**, 445 (1985); *Appl. Phys. Lett.* **44**, 1002 (1984).
- <sup>3</sup>N. Newman, M. Van Schligaarde, T. Kendelwicz, M. D. Williams, and W. E. Spicer, *Phys. Rev. B* **33**, 1146 (1986).
- <sup>4</sup>W. E. Spicer, I. Lindau, P. Skeath, and C. Y. Su, *J. Vac. Sci. Technol.* **17**, 1019 (1980).
- <sup>5</sup>W. Mönch and H. Gant, *Phys. Rev. Lett.* **48**, 512 (1982).
- <sup>6</sup>R. W. Grant, J. R. Waldrop, S. P. Kowalczyk, and E. A. Kraut, *J. Vac. Sci. Technol.* **19**, 477 (1981).
- <sup>7</sup>J. Massies, J. Chapiro, M. Laviro, and N. T. Linh, *Appl. Phys. Lett.* **38**, 693 (1981).
- <sup>8</sup>H. Brugger, F. Schäffler, and G. Abstreiter, *Phys. Rev. Lett.* **52**, 141 (1984).
- <sup>9</sup>P. Chiaradia, A. D. Katnani, H. W. Sang, Jr., and R. S. Bauer, *Phys. Rev. Lett.* **52**, 1246 (1984).
- <sup>10</sup>J. R. Waldrop, *Appl. Phys. Lett.* **47**, 1301 (1985).
- <sup>11</sup>S. D. Offsey, J. M. Woodall, A. C. Warren, P. D. Kirchner, T. I. Chappel, and G. D. Pettit, *Appl. Phys. Lett.* **48**, 475 (1986).
- <sup>12</sup>N. Braslau, J. B. Gunn, and J. L. Staples, *Solid-State Electron.* **10**, 381 (1967).
- <sup>13</sup>T. S. Kuan, P. E. Batson, T. N. Jackson, H. Rupprecht, and E. L. Wilkie, *J. Appl. Phys.* **54**, 6952 (1983).
- <sup>14</sup>C. J. Palmstrom and D. V. Morgan, *Gallium Arsenide*, edited by M. J. Howes and D. V. Morgan (Wiley, Chichester, 1985), Chap. 6, and references cited therein.
- <sup>15</sup>N. Braslau, *J. Vac. Sci. Technol.* **19**, 803 (1981); *J. Vac. Sci. Technol. A* **4**, 3085 (1986).
- <sup>16</sup>C. Y. Chang, Y. K. Fang, and S. M. Sze, *Solid-State Electron.* **14**, 541 (1971).
- <sup>17</sup>J. R. Waldrop and R. W. Grant, *Appl. Phys. Lett.* **50**, 250 (1987).
- <sup>18</sup>F. R. McFeely, S. P. Kowalczyk, L. Ley, R. A. Pollak, and D. A. Shirley, *Phys. Rev. B* **7**, 5228 (1973).
- <sup>19</sup>See J. R. Waldrop, R. W. Grant, and E. A. Kraut, *J. Vac. Sci. Technol. B* **5**, 1209 (1987).
- <sup>20</sup>R. N. Thomas and M. H. Francombe, *Appl. Phys. Lett.* **11**, 108 (1967).
- <sup>21</sup>J. R. Waldrop, E. A. Kraut, S. P. Kowalczyk, and R. W. Grant, *Surf. Sci.* **132**, 513 (1983).
- <sup>22</sup>R. S. List, P. H. Mahowald, J. Woicik, and W. E. Spicer, *J. Vac. Sci. Technol. A* **4**, 1391 (1986).
- <sup>23</sup>J. E. Davey, *Appl. Phys. Lett.* **8**, 164 (1966).
- <sup>24</sup>S. P. Kowalczyk, R. W. Grant, J. R. Waldrop, and E. A. Kraut, *J. Vac. Sci. Technol. B* **1**, 684 (1983).
- <sup>25</sup>C. E. C. Wood, *J. Vac. Sci. Technol.* **18**, 772 (1981).
- <sup>26</sup>R. A. Stall, C. E. C. Wood, K. Board, N. Dandekar, L. F. Eastman, and J. Devlin, *J. Appl. Phys.* **52**, 4062 (1981).
- <sup>27</sup>A. D. Katnani, P. Chiaradia, H. W. Sang, Jr., and R. S. Bauer, *J. Electron. Mater.* **14**, 25 (1985).
- <sup>28</sup>P. Chen, D. Bolmont, and C. A. Sebenne, *J. Phys. C* **15**, 6101 (1982).
- <sup>29</sup>A. A. Lakhani and D. R. Urech, *Mater. Res. Soc. Symp. Proc.* **25**, 551 (1984).

# Metal contacts to GaAs with 1 eV Schottky barrier height

J. R. Waldrop and R. W. Grant

Rockwell International Science Center, Thousand Oaks, California 91360

(Received 27 January 1988; accepted for publication 22 March 1988)

Metal Schottky barrier contacts to *n*-type (100) GaAs are described in which a 1 eV Schottky barrier height  $\phi_B$  is achieved by using a very thin Si interface layer to influence the interface Fermi energy  $E'_F$ . The metals investigated are Au, Cr, and Ti. The contact structure consists of a thick metal in combination with a  $\sim 15$ – $30$  Å heavily *p*-type Si interface layer. The  $E'_F$  and interface composition during initial contact formation were obtained by x-ray photoemission spectroscopy (XPS); the  $\phi_B$  for the corresponding thick contacts was measured by current-voltage (*I-V*) and capacitance-voltage (*C-V*) techniques. The XPS, *I-V*, and *C-V* measurements gave consistent results. The 1 eV  $\phi_B$  for the Si interface layer contact structure is independent of the contact metal.

The metal contacts to GaAs commonly used in device applications generally exhibit a restricted range of Schottky barrier height  $\phi_B$  that is between  $\sim 0.7$  and  $0.9$  eV. The performance of many GaAs device designs which include Schottky barrier contacts is improved, however, if a larger  $\phi_B$  contact can be employed. Some unconventional Schottky barrier contacts where  $\phi_B$  is  $\sim 1$  eV have been reported; for example, polymeric (SN)<sub>x</sub>,<sup>1</sup> amorphous Si-Ge-B material,<sup>2</sup> and Au with interface chalcogen.<sup>3</sup> Thus, an upper limit for  $\phi_B$  established for ideal metal contacts<sup>4</sup> (no interface oxide) is not an intrinsic property of all GaAs Schottky barrier interfaces.

This letter reports 1 eV  $\phi_B$  metal Schottky barrier contacts to GaAs in which the barrier increase is accomplished by influencing the interface Fermi energy  $E'_F$  with a very thin Si interlayer. The metals investigated are Au, Cr, and Ti. The contact structure consists of a thick metal and a  $\sim 15$ – $30$  Å Si interface layer made heavily *p* type with Ga. During initial contact formation  $E'_F$  and interface composition were observed by x-ray photoemission spectroscopy (XPS). For thick contacts,  $\phi_B$  was measured by current-voltage (*I-V*) and capacitance-voltage (*C-V*) techniques on the same interfaces characterized by XPS. The XPS, *I-V*, and *C-V* measurements gave consistent results.

The contacts were prepared in the ultrahigh vacuum environment ( $10^{-10}$  Torr range base pressure) of an XPS apparatus that consists of a HP5950 electron spectrometer ( $h\nu = 1486.6$  eV monochromatic x-ray source,  $\sim 16$  Å effective photoelectron escape depth) and a custom sample preparation chamber. XPS spectra of the As 3*d*, Ga 3*d*, and of other appropriate core levels were obtained at different stages of initial contact interface formation. Electrical measurements were made with a computerized system that includes a HP4140B pA meter/voltage source and a HP4275A capacitance meter.

The GaAs used was (100) Bridgman-grown *n*-type ( $\sim 5 \times 10^{16}$  cm<sup>-3</sup> Si) wafers. To prepare a sample, a  $\sim 8 \times 8$  mm GaAs piece is etched in fresh 4:1:1 H<sub>2</sub>SO<sub>4</sub>:H<sub>2</sub>O<sub>2</sub>:H<sub>2</sub>O solution for  $\sim 30$  s to remove polishing damage, mounted on a Mo plate with In, and immediately put into the XPS system. The native oxide is removed from the GaAs surface by momentary heating to the minimum necessary temperature ( $\sim 575$  °C). This thermally cleaned surface is free of O

and C (as shown by XPS), and is ordered (exhibits a characteristic low-energy electron diffraction pattern). The Si layer evaporation source was a Ta basket filled with heavily *p*-type (B) Si. The Ga evaporation source was a miniature W basket located near the sample. Au, Cr, and Ti contact metals were evaporated from W baskets. After XPS analysis of an initial thin metal overlayer ( $\sim 10$ – $15$  Å), a final thick metal layer of  $> 2000$  Å was deposited. An array of circular  $2.54 \times 10^{-2}$  cm diameter contacts was defined by photolithography and etching. The electrical measurements were thus taken on the same interfaces characterized by XPS.

The Si interface layers, which ranged from 17 to 28 Å, were deposited at  $\sim 0.1$  Å/s onto clean GaAs surfaces held at 250 °C (the layer thickness was measured by noting the attenuation of the As 3*d* peak from the GaAs substrate). Low  $E'_F$  (large  $\phi_B$ ) results were obtained most consistently when both a monolayer of Ga was deposited during the first few seconds of the Si overlayer growth and the chamber was backfilled with  $\sim 2 \times 10^{-6}$  Torr H<sub>2</sub>. This amount of Ga is in excess of what can be incorporated into Si films in the thickness range used, thus ensuring that sufficient *p*-type dopant is available to produce degeneracy. The resultant Si layer is designated Si(Ga). The hydrogen background seems to assist in making the Si films *p* type. Although we surmise that hydrogen helps by minimizing the amount of electrically active deep levels in the Si, the exact mechanism(s) involved is not clear. Other Si deposition conditions also yielded low  $E'_F$  interfaces, as will be briefly discussed later.

The As 3*d* data in Fig. 1 illustrate how XPS was used to measure  $E'_F$  (and  $\phi_B$ ) during contact interface formation (other details on the XPS technique can be found elsewhere<sup>5</sup>). The top three peaks are for sequential treatments to the same sample; the bottom peak is for the indicated two overlayers (peak heights are normalized). The inset in Fig. 1 depicts the relationship between the As 3*d* core level in GaAs at the interface and  $E'_F$  (the photoelectron escape depth is much smaller than the band bending depth). Thus,  $E'_F = E_{As\ 3d} - 40.74$  eV, where  $(E_{As\ 3d} - E_v) = 40.74 \pm 0.03$  eV is the constant As 3*d* to valence-band maximum energy difference in GaAs<sup>6</sup> (note that the XPS binding energy  $E_B$  scale is zero at the sample Fermi energy). The vertical line indicating the center (midpoint of the width at half-maximum) of the clean surface As 3*d* peak at 41.58 eV

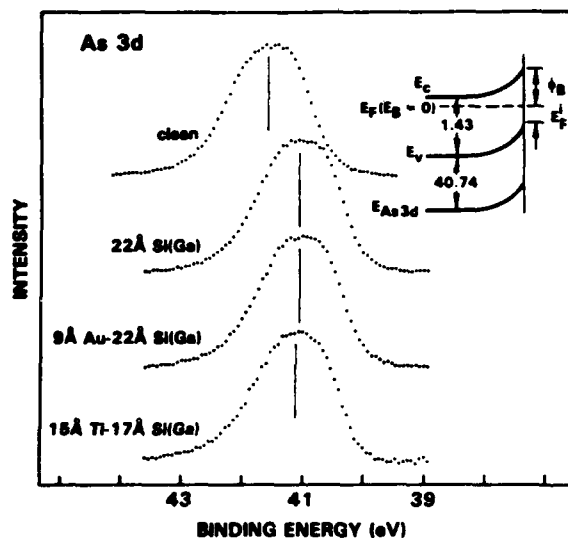


FIG. 1. XPS As 3d core level spectra for various thin overlayers on clean n-type GaAs (100) surfaces. Inset shows relationship between As 3d binding energy and  $E_F^i$ .

therefore gives an  $E_F^i$  (clean) measurement of 0.84 eV (the average value for four samples was 0.79 eV).

Deposition of 22 Å of Si(Ga) onto the clean GaAs surface caused a 0.51 eV decrease of the As 3d binding energy to 41.07 eV, which gives  $E_F^i = 0.33$  eV (compare upper two peaks in Fig. 1). Similar  $E_F^i$  data for the other samples are listed in Table I. Each sample has a low (0.33–0.47 eV)  $E_F^i$  value after deposition of a Si(Ga) overlayer.

Is the low  $E_F^i$  value at the Si(Ga)-GaAs interface retained after deposition of a contact metal? The third As 3d peak in Fig. 1 at 41.06 eV demonstrates that a 9 Å Au overlayer essentially did not change  $E_F^i$  for the 22 Å Si(Ga) sample ( $E_F^i = 0.32$  eV). Similarly, the bottom As 3d peak at 41.12 eV ( $E_F^i = 0.38$  eV) is for a 15 Å Ti overlayer on the 17 Å Si(Ga)-GaAs interface. Thus, deposition of a metal does not increase the low  $E_F^i$  value established by the Si(Ga) layer.

The  $E_F^i$  measured with a metal overlayer is related to the Schottky barrier height (inset in Fig. 1) by  $\phi_B = 1.43$

TABLE I. Schottky barrier height of metal contacts to GaAs that contain a thin Si(Ga) interface layer.

Contact	$E_F^i$ (eV)	$\phi_B^{XPS}$ (eV)	$n$	$\phi_B^{IV}$ (eV)	$\phi_B^{CV}$ (eV)
Au-22 Å Si(Ga)	0.33	1.11	1.08	1.01	1.01
Cr-28 Å Si(Ga)	0.41	...	1.11	0.99	1.10
Ti-17 Å Si(Ga)	0.39	1.05	1.11	0.98	1.14
Ti-26 Å Si(Ga)	0.47	1.01	1.10	0.97	1.06
Au-ideal			1.05	0.89	
Cr-ideal			1.05	0.76	
Ti-ideal			1.04	0.83	

<sup>a</sup>Si(Ga) overlayer only.

<sup>b</sup>Includes + 0.04 eV image force correction.

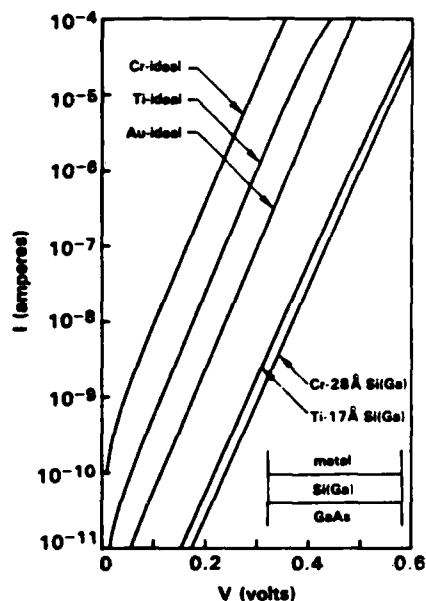


FIG. 2. Representative  $I-V$  data for Cr-Si(Ga) and Ti-Si(Ga) contacts compared to corresponding ideal contacts [Au-Si(Ga) data not shown because of overlap with Cr-Si(Ga) data]. Contact area =  $5.07 \times 10^{-4}$  cm<sup>2</sup>.

eV -  $E_F^i$ . The values of  $\phi_B^{XPS}$  for the Au and Ti samples are given in Table I [the Cr  $\phi_B^{XPS}$  could not be measured because the As 3d and Cr 3p peaks overlap and there was an additional 0.05 eV decrease in  $E_F^i$  at the 26 Å Si(Ga)-GaAs interface upon Ti deposition]. Thus, XPS measurements show that thin metal contacts to Si(Ga)-GaAs interfaces have ~1 eV Schottky barrier heights.

Representative  $I-V$  data for the thick metal Cr-28 Å Si(Ga) and Ti-17 Å Si(Ga) contacts are plotted in Fig. 2 [the Au-22 Å Si(Ga) data are not shown because of overlap with the Cr-Si(Ga) data]. For comparison,  $I-V$  data for ideal contacts of these metals (metal deposited onto clean GaAs surface) are also shown. A substantial increase in barrier height is evident for the contacts with the Si(Ga) interlayer. The  $I-V$  data were analyzed with respect to the thermionic emission model<sup>7</sup> for current transport:

$$I = I_S \exp(qV/nkT) [1 - \exp(-qV/kT)] A,$$

where the ideality factor  $n$  (~1.02 is ideal) and  $I_S$  were determined by a least-squares fit. The Schottky barrier height  $\phi_B^{IV}$  is related to  $I_S$  by  $I_S = SA^*T^2 \times \exp[-q(\phi_B^{IV} - \Delta\phi)/kT] A$ , where  $S$  is the contact area,  $A^* = 8.16$  is the effective Richardson constant, and  $\Delta\phi = 0.04$  eV is the calculated image force correction. The corresponding  $C-V$  data for each contact, taken at 1 MHz over a +0.2 to -2.0 V range, were analyzed according to the conventional model<sup>8</sup> that gives  $\phi_B^{CV}$  in terms of the intercept  $V_i$  (found by a least-squares fit) on the voltage axis of a  $1/C^2$  vs  $V$  plot. There were no significant deviations from linearity in these  $1/C^2$  vs  $V$  plots. Table I lists the average values of  $n$ ,  $\phi_B^{IV}$ , and  $\phi_B^{CV}$  for each metal-Si(Ga) sample (~10 contacts per sample,  $< \pm 0.01$  eV estimated measurement uncertainty). The  $\phi_B^{IV}$  for the corresponding ideal contact is also given.

The electrical measurements on the thick contacts confirm the 1.0 eV barriers measured by XPS. Why  $\phi_B^{CV}$  is  $\sim 0.1$  eV larger than  $\phi_B^{IV}$  for the Cr-Si(Ga) and Ti-Si(Ga) contacts is unexplained but is most likely an artifact of the C-V model used; the close agreement of the values for the Au-Si(Ga) contact shows this difference is not an intrinsic feature of the metal-Si(Ga)-GaAs interface. For this reason the  $\phi_B^{IV}$  values will be considered the most accurate measure of the barrier height. The ideality factors are acceptably low. The increased  $\phi_B$  for the metal-Si(Ga) contact compared to the respective ideal contact ranges from 0.1 eV (Au) to 0.23 eV (Cr). In addition, the metal-Si(Ga)  $\phi_B$  is independent of the contact metal, which is in contrast with ideal contacts to GaAs.

The XPS results demonstrate that the large  $\phi_B$  is caused by a low  $E_F'$  created at the Si(Ga)-GaAs interface which remains after deposition of a thick contact metal. This method of achieving a large barrier contact is thus distinct from methods<sup>9</sup> in which an effective barrier height is controlled by tailoring the impurity profile, and hence the potential, in the GaAs depletion region near a metal-GaAs interface where  $\phi_B$  itself is fixed.

The critical factor for achieving a low  $E_F'$  at Si-GaAs interfaces is that the Si be heavily *p* type. In principle the Si layer should not be depleted. We have also produced low  $E_F'$  interfaces with boron-doped Si deposited at 200 and 350 °C in vacuum. Thus, neither the kind of *p* dopant nor the precise substrate temperature is a crucial parameter. The nonepitaxial nature of the Si and large lattice mismatch with GaAs also indicates that interface perfection need not be approached to obtain a low  $E_F'$ . Furthermore, a large  $E_F' = 1.23$  eV value was recently reported<sup>10</sup> for the Si(As)-GaAs interface grown at 250 °C. Thus,  $E_F'$  is unpinned and can be varied up to  $\sim 0.9$  eV at Si-GaAs interfaces by making the Si either *p* or *n* type. This observation suggests that the lower limit to  $E_F'$  values at Si-GaAs interfaces may be set by where the Si valence-band maximum falls within the GaAs band gap (that is, the Si-GaAs heterojunction valence-band offset  $\Delta E_v$ ). A  $\Delta E_v$  of  $0.23 \pm 0.1$  eV has

been measured,<sup>11</sup> which is fairly close to the  $E_F'$  values for the metal-Si(Ga)-GaAs contacts.

Our results offer a possible basis for understanding the high barrier measured for thick amorphous Si-Ge-B contacts<sup>2</sup> to GaAs. If heavily *p*-type material in intimate contact with the GaAs was produced by the chemical vapor deposition process that was used, then  $E_F'$  may have been unpinned in the same way as at the Si(Ga)-GaAs interfaces described here.

In summary, the  $\phi_B$  of metal contacts to GaAs can be increased to 1.0 eV by inclusion of a very thin  $\sim 15$ – $30$  Å Si(Ga) interface layer to control  $E_F'$ . The metals investigated were Au, Cr, and Ti. The increased  $\phi_B$  for these metals (compared to ideal contacts) ranges from 0.1 to 0.23 eV. Thus, use of the Si(Ga) interlayer also makes  $\phi_B$  independent of the contact metal. Because of the diverse properties of Au, Cr, and Ti, we expect that other metals will also exhibit an increased  $\phi_B$  when used in a similar metal-Si(*p*-type)-GaAs contact structure.

This work was supported by Air Force Office of Scientific Research contract No. F49620-85-C-0120.

<sup>1</sup>R. A. Scranton, J. S. Best, and J. O. McCaldin, *J. Vac. Sci. Technol.* **14**, 930 (1977).

<sup>2</sup>M. Suzuki, K. Murase, K. Asai, and K. Kurumada, *Jpn. J. Appl. Phys.* **22**, L709 (1983).

<sup>3</sup>J. R. Waldrop, *Appl. Phys. Lett.* **47**, 1301 (1985).

<sup>4</sup>J. R. Waldrop, *Appl. Phys. Lett.* **44**, 1002 (1984); *J. Vac. Sci. Technol. B* **2**, 445 (1984).

<sup>5</sup>R. W. Grant, J. R. Waldrop, S. P. Kowalczyk, and E. A. Kraut, *J. Vac. Sci. Technol.* **19**, 477 (1981).

<sup>6</sup>J. R. Waldrop, R. W. Grant, and E. A. Kraut, *J. Vac. Sci. Technol. B* **5**, 1209 (1987).

<sup>7</sup>E. H. Rhoderick, *Metal-Semiconductor Contacts* (Clarendon, Oxford, 1977).

<sup>8</sup>A. M. Goodman, *J. Appl. Phys.* **34**, 329 (1963).

<sup>9</sup>For example, J. M. Shannon, *Solid-State Electron.* **19**, 537 (1976).

<sup>10</sup>R. W. Grant and J. R. Waldrop, *J. Vac. Sci. Technol. B* **5**, 1015 (1987).

<sup>11</sup>R. S. List, J. Woicik, P. H. Mahowald, I. Lindau, and W. E. Spicer, *J. Vac. Sci. Technol. A* **5**, 1459 (1987).

# Wide range of Schottky barrier height for metal contacts to GaAs controlled by Si interface layers

J. R. Waldrop and R. W. Grant

Rockwell International Science Center, Thousand Oaks, California 91360

(Received 3 February 1988; accepted 21 April 1988)

Metal (Au, Cr, and Ti) contacts to *n*-type (100) GaAs are described in which the Schottky barrier height  $\phi_B$  is controlled by using a very thin Si interface layer to influence the interface Fermi energy  $E_F^i$ . The contact structure consists of a thick metal and an  $\sim 15$ – $30$  Å Si interface layer that is heavily either *p*-type or *n*-type. A large 1 eV  $\phi_B$  is found for the metal–Si(*p*-type)–GaAs structure and a small 0.5 eV  $\phi_B$  for the metal–Si(*n*-type)–GaAs structure. X-ray photoemission spectroscopy (XPS) was used to obtain  $E_F^i$  and interface composition during initial contact formation; the  $\phi_B$  for the thick contacts was measured by *I*–*V* and *C*–*V* techniques.

## I. INTRODUCTION

Ideal metal contacts (no interface oxide) to *n*-type GaAs generally have a range in Schottky barrier height  $\phi_B$  that is between  $\sim 0.7$  and  $0.9$  eV.<sup>1</sup> However, this restricted  $\phi_B$  range is not an intrinsic property associated with all GaAs contacts. For example, some unconventional large height Schottky barrier contacts where  $\phi_B$  is  $\sim 1$  eV are polymeric (SN)<sub>x</sub>,<sup>2</sup> amorphous Si–Ge–B material,<sup>3</sup> and Au with interface chalcogen.<sup>4</sup> In contrast, low  $\phi_B$  ( $< 0.4$  eV) contacts have also been reported, including Al with interface chalcogen<sup>5,6</sup> and Au contacts that have a thin ( $\sim 10$  Å) Ge interface layer.<sup>7</sup> Such an extended range in  $\phi_B$  is of benefit in many GaAs device designs. Investigation of the conditions under which a wide range of  $\phi_B$  can be attained at GaAs interfaces is thus of interest for both Schottky barrier contact and Ohmic contact device applications.

This paper reports metal (Au, Cr, and Ti) contacts to *n*-type GaAs in which  $\phi_B$  is controlled over a wide range by influencing the interface Fermi energy  $E_F^i$  with a very thin Si interface layer. The contact structure is a thick metal and an  $\sim 15$ – $30$  Å Si interface layer. For large  $\phi_B$  contacts the Si is made heavily *p*-type with Ga or B. For small  $\phi_B$  the Si is made heavily *n*-type with P. X-ray photoemission spectroscopy (XPS) was used to obtain interface composition and  $E_F^i$  during initial contact formation. For thick contacts, electrical measurement of  $\phi_B$  was by *I*–*V* and *C*–*V* techniques. The XPS, *I*–*V*, and *C*–*V* measurements gave consistent values for  $\phi_B$  and  $E_F^i$ .

## II. EXPERIMENTAL

The thin Si–GaAs interfaces and subsequent thick metal contact layers were prepared within an XPS system that consists of a HP5950 electron spectrometer ( $h\nu = 1486.6$  eV monochromatic Al  $K\alpha$  x-ray source,  $\sim 16$  Å effective photoelectron escape depth) and a custom ultrahigh vacuum ( $10^{-10}$  Torr range base pressure) sample preparation chamber. XPS spectra of the As 3*d*, Ga 3*d*, and other pertinent core levels were obtained at several stages of interface formation. Electrical measurements on thick contacts were made with a computerized system that includes a HP4140B

pA meter/voltage source and a HP4275A capacitance meter. *I*–*V* data were taken in 0.01 V forward bias increments to a current limit of 1 mA; *C*–*V* data were taken at 1 MHz in 0.1 V increments to a reverse bias of  $-2$  V.

The GaAs used was (100) oriented bulk grown *n*-type ( $\sim 5 \times 10^{16}$  cm<sup>-3</sup>) wafers. Samples were prepared by etching an  $\sim 8 \times 8$  mm GaAs piece in fresh 4:1:1 H<sub>2</sub>SO<sub>4</sub>:H<sub>2</sub>O<sub>2</sub>:H<sub>2</sub>O solution for  $\sim 30$  s to remove polishing damage, mounting it on a Mo plate with In, followed by immediate placement into the XPS system. A clean surface was obtained by momentary heating to the minimum temperature ( $\sim 575$  °C) required to remove the thin,  $\sim 10$  Å, GaAs native oxide composed of Ga<sub>2</sub>O<sub>3</sub> and As<sub>2</sub>O<sub>3</sub>. The resultant GaAs surface both is ordered [displays a characteristic low-energy electron diffraction (LEED) pattern] and is shown by XPS to be free of O and C. The Si source was an enclosed Ta wire basket. Si impurity dopant sources were a miniature W basket located near the sample for Ga, elemental B included in the Si source for B, and a piece of InP wrapped in resistively heated Ta wire for P. Au, Cr, and Ti contact metals were evaporated from W baskets. After XPS analysis of thin overlayer(s) a final thick metal overlayer of  $> 2000$  Å was deposited. Circular  $2.54 \times 10^{-2}$ -cm-diam contacts for electrical measurements were defined by photolithography and etching. Electrical measurements were thus obtained from the same interfaces that were characterized by XPS.

Si layers of  $\sim 10$ – $30$ -Å thickness were deposited at  $\sim 0.1$  Å/s onto clean GaAs surfaces held between 200 and 350 °C (measurement of layer thickness was by noting the attenuation of the As 3*d* peak from the underlying GaAs). For the B doped Si layers, designated Si(B), material from the Si source was evaporated in vacuum. The procedure for the Ga doped layers, Si(Ga), was somewhat more complex. The same Si source as for the Si(B) layers was used. Ga was introduced into the Si by depositing a monolayer of Ga during the first few seconds of Si growth. This amount of Ga is more than can be incorporated into the Si in the thickness range used, which ensures that sufficient Ga is available to produce degeneracy. The most consistent low  $E_F^i$  Si(Ga)–GaAs interfaces were obtained when the chamber was back-

filled with  $\sim 2 \times 10^{-6}$  Torr  $H_2$  during the Si deposition. Evidently, the hydrogen assists in the  $p$ -type doping process by minimizing the number of electrically active deep levels in the Si, but the precise mechanism(s) involved is not obvious. Si layers with incorporated P, Si(P), were obtained by evaporation of lightly  $n$ -type (P) Si in an  $\sim 2 \times 10^{-6}$  Torr  $P_2$  background pressure.

Figure 1 illustrates how XPS is used to measure  $E_F^i$  from the binding energy  $E_B$  of the As 3d core level peak in GaAs at an interface, designated  $E_{As\ 3d}$  ( $E_B$  is zero at the sample Fermi energy). The escape depth for As 3d photoelectrons is much smaller than the GaAs band bending depth. Thus referring to Fig. 1,  $E_F^i = E_{As\ 3d} - 40.74$  eV, where  $(E_{As\ 3d} - E_v) = 40.74$  eV is the constant As 3d to valence band maximum binding energy difference in GaAs.<sup>8</sup>  $E_F^i$  can be conveniently measured for overlayer(s) up to approximately twice the escape depth. If one of the overlayers is a metal, then  $\phi_B^{XPS} = 1.43$  eV  $- E_F^i$ .

$I$ - $V$  data were analyzed by using the thermionic emission model<sup>9</sup>:  $I = I_S \exp(qV/nkT) [1 - \exp(-qV/kT)]$ ,  $A$ , where the ideality factor  $n$  ( $\sim 1.02$  is ideal) and  $I_S$  were determined by a least-squares fit. The Schottky barrier height  $\phi_B^{IV}$  is related to  $I_S$  by  $I_S = SA^*T^2 \exp[-q(\phi_B^{IV} - \Delta\phi)/kT]$ , where  $S$  is the contact area,  $A^* = 8.16$  is the effective Richardson constant, and  $\Delta\phi$  is the calculated image force correction ( $\Delta\phi = +0.04$  eV for  $\phi_B > 0.7$  eV and  $+0.03$  eV for  $\phi_B < 0.7$  eV).  $C$ - $V$  data were analyzed in terms of a conventional model<sup>10</sup> whereby  $\phi_B^{CV}$  is related to the intercept  $V_i$  (which was found by a least-squares fit) on the voltage axis of a  $1/C^2$  vs  $V$  plot. With the present GaAs material,  $\phi_B^{CV} = V_i + 0.08$  eV. The estimated measurement uncertainty in  $\phi_B^{IV}$  and  $\phi_B^{CV}$  is  $< \pm 0.01$  eV.

### III. RESULTS

Figure 2 shows representative As 3d core level spectra to demonstrate the range in  $E_F^i$  that results from Si(P), Si(B),

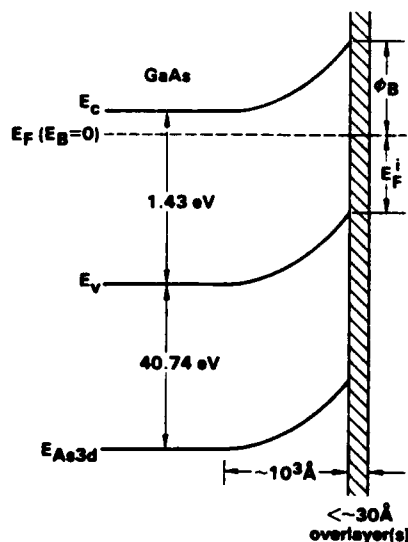


FIG. 1. Schematic interface band diagram that illustrates the XPS measurement of  $E_F^i$  and  $\phi_B$  by using the As 3d core level in GaAs.

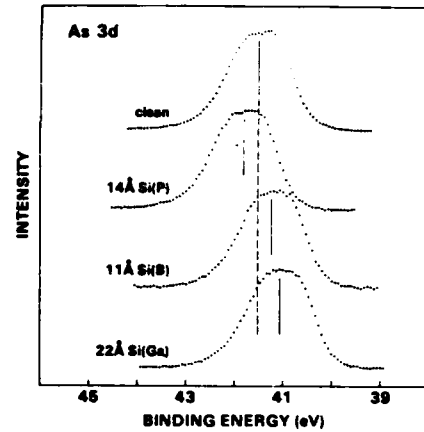


FIG. 2. XPS As 3d core level spectra for thin  $p$ -type and thin  $n$ -type Si layers deposited on clean  $n$ -type GaAs (100) surfaces.

and Si(Ga) overlayers deposited onto clean GaAs (100) surfaces (peak heights are normalized). The upper two peaks are for the same sample. Thus, the vertical line that indicates the center (midpoint of the width at half-maximum) of the clean surface As 3d peak at  $E_{As\ 3d} = 41.52$  eV corresponds to  $E_F^i$  (clean) = 0.78 eV (the average value for 14 samples was 0.79 eV). Deposition of a 14  $\text{\AA}$  Si(P) overlayer onto this clean surface results in a 0.30 eV increase in binding energy to  $E_{As\ 3d} = 41.82$  eV, which is a  $E_F^i$  increase to  $E_F^i = 1.08$  eV. In contrast, overlayers of Si(B) (third peak,  $E_{As\ 3d} = 41.24$  eV) and Si(Ga) (bottom peak,  $E_{As\ 3d} = 41.07$  eV) have a decrease in  $E_B$  relative to the clean surface, which is thus a  $E_F^i$  decrease to 0.50 and 0.33 eV, respectively. In this example, therefore, the range in  $E_F^i$  at these Si-GaAs interfaces is 0.75 eV. Table I lists similar data for a number of samples in which thin Si(Ga), Si(B), and Si(P) overlayers were deposited onto clean GaAs surfaces. Also listed is a recently reported<sup>11</sup> value for  $E_F^i$  at a Si(As)-GaAs (100) interface. The maximum range in  $E_F^i$  for the Si-GaAs interfaces in Table I is 0.90 eV.

To make a Schottky barrier contact a metal is deposited onto the thin Si layers. Is the  $E_F^i$  value established at the Si-GaAs interface affected by such metal deposition? To answer this question the value of  $E_F^i$  (and thus  $\phi_B$ , as discussed in Sec. II) after deposition of a thin ( $\sim 10$ - $20$   $\text{\AA}$ ) metal layer onto the Si layer was measured by XPS for some of the samples. Table II lists the  $\phi_B^{XPS}$  measured for Au-Si(Ga), Ti-Si(Ga), and Au-Si( $\Gamma$ ) contacts (the Cr  $\phi_B^{XPS}$  could not be measured because the As 3d and Cr 3p peaks overlap). Thus, for the thin metal-Si(Ga) contacts  $E_F^i$  did not significantly change when a metal was deposited. There was, however, an  $\sim 0.1$  eV decrease in  $E_F^i$  for Au-Si(P). A large  $\sim 1$ -eV barrier is therefore predicted for thick contacts to Si(Ga)-GaAs and a small  $\sim 0.4$ -eV barrier for contacts to Si(P)-GaAs.

Representative  $I$ - $V$  data for thick metal Au-22  $\text{\AA}$  Si(Ga), Cr-24  $\text{\AA}$  Si(B), and Au-25  $\text{\AA}$  Si(P) contacts are plotted in Fig. 3. Also shown for comparison are data for ideal contacts of these metals (metal deposited onto a clean GaAs surface).

TABLE I. Interface Fermi energy  $E'_F$  after deposition of various thin Si layers which contain  $n$ -type or  $p$ -type impurities onto clean  $n$ -type GaAs(100) surfaces.

Impurity	Si thickness <sup>a</sup> (Å)	$E_{As\ 3d}$ <sup>b</sup> (eV)	$E'_F$ (eV)
Ga	17	41.13	0.39
Ga	22	41.07	0.33
Ga	26	41.21	0.47
Ga	28	41.15	0.41
B	11 <sup>c</sup>	41.24	0.50
B	24 <sup>c</sup>	41.28	0.54
B	25 <sup>d</sup>	41.23	0.49
P	14	41.82	1.08
P	25	41.84	1.10
As <sup>e</sup>	14		1.23

<sup>a</sup>Except as noted, Si deposited at 250 °C.

<sup>b</sup>As 3d binding energy in GaAs with Si overlayer.

<sup>c</sup>200 °C.

<sup>d</sup>350 °C.

<sup>e</sup>Reference 11.

A significant increase in barrier height is apparent for Si(Ga) and Si(B) interlayer contacts as is a significant decrease for the Si(P) contact. Table II gives the average  $n$  and  $\phi_B^{IV}$  measured for each Si interlayer contact sample (also given is the  $\phi_B^{IV}$  for the corresponding ideal metal contact).

Representative  $C-V$  data for the Au-Si(Ga), Au-Si(P), and Au-ideal contacts are shown in the  $1/C^2$  vs  $V$  plots of Fig. 4. The  $C-V$  data for the other contact samples were similar in form. The average  $\phi_B^{CV}$  measured for each sample is listed in Table II.

#### IV. DISCUSSION

The  $I-V$  and  $C-V$  electrical measurements of  $\phi_B$  on thick contacts are consistent with the  $E'_F$  ( $\phi_B$ ) values measured by XPS with thin overlayers. Why  $\phi_B^{CV}$  is  $\sim 0.1$  eV  $>$   $\phi_B^{IV}$  for the Cr and Ti contacts with Si(Ga) and Si(B) interlayers and an opposite sign difference of 0.07 eV is measured for the Au-Si(P) contact is not clear. The agreement between  $I-V$

TABLE II. Schottky barrier height  $\phi_B$  of metal contacts to GaAs that include a thin Si interface layer.

Contact	$\phi_B^{XPS}$ (eV)	$n$	$\phi_B^{IV}$ <sup>a</sup> (eV)	$\phi_B^{CV}$ (eV)
Au-22 Å Si(Ga)	1.11	1.08	1.01	1.01
Cr-28 Å Si(Ga)	...	1.11	0.99	1.10
Ti-17 Å Si(Ga)	1.05	1.11	0.98	1.14
Ti-26 Å Si(Ga)	1.01	1.10	0.97	1.06
Cr-24 Å Si(B)	...	1.09	0.92	0.97
Au-14 Å Si(P)	0.43	1.05	0.53	0.46
Au-25 Å Si(P)	0.42	1.06	0.49	0.42
Au-ideal		1.05	0.89	
Cr-ideal		1.05	0.76	
Ti-ideal		1.04	0.83	

<sup>a</sup>Includes image force correction, see the text.

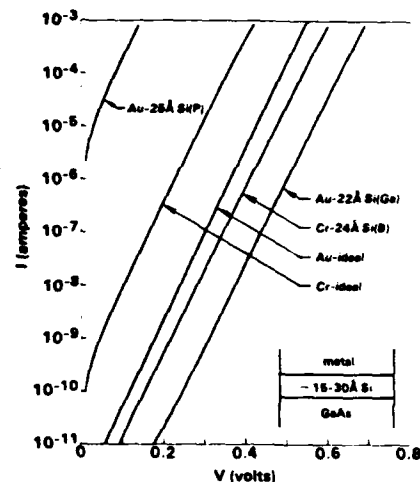


FIG. 3. Representative  $I-V$  data for Au-Si(Ga), Cr-Si(B), and Au-Si(P) contacts compared to Au-ideal and Cr-ideal contacts (contact area =  $5.07 \times 10^{-4}$  cm<sup>2</sup>).

and  $C-V$  values for the Au-Si(Ga) contact, however, indicates that such disparities are not an intrinsic characteristic of all metal-Si-GaAs contacts. Since the discrepancies are comparatively minor and may be an artifact of the  $C-V$  model, for discussion purposes the  $I-V$  values will be used: for the thick Si(Ga) contacts  $\phi_B = 1.0$  eV; for the Cr-Si(B) contact  $\phi_B = 0.92$  eV; and for the Au-Si(P) contact  $\phi_B = 0.5$  eV. The  $I-V$  ideality factors are acceptably small. Compared to the respective ideal contacts, the  $\phi_B$  increase ranges from 0.1 eV (Au) to 0.23 eV (Cr) while the  $\phi_B$  decrease for Au is 0.4 eV. By use of the metal-Si( $p$ -type)-GaAs structure  $\phi_B$  can be made essentially independent of the contact metal.

The XPS measurements show that the wide range in  $\phi_B$  for these metal-Si contacts is a direct consequence of the wide range in  $E'_F$  that can be induced at the Si-GaAs interface. This mechanism for achieving a wide range in  $\phi_B$  is thus quite unlike methods<sup>12</sup> in which a variable effective barrier height is created by tailoring the impurity profile, and therefore the potential, in the GaAs depletion region adjacent to a

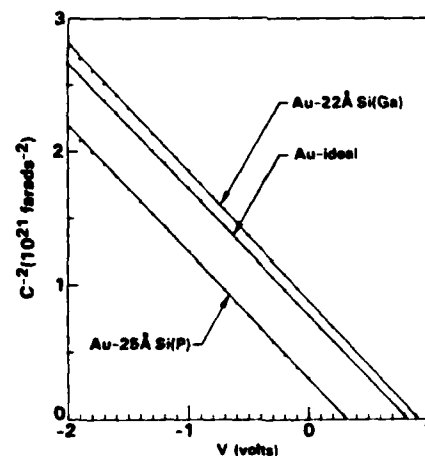


FIG. 4. Representative  $C-V$  data for Au-Si(Ga), Au-Si(P), and Au-ideal contacts. Line is least squares fit extrapolation to  $V'_s$ .

metal-GaAs interface where  $\phi_B$  itself remains constant.

Low  $E_F^i$  (high  $\phi_B$ ) values have been obtained both with Ga and with B heavily doped Si layers and high  $E_F^i$  (low  $\phi_B$ ) values both with P and with As heavily doped layers (in principle the Si layer should be degenerate and undepleted). Deposition temperatures between 200 and 350 °C were used. A LEED pattern was observed for the 350 °C growth which indicated epitaxy, but the lower temperature growths were either amorphous or polycrystalline. Thus, neither a precise Si growth temperature (although the lower and upper limits have not been determined) nor a particular Si impurity are crucial. The large lattice mismatch of Si and GaAs and the generally nonepitaxial nature of the Si layers also show that the degree of Si-GaAs interface perfection is unimportant. The essential condition influencing  $E_F^i$  at the Si-GaAs interface is that the Si be heavily either *n*-type or *p*-type.

Some difficulty was encountered in growing sufficiently heavy *p*-type Si films. The results with the B dopant were erratic with the method employed and there were some samples where the Si-GaAs  $E_F^i$  was not low because the Si apparently failed to be heavily *p*-type. Although lower  $E_F^i$  values were obtained with Ga, this should not be considered an inherent limitation of using B as a dopant but rather a requirement for good control over the Si dopant incorporation process. In this respect, the procedure for the Ga doped films yielded better consistency in producing low  $E_F^i$  interfaces, although the importance of the hydrogen background needs to be clarified. On the other hand, heavily *n*-type Si by P incorporation was readily obtained. Under the conditions used the Si layer had a large P excess detected by XPS; the amount of P can probably be controlled by changing the level of P overpressure or the substrate temperature.

A  $E_F^i$  range of ~0.7 eV at thin Ge-GaAs interfaces [*n*-type (100) GaAs] that results from making the Ge heavily either *n*-type or *p*-type has been reported.<sup>7,11</sup> This range is similar to the 0.66 eV band gap of Ge and consistent with the Ge-GaAs band lineup, which thus strongly suggests that the Ge band gap magnitude is what determines the extent to which  $E_F^i$  can be varied at this interface. In Table I the maximum  $E_F^i$  unpinning range for thin Si-GaAs interfaces is ~0.7 eV for the present data [~0.8 eV if the previously reported Si(As)-GaAs interface is included]. By analogy with the Ge-GaAs interface, an  $E_F^i$  range of ~1.1 eV is predicted at the Si-GaAs interface based on the 1.12 eV crystalline Si band gap. It is reasonable to expect that the value of  $E_F^i$  at its lower limit will be approximately set by where the Si valence band maximum lies within the GaAs band gap, which is the Si-GaAs heterojunction valence band offset  $\Delta E_v$ . A  $\Delta E_v$  of  $0.23 \pm 0.1$  eV has been measured<sup>13</sup> for the Si-GaAs interface, a value less than but in fair accord with the Si(Ga)-GaAs  $E_F^i$  results. Thus, an additional decrease in  $E_F^i$  at Si(*p*-type)-GaAs interfaces and an increase at Si-(*n*-type) interfaces amounting to ~0.3 eV in total (~0.4 for the Ga, B, and P dopants) is probable by refinement of the Si deposition process.

Unlike the comparatively constant  $E_F^i$  at Si(*p*-type)-GaAs interfaces with metal deposition, the Si(P)-GaAs  $E_F^i$  decreased ~0.1 eV with a Au overlayer. This effect may thus

occur for other metals. For many Ohmic contact applications the 0.5 eV  $\phi_B$  obtained at the Au-Si(P)-GaAs contact may be sufficiently low. However, it is likely that the highest  $E_F^i$  at Si(*n*-type)-GaAs interfaces can be retained by interposing a thin layer of a nonmetal electrical conductor between the contact metal and the Si(*n*-type)-GaAs interface. This structure would thus be similar to that used for a GaAs nonalloyed Ohmic contact design<sup>7</sup> in which a high  $E_F^i$  at an ~10 Å Ge(As)-GaAs interface is maintained by such an interlayer (in one example NiAs<sub>x</sub> was used). If found necessary in some instances, the same principle of an electrically conducting isolation layer could also be applied to optimally maintain a low  $E_F^i$  at Si(*p*-type)-GaAs interfaces.

Like GaAs, other III-V compound semiconductors (InP, for example) tend to have a limited range of  $\phi_B$  for metal contacts. If the mechanism that restricts  $\phi_B$  in other III-V semiconductors is analogous to that for GaAs, the present results suggest that appropriately doped Si or Ge interlayers will also increase the  $\phi_B$  range for metal contacts to such semiconductors.

## V. SUMMARY

$E_F^i$  values of 0.4 eV for Si(Ga), 0.5 eV for Si(B), and 1.1 eV for Si(P) are measured by XPS at Si-GaAs(100) interfaces, where the Si is an ~15-30-Å overlayer [a value of 1.2 eV has also been reported for Si(As)]. Thus,  $E_F^i$  at the Si-GaAs(100) interface is not pinned and can be moved over a wide 0.7-0.8-eV range by making the Si layer either *p*-type or *n*-type. For thick metal Au, Cr, and Ti contacts to the Si(Ga)-GaAs interface  $\phi_B = 1.0$  eV; for Cr to Si(B)-GaAs  $\phi_B = 0.92$  eV; and for Au to Si(P)-GaAs  $\phi_B = 0.5$  eV. Inclusion of a thin ~15-30 Å heavily *p*-type or heavily *n*-type Si interface layer therefore allows the design of metal contacts to GaAs with an extended barrier height range compared to conventional metal contacts.

## ACKNOWLEDGMENT

This work was supported by AFOSR Contract No. F49620-85-C-0120.

- <sup>1</sup>J. R. Waldrop, *Appl. Phys. Lett.* **47**, 1002 (1984); *J. Vac. Sci. Technol. B* **2**, 445 (1984).
- <sup>2</sup>R. A. Scranton, J. S. Best, and J. O. McCaldin, *J. Vac. Sci. Technol.* **14**, 930 (1977).
- <sup>3</sup>M. Suzuki, K. Murase, K. Asai, and K. Kurumada, *Jpn. J. Appl. Phys.* **22**, L709 (1983).
- <sup>4</sup>J. R. Waldrop, *J. Vac. Sci. Technol. B* **3**, 1197 (1985).
- <sup>5</sup>J. Massies, J. Chaplart, M. Laviron, and N. T. Linh, *Appl. Phys. Lett.* **38**, 693 (1981).
- <sup>6</sup>J. R. Waldrop, *Appl. Phys. Lett.* **47**, 1301 (1985).
- <sup>7</sup>J. R. Waldrop and R. W. Grant, *Appl. Phys. Lett.* **50**, 250 (1987).
- <sup>8</sup>J. R. Waldrop, R. W. Grant, and E. A. Kraut, *J. Vac. Sci. Technol. B* **5**, 1209 (1987).
- <sup>9</sup>E. H. Rhoderick, *Metal-Semiconductor Contacts* (Clarendon, Oxford, 1977).
- <sup>10</sup>A. M. Goodman, *J. Appl. Phys.* **34**, 329 (1963).
- <sup>11</sup>R. W. Grant and J. R. Waldrop, *J. Vac. Sci. Technol. B* **5**, 1015 (1987).
- <sup>12</sup>See, for example, J. M. Shannon, *Solid State Electron.* **19**, 537 (1976).
- <sup>13</sup>R. S. List, J. Woicik, P. H. Mahowald, I. Lindau, and W. E. Spicer, *J. Vac. Sci. Technol. A* **5**, 1459 (1987).

Variations of GaAs (100) Interface Fermi Level  
for Model AuGeNi Ohmic Contacts\*

R.W. Grant and J.R. Waldrop  
Rockwell International Science Center  
Thousand Oaks, CA 91360

The AuGeNi alloyed ohmic contact is widely used for n-GaAs. The heterogeneous nature of the alloyed metallization complicates analysis of the ohmic contact formation mechanism. It is usually assumed, however, that the interface Fermi level ( $E_F^i$ ) position (relative to the valence band maximum) for the alloyed contact is  $\sim 0.5-0.7\text{eV}$  (consistent with Schottky barrier ( $\phi_B$ ) heights observed for most metal contacts to n-GaAs) and that a large donor concentration associated with Ge indiffusion near the GaAs interface region during alloying produces a low resistance tunnel contact.

Model AuGeNi contacts to n-GaAs that involve layered structures have been investigated to correlate  $E_F^i$  with interface composition. The layers (prepared in ultra high vacuum) were fabricated from the Au, Ge, and Ni components used in the alloyed contact in addition to As and Te; these contacts were not alloyed in order to preserve interfaces of known composition. X-ray photoemission spectroscopy (XPS) and current-voltage (I-V) measurements were used to analyze the samples.

For very thin ( $\sim 10\text{\AA}$ ) Ge epitaxial layers grown on n-GaAs under conditions where As was incorporated in the Ge [i.e., Ge(As)], an unusually large  $E_F^i = 1.0-1.2\text{eV}$  was observed by XPS; Ge grown in the same temperature range without As incorporation or deposited at room temperature yielded  $E_F^i = 0.4-0.7\text{eV}$ . Whether or not the large  $E_F^i$  ( $1.0-1.2\text{eV}$ ) associated with the  $\sim 10\text{\AA}$  Ge(As) layer could be retained depended on the composition of the next deposited layer. For example, deposition of thin NiAs<sub>x</sub> or Te onto the Ge(As) preserved the large  $E_F^i$  values (as determined by XPS), while deposition of thin Au or Ni layers shifted  $E_F^i$  from  $\sim 1.1$  to  $\sim 0.7\text{eV}$ . I-V measurements of  $\phi_B$  on these samples after making the overlayer thickness sufficient to fabricate contacts demonstrated that this  $E_F^i$  variation was preserved. Thus, Au-NiAs<sub>x</sub>-Ge(As) and Au-Te-Ge(As) contacts with high  $E_F^i$  ( $\sim 1.0-1.2\text{eV}$ ) have low  $\phi_B$  ( $\sim 0.25-0.4\text{eV}$ ) while Au-Ge(As) and Ni-Ge(As) contacts have  $\phi_B$   $0.6-0.8\text{eV}$ . It is therefore possible to obtain the unusually large  $E_F^i$  values in thick contacts by an appropriate choice of layer structure.

The present results on model AuGeNi ohmic contacts suggest that microscopic nonuniform regions with low  $\phi_B$  may be associated with alloyed AuGeNi ohmic contact formation. The unusually large  $E_F^i$  values observed may also provide a guide for the design of nonalloyed ohmic contacts.

\* This work was supported by AFOSR contract No. F49620-85-C-0120.

## Large Range of Interface Fermi Energy in n-GaAs (100) Induced by Thin Si Layers

J. R. Waldrop and R. W. Grant  
Rockwell International Science Center  
Thousand Oaks, CA 91360

Clean surfaces of n-type GaAs (100) have interface Fermi energy  $E_F^i$  values (relative to the valence band maximum) near midgap. Several ways to significantly increase  $E_F^i$  with respect to these vacuum-clean surface values are known. For example, deposition of a  $\sim 15$  Å Si layer with incorporated As results in an  $E_F^i$  of 1.23 eV.<sup>1</sup> We here report x-ray photoemission spectroscopy (XPS) interface data and electrical measurements on thick Schottky barrier contacts which show that thin ( $\sim 15$  Å) Si layers evaporated from a source containing B onto clean n-type GaAs (100) surfaces will cause a decrease in  $E_F^i$  to values as low as 0.43 eV. Thus, a large 0.8 eV range in  $E_F^i$  at Si-GaAs (100) interfaces can be induced via the dopant type in the thin Si overlayer. The ultimate  $E_F^i$  range at these interfaces appears to be limited by the magnitude of the Si bandgap. The Si-GaAs (100) results further demonstrate that  $E_F^i$  is not necessarily pinned within a narrow set of values at interfaces that involve n-type GaAs (100).

The samples were prepared in the UHV chamber of the XPS system. The Si overlayers were deposited onto thermally cleaned GaAs substrates that were at a temperature between 200 and 350°C. Although epitaxy was observed at 350°C the Si deposited at lower temperatures was not epitaxial. Thus, the Si-GaAs interface perfection was not a crucial factor for achievement of a low  $E_F^i$  value. The  $E_F^i$  during interface formation was measured by analysis of XPS core level peaks. Schottky barrier contacts for electrical characterization were formed by depositing a thick layer of metallization onto the  $\sim 15$  Å Si overlayer. For chromium and conducting chromium phosphide contacts the low  $E_F^i$  values at the Si-GaAs interface were retained and barrier heights of  $\sim 1$  eV were measured by I-V and C-V techniques consistent with the associated XPS measurements. The corresponding Schottky barrier heights for ideal (no Si interlayer) contacts of these metallizations are  $\sim 0.2$  eV lower. Thus, use of a thin p-type Si interlayer at n-GaAs (100) Schottky barrier contacts is a method to considerably increase barrier height compared to that generally obtained with ideal metal contacts.

This work was supported by AFOSR Contract No. F49620-85-C-0120

1. R.W. Grant and J.R. Waldrop, J. Vac. Sci. Technol. B5, 1015 (1987)

Materials Research Society Symposia  
1989 Spring Meeting - April 1989  
Symposium D: Chemistry and Defects in Semiconductor  
Heterostructures

EFFECT OF Si AND Ge INTERFACE LAYERS ON THE SCHOTTKY  
BARRIER HEIGHT OF METAL CONTACTS TO GaAs. J. R.  
Waldrop and R. W. Grant, Rockwell International  
Science Center, Thousand Oaks, CA 91360.

Conventional metal contacts to GaAs generally have a relatively narrow Schottky barrier height  $\phi_B$  range of  $\sim 0.7$ - $0.9$  eV for n-type material and  $\sim 0.5$ - $0.6$  eV for p-type. We describe recent results in which it has been found that the metal contact  $\phi_B$  range for both n-type and p-type GaAs can be significantly extended by inclusion of very thin Si or Ge interlayers that directly influence the interface Fermi energy  $E_F^i$ . X-ray photoemission spectroscopy was used to obtain  $E_F^i$  and composition during contact formation; the  $\phi_B$  for the corresponding thick contacts was measured by electrical methods. The Si and Ge interlayers are  $\sim 15$ - $30$  Å thick and are heavily either n type or p type. In an appropriate structure, the  $\phi_B$  range for contacts to n-type GaAs can be as large as  $\sim 0.25$  to 1 eV. For p-type GaAs,  $\phi_B$  values of  $\sim 0.7$ - $0.9$  eV have been obtained. The results will be discussed in terms of a simple heterojunction model of the interlayer-GaAs interface.

Supported in part by the AFOSR

J.R. Waldrop  
Rockwell International Science Center  
P.O. Box 1085  
Thousand Oaks, CA 91360  
(805) 373-4249

DISCLOSURE  
OF  
INNOVATION OR INVENTION

Title Design of Nonalloyed Ohmic Contacts with Low Barrier Heights

Docket No. 87SC36

INNOVATOR OR INVENTOR	DEPT. NO. & MAIL ADDRESS	SERIAL NO.	SOC. SEC. NO.	PHONE NO.	SUPERVISOR
J.R. Waldrop	311 A16		557-60-0219	4249	R.W. Grant
R.W. Grant	311 A16		276-34-1884	4219	C.A. Liechti

THE PROBLEM: Reduction of barrier height at semiconductor interfaces for nonalloyed tunneling ohmic contact applications.

DESCRIPTION OF SOLUTION: (Succinct statement of broad solution together with detailed description, illustrated by sketches where appropriate, of the structure, operation, physical characteristics -- electrical, chemical, mechanical -- describing the new result. Attach additional material, preferably on Form 74-S.)

Nonalloyed ohmic contacts to GaAs and other semiconductors are increasingly important as device dimensions decrease. Many semiconductors (including GaAs) exhibit a narrow range of Fermi level positions at the interfaces of electrical contacts. This range is typically not optimum for nonalloyed tunneling ohmic contact applications because the specific contact resistance depends exponentially on barrier height. Gallium Arsenide is a semiconductor where the Schottky barrier height on n-type material is usually limited to a narrow range (0.7 to 0.9 eV) for metal contacts. This large barrier is thus an impediment to achieving a low ohmic contact resistance. A solution to the problem is to deposit very thin layers (on the order of  $10\text{\AA}$ ) of another heavily doped semiconductor onto the semiconductor being considered. For n-GaAs it is observed that heavily n-type doped Ge or Si can lower the Schottky barrier height to  $-0.25 - 0.4$  eV. By use of a suitable nonmetallic conducting diffusion barrier, this low Schottky barrier height can be retained for metal contacts of thickness ( $>2000\text{\AA}$ ) that are suitable for practical applications. (The low barrier is not retained if the contact metal is directly against the thin semiconductor overlayer.) The role of the diffusion barrier is thus to isolate the semiconductor interface from the metal contact material while also providing a conducting electrical contact. The intermediate conducting layer does not itself introduce any electrical potential barrier. The thin heavily doped semiconductor layer either removes or overcomes the mechanism responsible for the normally observed narrow range of interface Fermi level positions but is thin enough so as not to introduce significant series resistance.

DISCLOSURE  
OF  
INNOVATION OR INVENTION

Title Method for Obtaining Metal Contacts with Large Schottky Barrier Heights Docket No. 88SC46

INNOVATOR OR INVENTOR	DEPT. NO. & MAIL ADDRESS	SERIAL NO.	SOC. SEC. NO.	PHONE NO.	SUPERVISOR
J.R. Waldrop	312 A4		557-60-0219	4249	P.M. Asbeck
R.W. Grant	315 A16		276-34-1884	4219	D.T. Cheung

THE PROBLEM: Conventional metal Schottky barrier contacts to compound semiconductors have limited range of barrier height.

DESCRIPTION OF SOLUTION: (Succinct statement of broad solution together with detailed description, illustrated by sketches where appropriate, of the structure, operation, physical characteristics -- electrical, chemical, mechanical -- describing the new result. Attach additional material, preferably on Form 74-S.)

Metal contacts to n-type GaAs commonly used in device applications generally have a limited range of Schottky barrier height that is 0.7 and 0.9 eV; the actual barrier height value within this range depends on the metal involved. It would be advantageous for certain device applications both to increase the contact barrier height over that customarily obtainable and to make the height independent of the contact metal. Both these objectives can be accomplished by using a contact formation method that is based on influencing the barrier height with a very thin (~15 - 30Å), heavily p-type, Si interlayer. This Si interlayer serves to overcome (compensate) the mechanism(s) at the metal-GaAs interface which would otherwise fix the barrier height (interface Fermi energy) for a particular metal at a lower value. It has been found that Si doped with either Ga or B will produce the desired effect of increasing the barrier. For Au, Cr, and Ti contacts with such a Si interlayer heavily doped with Ga the barrier height is 1 eV, independent of the metal. The increased barrier for these metals compared to the corresponding ideal (no interlayer) contact ranges from 0.1 to 0.23 eV. Because of the diverse properties of Au, Cr, and Ti it is expected that other metals will also have an increased barrier when used in the metal-Si(p-type)-GaAs contact structure. It is further expected that for other compound semiconductors such as InP, a similar contact structure will also produce increased Schottky barrier heights.